DEFINING AN IN VIVO RODENT MODEL FOR STATIN MYALGIA

DETERMINING A RODENT MODEL TO INVESTIGATE GLUTAMATE AS A MECHANISM UNDERLYING STATIN MYALGIA

By ALLYSON M. SCHWEITZER, B.Sc. Kinesiology Honours

A Thesis Submitted to the School of Graduate Studies in Partial Fulfillment of the Requirements for the Degree Master of Science

McMaster University MASTER OF SCIENCE (2020), Hamilton, Ontario (Medical Sciences)

TITLE: Determining a rodent model to investigate glutamate as a mechanism underlying statin myalgia

AUTHOR: Allyson M. Schweitzer, B. Sc. Kinesiology Honours (McMaster University)

SUPERVISOR: Dr. Thomas Hawke

NUMBER OF PAGES: xv, 122

Lay Abstract

Statins, a class of cholesterol-lowering medications, are one of the most widely prescribed medications worldwide. They have been demonstrated to be very effective at reducing one's risk of cardiovascular-related death. Statins are generally very well tolerated, however, the most common negative side effects of their use are muscle related and include muscle pain, muscle inflammation and muscle damage. Muscle pain is the most common of these symptoms to present and interestingly, often presents without any clinical indication of muscle damage. The lack of a physical explanation for what is causing this pain makes treating statin-associated muscle pain quite difficult. A lot of effort has gone into determining the mechanism(s) for statin-associated muscle damage, however, there is a gap when it comes to investigating the mechanism(s) for statin-associated muscle pain. The studies herein, therefore, aimed to bridge this gap and investigated a potential mechanism for statin-associated muscle pain in a rodent model. The foundation for this model was built on a cell culture model that was previously developed in our lab. Our data suggest that a rodent model for statin-associated muscle pain may not be an appropriate representation of what occurs in humans. In particular, reduced blood cholesterol and substantial skeletal muscle oxidative stress were not demonstrated in our model as they have been in humans and in cell culture studies. This raised concern around the efficacy of rodent models for statin associated muscle symptoms in general and highlighted the importance of having standardized models. The differences between human/cell culture studies and rodent models also made it difficult to draw firm conclusions on whether the mechanism for statin myalgia investigated herein is supported.

Abstract

HMG-CoA reductase inhibitors, known commonly as statins are one of the most widely prescribed medications worldwide. Statins reduce circulating cholesterol levels and are very effective at reducing one's risk for all-cause and cardiovascular mortality. Though generally well tolerated, statin-associated muscle symptoms (SAMS) present in more than a quarter of statin users. The most common SAMS is myalgia or muscle pain. Statin myalgia often presents in the absence of myofibre damage, making its origin and treatment ambiguous. There are numerous rodent models for statin myopathy in the literature, but surprisingly there is no representation of statin myalgia that we are aware of. This is shocking given the high prevalence of statin myalgia compared to statin myopathy. Recently, our lab published an *in vitro* model of statin myalgia that focused on elevated xCT transporter activity and interstitial glutamate. This model explains that pain perceived in statin myalgia is the result of statins' downstream ability to elevate skeletal muscle interstitial glutamate concentrations, thereby activating peripheral nociceptors. The studies herein aimed to create an *in vivo* rodent model of statin myalgia based on the aforementioned *in vitro* model. We hypothesized that glutamate, sampled by way of skeletal muscle microdialysis, would be elevated in the skeletal muscle interstitium of rats following statin treatment. Drawing conclusions on the role of glutamate in statin myalgia was not a straightforward process and required multiple model adjustments due to confounding variables. Additionally, many of the recognized effects of statins that were assumed from human and *in vitro* studies did not translate well to our rodent model. This was the first attempt at creating an *in vivo* model of statin myalgia and evidence suggests that a rodent model may not be an appropriate representation of what occurs in humans. While these

studies also raised doubt on the efficacy of rodent models for SAMS investigations in general and highlighted the importance of having standardized models, certain limitations and assumptions of our model must be addressed before concrete conclusions can be drawn.

Acknowledgements

Firstly, I would like to thank my advisor, Dr. Thomas Hawke, for the guidance and support he has given me over the past two years and for providing me many opportunities to learn and grow as a young scientist. I would also like to express my gratitude to Dr. Irena Rebalka, whose unwavering mentorship, encouragement and friendship truly heightened my lab experience. Thank you for training me and for helping collect and analyze data. You inspired me every day, and I am so thankful to have shared this research experience with you.

Thank you, Dr. Chris Perry for reminding me that there will always be good and bad science days. Thank you to my committee members, Dr. Tarnopolsky and Dr. Raha, for your insightful questions and discussions.

Thank you to all of the scientists that worked in the Hawke Lab, past and present. Thank you, Cynthia, for your consistent willingness to help and for taking care of the lab, Athan, for providing new perspectives and hashing out ideas with me, Grace, for being a scope genius and for readily providing assistance and Mike, for being so positive and always offering a helping hand. Finally, a huge thank you to Maria, whose friendship in and out of the lab stayed with me through the thickest and thinnest. Life would not have been the same without you the past two years.

Last but definitely not least, I would like to thank my entire family for the love, support and encouragement they have shown me not only these last two years but throughout my entire university career.

Table of Contents

List of Figures and Tables

Figures from Review of Literature

Figure from Introduction

Figures from Section 1, Study One – Cardiotoxin Experiment

Figures from Section 2, Study Two – Statin Treatment *in vivo* (Nutella)

Figures from Section 3, Study Three – Statin Dosing (All-Natural Peanut Butter)

Figures and Table from Section 4, Study Four – Statin Treatment *in vivo* (Gavage)

Figures and Table from Section 5, Consolidating Discussion and Conclusions

Figures from Appendices

List of Abbreviations

ADP	Adenosine diphosphate
AMPA	α-amino-3-hydroxy-5-methyl-4-isoxazoleproprionic acid
ATP	Adenosine triphosphate
CNS	Central nervous system
CTX	Cardiotoxin
Cu,Zn-SOD	Copper-zinc-dependent superoxide dismutase
ECSOD	Extracellular superoxide dismutase
EDL	Extensor digitorum longus
ETC	Electron transport chain
FADH2	Flavin adenine dinucleotide
GPS	Gastrocnemius plantaris soleus
GSH	Reduced glutathione
GSSG	Oxidized glutathione
H-E	Hematoxylin-eosin
HMG-CoA	3-hydroxy-3-methyl-glutaryl-coenzyme A
H_2O_2	Hydrogen peroxide
LDL	Low density lipoprotein
mGlu	Metabotropic glutamate
Mn-SOD	Manganese-dependent superoxide dismutase
MSI-CE-MS	Multisegment injection-capillary electrophoresis-mass spectrometry
NADP	Nicotinamide adenine dinucleotide phosphate

NADPH	Nicotinamide adenine dinucleotide phosphate hydrogen
NMDA	N-methyl-D-aspartate
O_2^-	Superoxide
OCT	Optimal cutting temperature compound
ROS	Reactive oxygen species
SAMS	Statin associated muscle symptoms
SEM	Standard error of the mean
SOD	Superoxide dismutase
TA	Tibialis anterior
TCA	Tricarboxylic acid

Declaration of Academic Achievement

Allyson Schweitzer was the primary contributor. Dr. Irena Rebalka assisted with skeletal muscle microdialysis techniques and training. Molly Gingrich completed and analyzed cholesterol assays. Dr. Britz-McKibbon supervised the MSI-CE-MS analysis completed by Zachary Kroezen and Meera Shanmuganathan. Dr. Thomas Hawke and Dr. Irena Rebalka assisted with conceiving and designing the studies.

Review of Literature

Introduction to Skeletal Muscle and the Mitochondria

Skeletal muscle comprises approximately 40 percent of the average human's body mass and has important roles in respiration, heat provision and glucose regulation (Betts et al. 2017; Olson 2011). Most well-known, however, is that the contraction of this large and powerful organ is what makes locomotion, facial expressions, postural support and all voluntary movement possible. Skeletal muscle contraction and subsequent body movement requires the intricate coordination of numerous molecular processes and structures as they work together and respond to one another to create one fluid motion. Muscle cells/myofibres grouped together in a coordinated network with the skeletal, circulatory and nervous system, create a full and functional muscle. Human skeletal muscle is comprised of three types of myofibres: slow-oxidative, fast-oxidative and fast-glycolytic. They are classified based on how they produce adenosine triphosphate (ATP), the source of cellular energy that is used for muscle contraction (Betts et al. 2017). Fast glycolytic myofibres are the fastest to respond following stimuli for muscle contraction, but they also tend to fatigue the quickest. Contrastingly, slow oxidative myofibres respond slower but are able to sustain muscle contraction for longer durations. These phenomena are also related to how the myofibre generates ATP (Betts et al. 2017).

Myofibres are multinucleated, which facilitates the large production of enzymes and proteins that are required for muscle contraction. They are also cylindrical and in humans can be as long as 30 cm in muscles such as the sartorius (Betts et al. 2017). The striated appearance of myofibres under the microscope is a result of the arrangement of actin and myosin, two myofilament proteins that are integral in contraction. These myofilaments along with their

regulatory proteins make up the sarcomere, the functional unit of the myofibre responsible for contraction. Muscle contraction is a highly metabolically demanding process that requires an abundant supply of ATP. As previously mentioned, myofibres are able to produce ATP in different ways. Glycolytic myofibres rely primarily on anaerobic glycolysis for ATP production, whereas oxidative fibres rely more heavily on aerobic pathways (Betts et al. 2017). Anaerobic metabolism takes place in the cytosol of the myofibre. It provides quick energy and does not require oxygen but is an unsustainable energy source.

Alternatively, aerobic metabolism can maintain a constant supply of energy at rest or under periods of sustainable work. Aerobic ATP production occurs within the mitochondria in the myofibre (Betts et al. 2017; Dykens and Will 2008). The mitochondria are a double-membrane-bound organelle. The inner mitochondrial membrane folds in on itself and creates two distinct compartments within the organelle (Dykens and Will 2008). The space between the inner and outer membrane is termed the intermembrane space and the space interior to the inner mitochondrial membrane is called the mitochondrial matrix. The mitochondria produce the bulk energy required for skeletal muscle contraction through aerobic metabolism (Leninger 1964; Ribas, García-Ruiz, and Fernández-Checa 2014; Tzagoloff 1982). Aerobic metabolism includes the tricarboxylic acid (TCA) cycle and the electron transport chain (ETC). The TCA cycle takes place in the mitochondrial matrix and produces two ATP molecules per cycle (Dykens and Will 2008). It also produces reducing equivalents NADH and FADH2 that are used by the ETC (Dykens and Will 2008). The ETC is located on the inner mitochondrial membrane and is the main source of ATP production (Dykens and Will 2008). It consists of four enzyme complexes: I (NADPH ubiquinone oxidoreductase), II (succinate dehydrogenase), III (ubiquinol-cytochrome c

oxidoreductase) and IV (cytochrome c oxidase) (Betts et al. 2017; Dykens and Will 2008). The enzyme complexes are named for their position in the chain. The final complex involved in mitochondrial respiration, though not technically part of the ETC, is complex V, also known as ATP synthase (Dykens and Will 2008). With the help of coenzymes (coenzyme Q and cytochrome c) and reducing equivalents (NADPH/FADH2), electrons are transferred from one complex to the next in the ETC. The energy created through these redox reactions allows protons to be pumped from the mitochondrial matrix to the intermembrane space through certain ETC complexes (Betts et al. 2017; Dykens and Will 2008). As protons accumulate within the intermembrane space, an electrochemical gradient forms across the inner mitochondrial membrane (Nicholls and Ferguson 2002). This gradient drives the protons within the intermembrane space to pass through ATP synthase (Nicholls and Ferguson 2002). The energy release from protons shuttled through ATP synthase allows ADP to combine with an inorganic phosphate group and create ATP. During proper cellular functioning, energy requirements are matched by the mitochondria's ability to produce ATP and in skeletal muscle, the mitochondria can upregulate energy production to 20-fold their resting rate (Dykens and Will 2008).

Though imperative to proper cellular functioning, the mitochondria also play a role in programmed cell death or apoptosis (Kaufmann & Hengartner, 2001; Kroemer, 2003). This is achieved largely through the production of reactive oxygen species (ROS), which contribute to both programmed and necrotic mitochondrial-mediated cell death.

Reactive Oxygen Species and Oxidative Stress

ROS are important signalling molecules for processes such as skeletal muscle remodeling and regeneration (Nunes-Silva et al. 2014; Powers et al. 2010). In excess, however,

they have the ability to alter protein structure and function and cause detrimental cellular damage. Under normal physiological conditions, cellular antioxidants can abate and remove free radicals/ROS before cellular damage occurs. If the antioxidant capacity of a cell is compromised or ROS production exceeds its capacity, oxidative stress and cellular damage, dysfunction and/or cell death become more likely (Dykens and Will 2008; Ribas et al. 2014).

The main creator of ROS in mammalian cells are the mitochondria (Hoye et al. 2008; Li Li Ji, Fu, and Mitchell 1992; Venditti, Di Stefano, and Di Meo 2013). This is because as electrons transfer between protein complexes in the ETC, they have a tendency to leak into the surrounding oxygen-rich environment (Dykens and Will 2008). In this space, electrons react with and reduce oxygen to superoxide (O_2^-), a ROS. O_2^- is a highly reactive molecule capable of reacting with and altering the structure and function of lipids, proteins, enzymes and nucleic acids (Dykens and Will 2008; Ribas et al. 2014). While electron leak is most common at complexes I and III within the ETC (Adam-Vizi and Chinopoulos 2006; Grivennikova and Vinogradov 2006; Takeshige and Minakami 1979; Trumpower 1990; Turrens 2003; Venditti et al. 2013), complex II has also been implicated in electron leak (Quinlan et al. 2012). Numerous antioxidant defense systems exist to buffer mitochondrial ROS. Two of the most prevalent are the superoxide dismutase (SOD) enzymes and glutathione and its associated enzymes (Dykens and Will 2008; Fridovich 1989; Ribas et al. 2014).

The main role of SOD enzymes is to abate O_2^- accumulation. Three different SOD enzymes exist in mammals: SOD1/Cu,Zn-SOD in the cytoplasm, SOD2/Mn-SOD in the mitochondria and SOD3/ECSOD in the extracellular space (Miao and St. Clair 2009). Given that SOD2 exists exclusively within the mitochondrial matrix, it is one of the first to defend against

mitochondrial ROS (Dykens and Will 2008; Okado-Matsumoto and Fridovich 2001; Weisiger and Fridovich 1973). The SOD enzymes catalyze the dismutation of O_2^- to hydrogen peroxide (H_2O_2) and oxygen (O_2) (Dykens and Will 2008; Fridovich 1995). H_2O_2 is less reactive than O_2^- but can still cause deleterious cellular effects if accumulation occurs (Cadenas and Davies 2000; Dykens and Will 2008). H_2O_2 accumulation is controlled in part by glutathione and its associated enzymes.

SOD activity and mRNA expression are upregulated during periods of increased oxidative stress. Marius-Daniel, Stelian & Dragomir (2010) show increased SOD activity in rat skeletal muscle following acute exercise. Similarly, Zhao et al. (2013) demonstrated elevated SOD1/SOD2 mRNA expression in rat skeletal muscle following exercise. Furthermore, Avin et al. (2016) demonstrated greater SOD1/SOD2 mRNA expression in the skeletal muscle of rats with chronic kidney disease – a pathology associated with elevated oxidative stress.

In addition to the SOD enzymes, glutathione and its associated enzymes are integral in a cell's antioxidant defense system. Reduced glutathione (GSH) is a tripeptide thiol expressed ubiquitously in mammalian cells and is the main antioxidant defense against ROS (Meister, 1995; Ribas et al., 2014). GSH is synthesized *de novo* from cysteine, glutamate and glycine, with cysteine defined as the rate-limiting substrate for its production (Ribas et al. 2014). GSH is synthesized in the cytosol, following which it can be transported into the mitochondria (García-Ruiz et al. 1994; Griffith and Meister 1985; Mari et al. 2009, 2010). The antioxidant defense of GSH works in multiple ways, in isolation or in conjunction with different enzymes (Fig. 1). In isolation, GSH acts as a free radical scavenger by reducing target molecules through its subsequent oxidation (Ross 1988; Shan, Aw, and Jones 1990; Yang et al. 2014). Oxidized

glutathione (GSSG) is recycled back to GSH by glutathione reductase (Kelner and Montoya 2000). The GSH to GSSG ratio (GSH/GSSG) is commonly used as an indicator of the oxidative state within the cell (i.e. a smaller ratio indicates greater oxidative stress). Reduced GSH/GSSG ratios have been demonstrated in rodent skeletal muscle following exercise, in disease states and in response to xenobiotics, all of which implicate elevated oxidative stress (Bouitbir et al. 2016; Deminice and Jordao 2012; Hughes et al. 2019). Alternatively, GSH acts as a substrate for the enzyme glutathione peroxidase (Dykens and Will 2008; Ribas et al. 2014). Glutathione peroxidase is intrinsic to the mitochondrial matrix and catalyzes the reaction of H_2O_2 to water while subsequently oxidizing GSH (Fig. 1) (Dykens and Will 2008; Ribas et al. 2014). The efficiency and effectiveness of this enzyme relies heavily on the availability of GSH (Dykens and Will 2008).

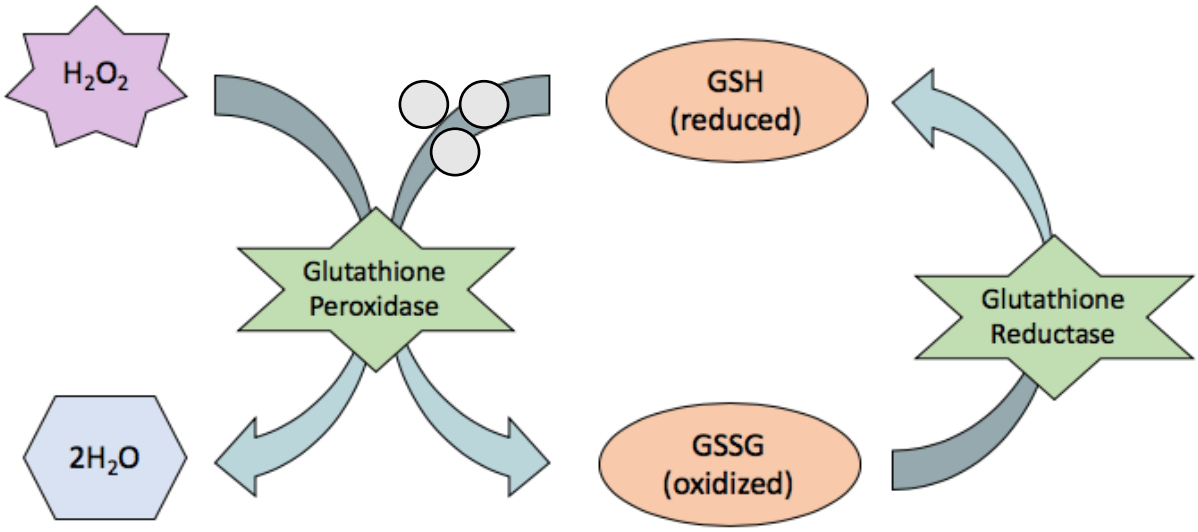

Figure 1: Antioxidant defense mechanism of glutathione and its associated enzymes. GSH reduces target molecules (grey circles) through its subsequent oxidation to GSSG. Glutathione reductase recycles GSSG back to GSH. Using GSH as a substrate, glutathione peroxidase catalyzes the reaction of hydrogen peroxide (H_2O_2) to two water ($2H_2O$) molecules.

The SOD enzymes and GSH mechanisms of antioxidant defense work in conjunction with each other to maintain proper cellular homeostasis. If either of these antioxidant defense systems are compromised, the risk of oxidative stress and cellular damage increases. Antioxidant capacity can be altered in many ways including protein expression, substrate availability, energy supply and transporter function (Banjac et al. 2008; Rebalka et al. 2019; Rimaniol et al. 2001; Ungard, Seidlitz, and Singh 2014).

Cystine, Cysteine and the xCT Transporter

When discussing antioxidants, it is important to distinguish between cysteine and cystine. Cystine is formed by the oxidation and formation of a disulfide bond between two cysteine molecules. Extracellular cystine is readily available to peripheral tissue due to the large synthesis and export of cysteine by the liver (Bannai 1986; Brigham, Stein, and Moore 1960; Muir et al. 2017; Vitvitsky et al. 2004). In the extracellular space cysteine is rapidly converted to cystine, its more stable form (Bannai 1986).

Intracellular cysteine content is the limiting factor of GSH synthesis because its intracellular production is very low (Combs and Denicola 2019; Ishii, Sugita, and Bannai 1987; Ribas et al. 2014). Some evidence exists that cysteine can be synthesized endogenously in human and rat skeletal muscle via transsulfuration of homocysteine, a product of the methionine cycle (Bao et al. 1998; Combs and Denicola 2019; Du et al. 2013; Mudd et al. 1965). The extent to which this pathway contributes to the intracellular pools in skeletal muscle, however, requires further elucidation.

More commonly, cysteine is imported through neutral amino acid transporters or cystine is imported through the system x_c^- cystine/glutamate exchange transporter to increase intracellular cysteine pools (Banjac et al. 2008). Given the low concentration of cysteine extracellularly, it is more often that cystine is imported (Arriza et al. 1994; Banjac et al. 2008; Mannery, Ziegler, and Jones 2007; Nkabyo et al. 2005).

System x_c^- is comprised of the xCT light chain, responsible for the specificity of the amino acid exchange reaction, and the 4F2 heavy chain (Banjac et al. 2008). Herein, xCT transporter will be used to refer to the activity of these two proteins involved in system x_c^-.

Transcription of the xCT gene increases as a result of oxidative stress as well as reduced intracellular cystine levels (Banjac et al. 2008) and xCT transporter activity has been demonstrated to play a major role in maintaining cellular homeostasis during periods of elevated oxidative stress (Sato et al. 2005; Siska et al. 2016; Sleire et al. 2015). Increased xCT expression drives increased cellular cystine uptake and subsequent antioxidant usage (Banjac et al. 2008; Gu et al. 2017; Martin and Gardner 2015; Sayin et al. 2017). To combat oxidative stress, intracellular cystine is used directly in the cystine/cysteine redox cycle or converted to cysteine and used for GSH synthesis (Banjac et al. 2008).

Overexpression of the xCT transporter has been demonstrated to rescue murine and human cells from L-buthionine-S, R-sulfoximine-mediated cell death (Banjac et al. 2008). This defense against oxidative stress, however, can become problematic. For example, some cancer cell lines have been demonstrated to overexpress the xCT transporter, increasing their resistance to cell death (Guo et al. 2011; Sugano et al. 2015). Ungard et al. (2019) suggest that xCT overexpression in cancer cells may also play a role in cancer-induced bone pain. The xCT transporter imports one cystine molecule for every glutamate molecule it extrudes (Rutten et al. 2005). Glutamate is a neurotransmitter that is involved in the activation and sensitization of nociceptive pathways when in high concentrations extracellularly (Alfredson, Thorsen, and Lorentzon 1999; Cairns et al. 2002; Castrillon et al. 2012; Gerdle et al. 2014; Svensson et al. 2005). The authors suggest that xCT overexpression in cancer cells is responsible for cancer-induced bone pain because it increases extracellular glutamate concentrations. They support this hypothesis by demonstrating that a reduction in xCT transporter content delays the onset of cancer-induced bone pain in mice (Ungard et al. 2019).

Collectively, this evidence suggests that the xCT transporter is a key mediator of two important antioxidant pathways: the cystine/cysteine redox pathway and GSH synthesis (Banjac et al. 2008; Ishii et al. 1987; Ribas et al. 2014). More recently, xCT and its link to glutamate has been suggested to play a key role in pain pathologies.

Glutamate and Skeletal Muscle Pain

Glutamate is an amino acid heavily involved in skeletal muscle metabolism and is also the major excitatory neurotransmitter in the mammalian central nervous system (CNS) (Conn 2003; Julio-Pieper et al. 2011; Robinson and Coyle 1987). As mentioned, glutamate is involved in the activation and sensitization of nociceptive pathways, and its extracellular concentrations are very low compared to its intracellular concentrations (Bergstrom et al. 1974). High extracellular glutamate concentrations can also cause neural or peripheral toxicity and have been associated with migraines, glaucoma and cancer (Dreyer et al. 1996; Dröge et al. 1988; Tapiero et al. 2002; Vaccaro et al. 2007).

In skeletal muscle, glutamate is the most abundant amino acid and has the highest intracellular to extracellular concentration gradient of all the amino acids (Bergstrom et al. 1974; Newsholme et al. 2003). While no difference in glutamate distribution between muscle type has been demonstrated in humans, it has been demonstrated that glutamate concentration is higher in more oxidative than glycolytic rat skeletal muscle (Engelen et al., 2004; Essen-Gustavsson & Blomstrand, 2002; Turinsky & Long, 1990). Within the myofibre, glutamate is a precursor for glutathione synthesis and plays a role in the TCA cycle (Rutten et al. 2005).

Extracellularly, glutamate activates N-methyl-D-aspartate (NMDA), α-amino-3-hydroxy-5-methyl-4-isoxazoleproprionic acid (AMPA), metabotropic glutamate (mGlu) and kainate receptors, all of which are expressed in the CNS as well as the periphery (Bleakman, Alt, and Nisenbaum 2006; Omote et al. 1998). Enhanced glutamate release acting on these peripheral receptors has been suggested to contribute to nociceptive signalling and pain perception (Bleakman et al. 2006; Omote et al. 1998). Much research has gone into investigating the role of interstitial glutamate in skeletal muscle pain pathology, in particular in cases where there is no obvious physical explanation for the pain. In human patients with chronic Achilles pain but no inflammation, interstitial glutamate concentrations were significantly elevated compared to patients without chronic pain (Alfredson et al. 1999). In support, Gerdle et al. (2014) demonstrated elevated interstitial glutamate levels in the trapezius muscle of patients with chronic widespread pain compared to patients without pain. Furthermore, glutamate injections into human skeletal muscle have been demonstrated to cause a significantly greater pain response than saline injections (Castrillon et al. 2012; Svensson et al. 2003). Glutamate-induced muscle pain has also been demonstrated in rats, with female rats exhibiting a greater response to pain than males (Cairns et al., 2002, 2007). Collectively, these studies suggest that elevated interstitial glutamate plays a role in skeletal muscle pain pathology.

The Physiology of Muscle Nociception

Nociception and pain perception, though closely related and often used interchangeably, are not the same. Nociception refers to the neural encoding of anticipated or actual tissue damage, whereas pain refers to the subjective response to the anticipated or

actual harm (IASP 2012). This distinction makes nociception, but not pain perception, observable in anaesthetized animals (Mense 1993). Muscle pain differs from cutaneous pain in many ways. Muscle pain is often described as aching or cramping, whereas cutaneous pain is described as sharp, pricking or burning (Mense 1993). Additionally, in contrast to cutaneous pain, it is common that muscle pain is difficult to localize or is referred to surrounding tissues (Mense 1993). It is generally believed that nociceptor density is the greatest in superficial tissues and decreases in deeper tissues (Craig and Kniftki 1985; Hoheisel and Mense 1990). Nociceptors are free nerve endings that react to noxious stimuli and relay nociceptive information to the CNS. The typical location of these free nerve endings within skeletal muscle is embedded in the surrounding arterioles or within the connective tissue surrounding the myofibre (Stacey 1969). Nociceptors in skeletal muscle have different activation thresholds and fire between 0.3–30 m/s (Mense 1993). The two major types of nociceptive nerve fibres are A-δ (group III) and C (group IV). A-δ fibres are thinly myelinated and have a smaller receptive field than C fibres. They are responsible for the initial perception of pain. C fibres are unmyelinated and relay information slower than A-δ fibres but provide information on pain intensity. Nociceptive stimuli depolarize first order neurons, causing an action potential to be fired and information to be relayed to the CNS. It is here that the stimulus is perceived as noxious (painful) or innocuous. Nociceptive stimuli can be mechanical (i.e. stretch), thermal (i.e. temperature changes) or chemical (i.e. elevations in noxious substances, such as glutamate).

Introduction to Statin Associated Muscle Symptoms

The 3-hydroxy-3-methyl-glutaryl coenzyme A (HMG-CoA) reductase inhibitors, commonly known as statins, are one of the most widely prescribed medications worldwide (IMS

Institute for Healthcare Informatics 2017). By competitively blocking the enzyme HMG-CoA reductase from binding to HMG-CoA, statins inhibit the mevalonate pathway in the liver, effectively reducing cholesterol biosynthesis and subsequently, circulating cholesterol levels (Hunninghake 1992). Concurrently, many peripheral tissues, including skeletal muscle, upregulate low density lipoprotein (LDL) cholesterol receptor expression, which further reduces the amount of cholesterol in circulation (Istvan and Deisenhofer 2001; Yokoyama et al. 2007). Statins have been demonstrated very effective for primary and secondary prevention of cardiovascular disease, as well as for prevention of cardiovascular and all-cause mortality (De Backer et al. 2004; Descamps et al. 2012; Ong 2005; Stone et al. 2014). In addition to reducing blood cholesterol, statins provide a number of pleiotropic benefits including improved endothelial function, mobilization of endothelial progenitor cells, stabilization of atherosclerotic plaques and reduced thromboembolism (Zhou and Liao 2010).

Though generally well tolerated, statin associated muscle symptoms, or SAMS, are the most common adverse side effect of treatment and have been demonstrated to be prevalent in up to 29 percent of statin users (Rosenson et al. 2014). These symptoms range from muscle pain/weakness/soreness (myalgia) and muscle damage (myopathy) to rare but extreme cases of rhabdomyolysis (Ramkumar, Raghunath, and Raghunath 2016; Toussirot, Michel, and Meneveau 2015). Of the SAMS, statin myalgia is by far the most common (Ramkumar et al. 2016). The origin and mechanism(s) of statin myalgia are ambiguous, given that there is often no obvious physical explanation for the pain. The current guidelines for the treatment of statin myalgia include reducing medication dose or changing the type of statin prescribed. SAMS and statin myalgia have been demonstrated to be more prevalent in users prescribed lipophilic

statins (Bruckert, Hayem, Dejager, Yau, & Bégaud, 2005; Dale, White, Henyan, Kluger, & Coleman, 2007; Jordon C. Irwin, Fenning, & Vella, 2020; Kaufmann et al., 2006; McKenney, 2003; Taha, De Moor, Barrett, & Gershkovich, 2014). The lipophilic statins (atorvastatin, simvastatin, lovastatin, fluvastatin, pitavastatin and cerivastatin) pass through cell membranes more easily and are less readily excreted by the renal system, thus they remain in circulation for a longer period of time and have a greater opportunity to become toxic (Ward, Watts, and Eckel 2019).

There are many hypotheses as to the mechanism(s) of SAMS including: altered mitochondrial metabolism, reduced serum vitamin D and coenzyme Q10 levels, impaired calcium homeostasis, genetic polymorphisms and elevated extracellular glutamate (Banach et al. 2015; Bouitbir et al. 2011, 2012, 2016; Brunham et al. 2012; Camerino et al. 2017; DeGorter et al. 2013; Kaufmann et al. 2006; Kwak et al. 2012; Michalska-Kasiczak et al. 2015; Morrison et al. 2016; Rebalka et al. 2019). Evidence for these mechanisms investigated in randomized-placebo controlled trials, however, often present as equivocal. Many investigations have demonstrated that statin prescription is associated with reductions in serum coenzyme Q10 levels, but coenzyme Q10 supplementation has little or no effect on SAMS (Bookstaver, Burkhalter, and Hatzigeorgiou 2012; Rott et al. 2016; Young et al. 2007). This could be because intramuscular coenzyme Q10 concentrations remain unchanged with statin treatment (Busanello et al. 2017; Camerino et al. 2017). Similar findings have been demonstrated with vitamin D supplementation (Eisen et al. 2014; Khayznikov et al. 2015; Kurnik et al. 2012).

It is widely accepted that statins alter skeletal muscle mitochondrial metabolism through reduced respiration and increased ROS production (Allard et al. 2018; Bouitbir et al.

2011, 2016; Busanello et al. 2017; Dohlmann et al. 2019; Rebalka et al. 2019), but the mechanism(s) of how altered mitochondrial metabolism leads to SAMS is yet to be fully elucidated.

Investigating Statin Associated Muscle Symptoms in a Rodent Model

In an attempt to elucidate the mechanism(s) behind SAMS, many different rodent models have been used. Studies differ by the type and dose of statin administered, treatment length and rodent gender and breed.

A time course study that treated female Wistar rats with 80 mg/kg/day of simvastatin evaluated muscle symptoms and necrosis at different time points throughout treatment (Westwood et al. 2005). Rats showed no muscle necrosis at any time point up to day 10 of treatment. By treatment day 12 and after, rats had muscle necrosis, elevations in serum creatine kinase and reduced bodyweight. These findings are corroborated in two follow-up studies in which female Wistar rats were treated with 80 mg/kg/day simvastatin or 150 mg/kg/day rosuvastatin (Sidaway et al. 2009; Westwood et al. 2008).

In another time course study, Schaefer et al. (2004) dosed female Sprague-Dawley rats with 0.1, 0.5 or 1.0 mg/kg/day cerivastatin and observed no histological changes on treatment day five or 10. They did, however, see histological changes by day 15. In combination, the findings of these time course studies suggest that a minimum 10 days of statin treatment is required before muscle necrosis presents. They also suggest that the type and dose of statin treatment is less influential than treatment length when inducing myopathy.

Similar to the findings in humans, multiple investigations have confirmed that statins induce oxidative stress in rat skeletal muscle. Measures of oxidative stress include

mitochondrial swelling, increased H_2O_2 production, reduced GSH/GSSG and reduced mitochondrial respiration (Bouitbir et al. 2011, 2012, 2016; La Guardia et al. 2013; Kaufmann et al. 2006; Sirvent et al. 2005).

All the models discussed in this section thus far have been rodent models for statin myopathy. There is currently a gap in the literature in terms of assessing the mechanism(s) for statin myalgia in a rodent model. As myalgia is the most common SAMS demonstrated in humans (Ramkumar et al. 2016), addressing this knowledge gap is of great importance. Recent investigations *in vitro* by Rebalka et al. (2019) provided insight into a potential mechanism of statin myalgia.

The Glutamate Hypothesis for Statin Myalgia

Following statin treatment *in vitro*, Rebalka et al. (2019) demonstrated that both murine and human-derived myotubes have elevated ROS production, extracellular glutamate and xCT protein content compared to untreated myotubes. The authors propose that this elevation in extracellular glutamate is caused by increased xCT activity and is the mechanism for statin myalgia. Statins have been demonstrated to reduce mitochondrial respiration and increase ROS production in both rats and humans (Allard et al. 2018; Bouitbir et al. 2011, 2016; Busanello et al. 2017; Dohlmann et al. 2019; Rebalka et al. 2019). Thus, it is hypothesized that xCT transporter content increases in order to upregulate certain antioxidant defenses, in particular GSH synthesis. Concurrent cystine import and glutamate export, therefore, elevates extracellular glutamate where it can activate and sensitize nociceptors. Rebalka et al. (2019) further supported their hypothesis that xCT is responsible for glutamate extrusion following

statin treatment by blocking the transporter with sulfasalazine; a pharmacological inhibitor of xCT. When xCT activity was blocked, statin-induced elevations in extracellular glutamate were not demonstrated. Importantly, this full mechanism proposed by Rebalka et al. (2019) (Fig. 2) offers an explanation for statin associated muscle pain in the absence of damage. While this model provides very valuable insight into a potential mechanism for statin myalgia, translation to an *in vivo* model is imperative to fully elucidate its implications (i.e. the induction of pain).

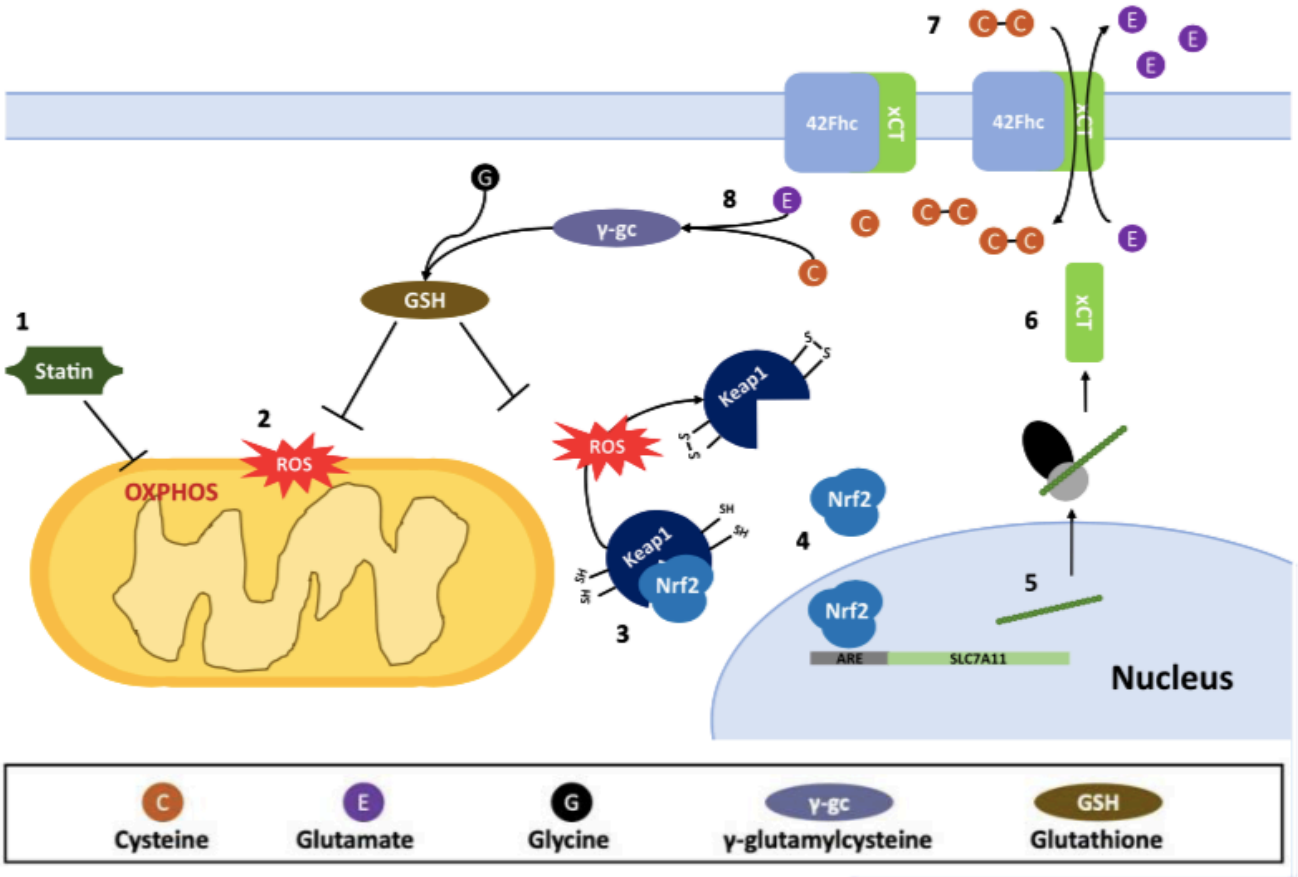

Figure 2: Proposed mechanism of statin associated myalgia. (1,2) Statin treatment impairs mitochondrial respiration which results in increased ROS production. (3) Under typical conditions, Kelch-like ECH-associated protein-1 (Keap1) targets transcription factor nuclear factor erythroid 2-related factor 2 (Nrf2) for degradation. (4) Oxidation of Keap1 by ROS results in the accumulation and nuclear translocation of transcription factor Nrf2. (5,6) Binding of Nrf2 to the antioxidant response element (ARE) increases xCT transcript expression and expression on the cell membrane. (7) Imported cystine (C-C) is reduced to cysteine and glutamate is released as a result, making glutamate available to bind to peripheral nociceptors and cause pain. (8) Cysteine is used in the synthesis of glutathione. Figure description and schematic derived and taken from Rebalka et al. (2019).

The Interstitium and Skeletal Muscle Microdialysis

Compartments within the human body are often described in a binary fashion; metabolites are either intracellular or extracellular. This binary classification fails to discriminate between compartments that exist within the extracellular environment, in particular, the interstitium (the fluid filled space that exists between cells). Though often neglected in mammalian physiology, this space plays an important role in numerous physiological functions and processes, including nociceptive pathways and pain perception. While nociceptive glutamate receptors are highly concentrated in the CNS, they also exist in the periphery, including in the skeletal muscle interstitium (Cairns and Dong 2008; Julio-Pieper et al. 2011; Zhu et al. 2020). Skeletal muscle microdialysis is used to collect the fluid in this space (interstitial fluid), which can then be tested for metabolites of interest.

Skeletal muscle microdialysis involves the insertion of a small, semipermeable probe in parallel to the myofibres of the muscle belly. The microdialysis tube length varies depending on the size of the muscle analyzed. The semipermeable microdialysis probe consists of two impermeable plastic ends, with a permeable plastic piece fitted between (Fig. 3). The permeable portion remains between the muscle fibres during sample collection. The pore size of this membrane can vary depending on the metabolite of interest. For example, a probe with a pore cut-off size of 6000 Da would be used to prevent any metabolite/protein larger than this size from being collected. During sample collection, saline, or a solution that closely mimics the interstitial fluid, is perfused though the microdialysis probe at a very slow flow rate (typically ranging from 2–5 μL/min)(Flodgren et al. 2010; Gerdle et al. 2014; Maggs et al. 1995; Miller et

al. 2004). This allows metabolites in the interstitial fluid to diffuse into the solution being perfused through the microdialysis probe and be collected for analysis (Fig. 3).

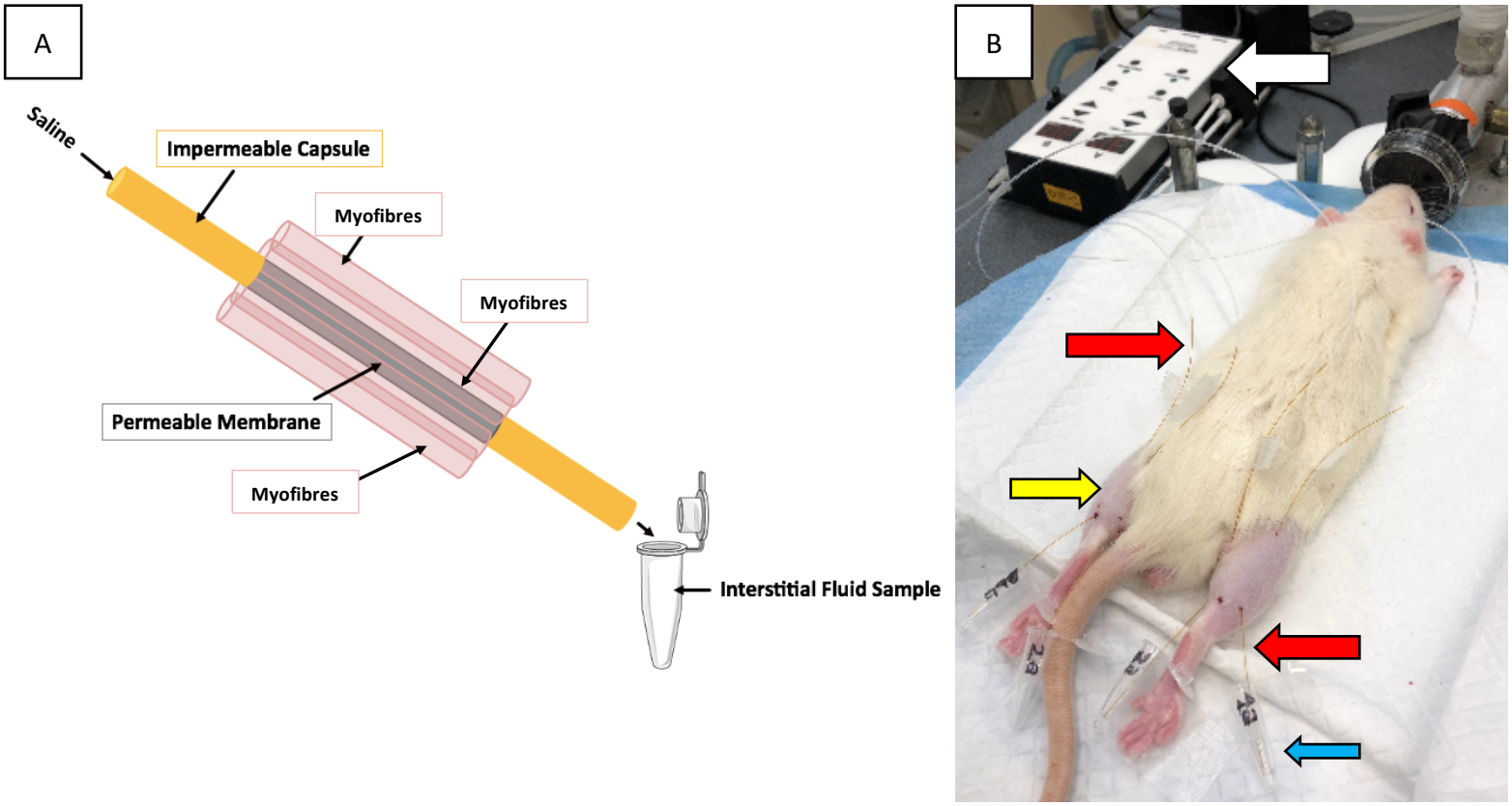

Figure 3: Schematic of skeletal muscle microdialysis probe insertion and visual of *in vivo* skeletal muscle microdialysis interstitial fluid collection. (A) The microdialysis probe (orange and grey) sits in parallel to the myofibres (pink) so that the permeable portion (grey) is in contact with the interstitium. Saline is perfused through the microdialysis probe so that metabolites in the interstitium can diffuse in it and be collected for analysis. (B) Demonstration of interstitial fluid collection *in vivo*. Selected highlighted components include the perfusion pump (white arrow), where the permeable portion of the microdialysis probe rests in the muscle belly (yellow arrow), the impermeable portions of the microdialysis tubing (red arrows), and the sample collection tube (blue arrow).

Importantly, microdialysis probe insertion does not largely disrupt the surrounding myofibre environment (Maclean, Vickery, and Sinoway 2001) (Fig. 4). To account for the small disturbances, a minimum washout/equilibration period of 45 minutes is undergone prior to sample collection (Maclean, Vickery, & Sinoway, 2001). The technique of skeletal muscle microdialysis is important for investigating the mechanisms of statin myalgia because it allows for collection and analysis of the metabolites that exist in the environment where nociceptors are activated and sensitized.

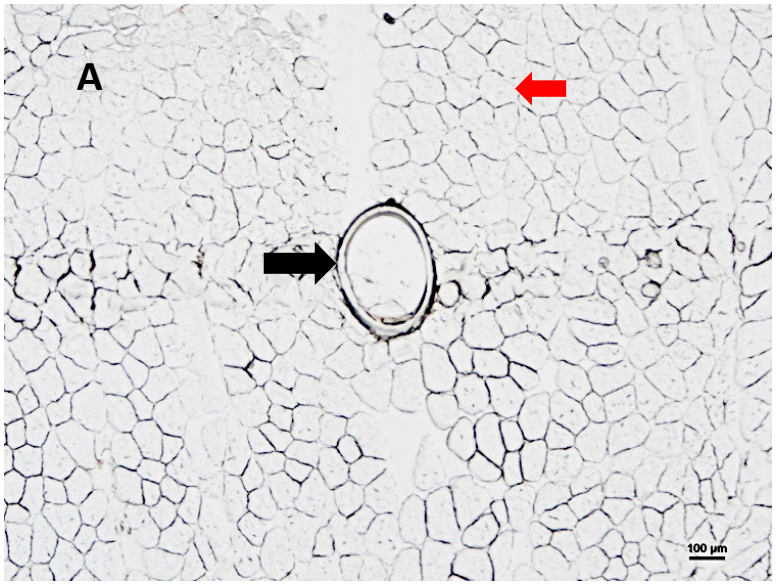

Figure 4: Cross sectional representation of microdialysis probe insertion. The microdialysis probe (black arrow) sits in parallel to the muscle fibres (red arrow) and does not largely disrupt the surrounding environment. Image acquired with 90i Eclipse Microscope (Nikon, Inc.). Scale bar represents 100 μm.

Study Objectives

In spite of the evidence that statins alter skeletal muscle metabolism (Allard et al. 2018; Dohlmann et al. 2019; Morville et al. 2019; Rebalka et al. 2019), they are widely prescribed because of their cardiovascular benefits. The current consensus is that the positive cardiovascular effects of statins outweigh the negative muscular effects (Pinal-fernandez et al. 2018), therefore, many statin users suffer from muscle pain daily. Identifying the underlying causes of SAMS will improve statin adherence and effectiveness. Additionally, certain subsets of the population, such as those prescribed multiple pharmaceuticals and those who engage in very vigorous physical activity seem to be at a greater risk for SAMS (Marot et al. 2011; Ozdemir et al. 2000; Parker et al. 2012; Yeter et al. 2007). The current consensus, therefore, may be particularly dangerous in a subset of people. While statin myalgia is the most prevalent of all SAMS, investigations into its mechanism(s) are the least represented in the literature. Addressing this knowledge gap has implications for millions of statin users worldwide. The aim of the studies detailed herein was to translate the *in vitro* glutamate hypothesis for statin myalgia (Rebalka et al. 2019) to an *in vivo* model using the technique of skeletal muscle microdialysis. We hypothesized that glutamate would be elevated in the interstitial space of rat skeletal muscle following 10 days of statin treatment.

Determining a Rodent Model to Investigate Glutamate as a Mechanism Underlying Statin Myalgia

Allyson Schweitzer, Irena Rebalka, Zachary Kroezen, Meera Shanmuganathan, Philip Brtiz-McKibbon and Thomas Hawke

Department of Health Sciences, McMaster University, Hamilton, Ontario, Canada, L8S4L8

Introduction

Skeletal muscle is a dynamic tissue that constantly responds to changes in its intracellular and extracellular environment. The fully functional muscle is comprised of tens to hundreds of muscle fibres (myofibres) bundled together with blood vessels from the circulatory system and peripheral nerve fibres from the nervous system. Skeletal muscle requires constant innervation from the nervous system for contraction and voluntary movement to occur. It also requires constant blood supply because of its high metabolic demand. The circulatory system supplies oxygen and nutrients to the myofibres. To sustain the metabolic demands of muscle contraction, these nutrients are converted to energy in the form of ATP. The majority of ATP is produced through oxidative phosphorylation (Leninger 1964; Ribas et al. 2014; Tzagoloff 1982). This takes place at the ETC on the inner membrane of the mitochondria.

In addition to ATP production, the mitochondria are also the main creators of ROS in mammalian cells (Hoye et al. 2008; Li Li Ji et al. 1992; Venditti et al. 2013). These ROS are created when electrons leak during transfer between complexes in the ETC and react in the surrounding oxygen-rich environment (Dykens and Will 2008). Here they form highly reactive radicals, such as O_2^-, that readily react and oxidize proteins, lipids and nucleic acids (Dykens and Will 2008; Ribas et al. 2014). Though essential to proper cellular functioning, if accumulated, ROS can cause irreversible damage and/or cell death. To ensure they do not accumulate within the mitochondria or the cytoplasm, many cellular antioxidants exist to abate ROS. Two of the most potent are the SOD enzymes and GSH and its associated enzymes.

The SOD enzymes consist of SOD1, found in the cytosol, SOD2, found in the mitochondria and SOD3, found in the extracellular space (Miao and St. Clair 2009). These

enzymes convert O_2^- to the less reactive ROS, H_2O_2 (Dykens and Will 2008; Fridovich 1995). If accumulated, however, H_2O_2 can also be quite dangerous. Glutathione peroxidase, therefore, helps to abate this accumulation by converting H_2O_2 to water using GSH as a substrate (Dykens and Will 2008; Ribas et al. 2014). Additionally, GSH is able to reduce O_2^- or other target molecules through its subsequent oxidation to GSSG (Ross 1988; Shan et al. 1990; Yang et al. 2014). Glutathione reductase then recycles GSSG back to GSH (Kelner and Montoya 2000) (Fig. 1). The GSH to GSSG ratio (GSH/GSSG) is a common indicator of cellular oxidative stress; a smaller ratio indicating higher oxidative stress.

The rate limiting substrate for GSH synthesis is cysteine (Combs and Denicola 2019; Ishii et al. 1987; Ribas et al. 2014), not to be confused with its oxidized form, cystine. During periods of high oxidative stress, the need for cysteine is augmented to meet the elevated GSH production demand. Cysteine is not readily produced in the myofibre and therefore must be brought in from the extracellular environment in its oxidized form (cystine) through the xCT transporter (Combs and Denicola 2019; Ishii et al. 1987; Ribas et al. 2014). Once inside the cell, cystine is reduced to cysteine. Elevated xCT transporter activity and protein expression have been demonstrated to play a role in maintaining cellular homeostasis during periods of oxidative stress (Banjac et al. 2008; Gu et al. 2017; Martin and Gardner 2015; Sato et al. 2005; Siska et al. 2016; Sleire et al. 2015; Sayin et al. 2017). Adaptive xCT transporter activity can become problematic, such as in the cancer cells, in which elevated activity makes cells more resistance to cell death (Guo et al. 2011; Sugano et al. 2015). It has also been suggested that elevated xCT transporter activity in cancer cells may be linked to cancer induced bone pain (Ungard et al. 2019, 2014; Zhu et al. 2020).

The xCT transporter is an antiporter that extrudes one glutamate for every cystine that is brought into the cell (Rutten et al. 2005). Glutamate is an amino acid heavily involved in skeletal muscle metabolism, but is also the most abundant excitatory neurotransmitter in the CNS (Conn 2003; Julio-Pieper et al. 2011; Robinson and Coyle 1987). When in high concentrations extracellularly, glutamate has been suggested to activate and sensitize nociceptive signalling and pain perception (Bleakman et al. 2006; Omote et al. 1998). Thus, Ungard et al. (2019) propose that the increase in xCT transporter activity in cancer cells leads to elevated extracellular glutamate, nociceptor activation and pain perception.

In the interstitium of skeletal muscle, glutamate concentration has been demonstrated to have similar positive correlations to pain (Alfredson et al. 1999; Cairns et al. 2002; Castrillon et al. 2012; Gerdle et al. 2014; Svensson et al. 2005). Furthermore, injections of glutamate into skeletal muscle have been demonstrated reliable at evoking a pain response in humans and rats (Cairns et al. 2002; Castrillon et al. 2012; Shimada et al. 2016; Svensson et al. 2003) and elevated interstitial glutamate have been demonstrated in patients with chronic pain and fibromyalgia (Alfredson et al. 1999; Sarchielli et al. 2007). Importantly, these pathologies involve pain perception in the absence of any cellular damage. This combinative evidence led to the hypothesis that xCT transporter activity and glutamate may play a role in statin myalgia.

Statins, known formally as the 3-hydroxy-3-methylglutaryl coenzyme-A (HMG-CoA) reductase inhibitors are one of the most widely prescribed medications worldwide (IMS Institute for Healthcare Informatics 2017). Statins competitively block the enzyme HMG-CoA reductase in the liver and inhibit cholesterol biosynthesis, effectively reducing the amount of total and LDL circulating cholesterol (Hunninghake 1992). This has numerous positive vascular

effects including stabilized atherosclerotic plaques, reduced thromboembolism and improved endothelial function (Zhou and Liao 2010). Importantly, statins reduce one's risk for cardiovascular and all-cause mortality (De Backer et al. 2004; Descamps et al. 2012; Ong 2005; Stone et al. 2014).

Though generally well tolerated, statin associated muscle symptoms (SAMS) present in up to 29 percent of statin users (Rosenson et al. 2014). Symptoms include myalgia, myositis, myopathy and in extreme cases rhabdomyolysis. The most common of these symptoms by far is myalgia (Ramkumar et al. 2016), referred to as statin myalgia. Statin myalgia commonly presents without clinical signs of muscle damage, making the discovery of its origin and treatment very difficult. While many different models exist in the literature for statin myopathy, there is currently no rodent model for statin myalgia that we are aware of. Recently, our lab published an *in vitro* model for statin myalgia that focused on elevated xCT transporter activity and interstitial glutamate (Rebalka et al. 2019). The authors showed that both human and murine myotubes treated with statins have increased mitochondrial ROS production, xCT transporter protein expression and extracellular glutamate concentration compared to untreated myotubes (Rebalka et al. 2019) (Fig. 2). It is hypothesized that the elevation in extracellular glutamate is responsible for the pain that is felt in statin myalgia. Importantly, this mechanism offers an explanation for pain in the absence of damage.

The current studies aimed to determine if this *in vitro* model could be replicated *in vivo*. To collect the interstitial fluid from between the myofibres, where glutamate is anticipated to be elevated, skeletal muscle microdialysis was employed. This technique involves the insertion

of a very small, semipermeable microdialysis probe into the muscle belly. The probe consists of two impermeable plastic ends and a permeable plastic piece fitted between (Fig. 5).

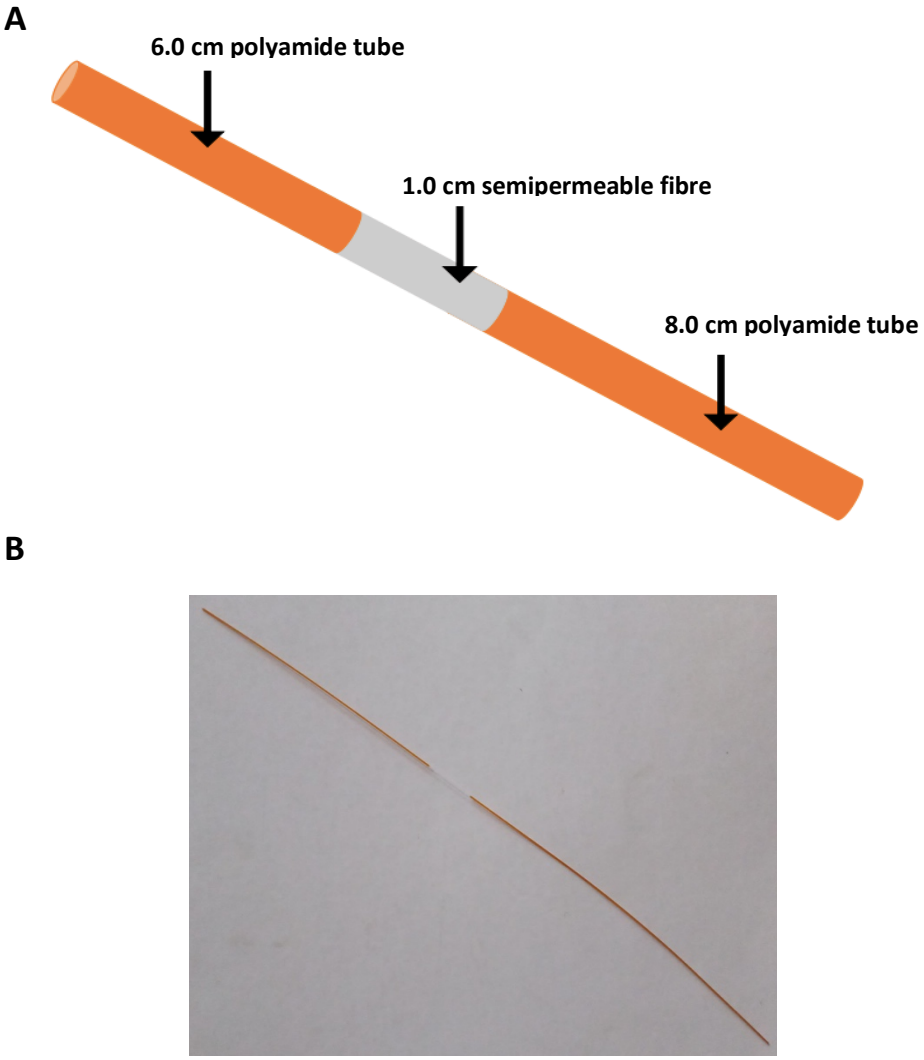

Figure 5: Microdialysis probe construction. (A) Microdialysis probes were constructed using permeable fibres, cutoff weight 6000 Da (grey) and polyamide tubing (orange). Polyamide tubes were cut to lengths of 6.0 and 8.0 cm. Permeable fibres were inserted into the polyamide tubes and glued so that 1.0 cm remains exposed. (B) Image of constructed microdialysis probe.

The permeable portion of the probe rests within the muscle belly, in parallel and in contact with the myofibres (Fig. 3). Importantly, the insertion of the microdialysis probe does not largely disrupt the surrounding cellular environment (Maclean et al. 2001) (Fig. 4). Saline is perfused through the probe at a very slow flow rate, allowing the metabolites that exist in the interstitial space to be collected through passive diffusion.

Statin myalgia is the most prevalent of the SAMS, yet investigations into its mechanism(s) lack representation in the literature. Addressing this knowledge gap has implications for millions of statin users worldwide. The current studies were the first attempt at creating a rodent model for statin myalgia and were based on Rebalka et al.'s (2019) *in vitro* model. We hypothesized that glutamate would be elevated in rat skeletal muscle interstitium following statin treatment.

Section 1

Study One – Cardiotoxin Experiment

1.1 Rationale

Cardiotoxin (CTX) is a toxin isolated from the venom of the red-spitting cobra (*Naga* pallida) (Mahdy 2019). It is used to elicit skeletal muscle damage in experimental animal models through specific binding of the sarcolemma and its subsequent lysis (Mahdy 2019). The specificity, reproducibility and acute response of CTX allows researchers to investigate tissue regeneration, healing and adaptation (Mahdy 2019). The current experiment aimed to induce single-leg, acute myofibre injury to the gastrocnemius of adult female Sprague-Dawley rats via CTX injection, and to assess the associated changes in interstitial glutamate concentrations. Glutamate has the highest intracellular to extracellular concentration gradient of all the amino acids (Bergstrom et al. 1974). Breaking the barrier (the sarcolemma) through CTX injection, would be expected to cause glutamate to leak into the interstitium. We postulated this elevation would be transient given that high extracellular glutamate is toxic to neurons and has been associated with a number of pathologies including migraines, glaucoma and cancer (Dreyer et al. 1996; Dröge et al. 1988; Tapiero et al. 2002; Vaccaro et al. 2007). The current experiment aimed to elucidate whether an elevation in interstitial glutamate in response to a skeletal muscle CTX injection could be captured quantitatively. To increase the likelihood of capturing these changes, sample was collected at three different time points post-CTX injection. 12-, 24- and 48-hours post-injection were chosen because these time points span the time when sarcolemma lysis is high (Hawke and Garry 2001). In addition, this experiment was conducted to determine the upper level/concentration of glutamate that will present in the

skeletal muscle interstitium. We hypothesized that interstitial glutamate concentrations would increase following sarcolemma lysis and that these differences would be capturable between 12- and 48-hours post-injection.

1.2 Methods

Pre-Experimental Procedures

Animals

Female Sprague-Dawley rats (250-300 g) were obtained from Charles Rivers Laboratories, housed in pairs, provided enrichment material and fed a 22/5 (Envigo, Teklad 8640, Mississauga, ON) rodent diet *ad libitum*. Animal housing conditions were maintained at 21°C, 50% humidity and a 12h/12h light/dark cycle. Experimentation was approved by the McMaster University Animal Research Ethics Board in accordance with the Canadian Council for Animal Care guidelines (AUP# 18-02-10). Experiments began following a one-week acclimation period after import.

CTX Injections

Rats were randomly assigned to one of three experimental groups. Treatment group one had skeletal muscle interstitial fluid collected 12-hours post-CTX injection (CTX12, n = 2 animals, 2 probes per animal), group two had skeletal muscle interstitial fluid collected 24-hours post-CTX injection (CTX24, n = 2 animals, 2 probes per animal) and group three had skeletal muscle interstitial fluid collected 48-hours post-CTX injection (CTX48, n = 2 animals, 2 probes per animal). Each rat received an approximate 100 μL injection of 5 μM CTX into their left

gastrocnemius, while the right leg of each animal acted as a control (n = 6 animals, 2 probes per animal).

Microdialysis Probe Construction

Microdialysis probe construction has been previously described (MacLean et al. 1998). Briefly, microdialysis probes were constructed using permeable fibres (Spectrum Laboratories, Laguna, CA) and polyamide tubing. Fibres had a molecular cutoff weight of 6000 Da and polyamide tubing was cut to 6.0 and 8.0 cm lengths. The ends of the hollow fibre were inserted into the polyimide tubing (one end into the 6.0 cm piece and the other end into the 8.0 cm piece) and glued so that 1.0 cm of hollow fibre remained exposed (Fig. 5).

Experimental Procedures

Microdialysis Probe Insertion

12-, 24- or 48- hours post-CTX injection, rats were anaesthetized with isoflurane gas.

Once deemed stable under anesthetic, both hindlegs were shaved and hind paws were taped down, immobilizing and exposing the gastrocnemius. An 18-gauge, curved cannula was inserted rostral-caudal into the gastrocnemius, along the natural orientation of the muscle fibres. Once the cannula was in place, the 8.0 cm end of the microdialysis probe was inserted into the caudal end of the cannula and fed through so that the 6.0 cm portion of the polyamide tubing extended past the paw. Once the microdialysis probe was positioned so that the 1.0 cm hollow

fibre sat within the muscle belly, the 6.0 cm portion of the polyimide tubing was held in place and the cannula was retracted, leaving the microdialysis probe in place (Fig. 3).

Experimental Protocol

Two microdialysis probes were inserted into each triceps surae, one in the lateral gastrocnemius and one in the medial gastrocnemius so that each animal had a total of four probes inserted. Following insertion, microdialysis probes were perfused (microdialysis syringe pump model 102, CMA, Harvard Apparatus Canada) with 0.9% sodium chloride solution at a rate of 2 μL/min. As probe insertion results in some cellular disruption, a 60-minute equilibration period took place before sample collection. 15 minutes were added onto the recommended 45-minute equilibration time to ensure the external environment around the probe had stabilized and any cellular damage had dissipated (Maclean et al. 2001). Following this equilibration period, interstitial dialysate was collected for three 30-minute periods. Interstitial dialysate samples were collected in 0.5 mL Eppendorf tubes. Eppendorf tubes were weighed pre and post dialysate collection to allow for weighing of interstitial fluid and to account for fluctuations in flow rate. Following each 30-minute collection period, dialysate samples were weighed, sealed and stored on ice until the completion of the experiment in which they were stored at -21°C until analysis. Once interstitial fluid collection was complete, animals were euthanized. Left and right gastrocnemius-plantaris-soleus (GPS) muscle complexes were then harvested and bisected longitudinally so that each piece of muscle contained one microdialysis probe. Following bisection, muscle was embedded in optimal

cutting temperature compound (OCT), frozen in isopentane cooled by liquid nitrogen and stored at -80°C for future analysis.

Sample Analysis

Skeletal Muscle Interstitial Fluid Metabolite Quantification

Metabolites were quantified through use of multisegment injection-capillary electrophoresis-mass spectrometry (MSI-CE-MS) as previously described (Saoi et al. 2019). Briefly, analysis was performed on an Agilent 7100 capillary CE instrument (Agilent Technologies Inc., Mississauga, ON, Canada) coupled to an Agilent 6230 Time-of-Flight Mass Spectrometer (TOF-MS; Agilent Technologies Inc.). Due to the purity of the interstitial fluid samples, as a result of the 6000 Da microdialysis probe pore cut-off size, no protein purification was required. Samples were injected neat on the CE uncoated fused-silica capillary with 50 μm inner diameter and 120 cm length (Polymicro Technologies, AZ, USA). Background electrolyte consisted of 1 M formic acid, pH 1.8, with 15% acetonitrile for positive ion mode and 50 mM ammonium bicarbonate, pH 8.5, for negative ion mode. Separations were performed with an applied voltage of 30 kV at 25°C. Data acquisition was performed in full-scan mode on the TOF-MS, spanning a mass range of 50-1700 m/z.

Histology

Muscle (GPS) was sectioned into 6 μm cryosections and air-dried for 30 minutes. Hematoxylin-eosin (H-E) staining was performed following a standard protocol. All images were obtained with a 90i Eclipse Microscope (Nikon, Inc., Melville, NY). Indication of altered myofibre

morphology was assessed visually by presence of mononuclear infiltrate and necrotic myofibres.

Statistics

All statistics were performed using Prism 7 (GraphPad Software, La Jolla, CA). Statistical significance was determined using one-way ANOVA followed by Tukey's multiple comparison post hoc-test. Data presented are mean $\pm$ SEM. Individual points are included for transparency. Statistical significance was defined as $p \leq 0.05$.

1.3 Results

CTX injection induced myofibre necrosis and mononuclear infiltration to the area of injury at all time points post-injection. To determine if CTX injection was successful at eliciting sarcolemma lysis and myofibre injury, H-E staining was completed and analyzed for visual differences in mononuclear infiltrate and necrotic myofibres. All 24- and 48- hour time point animals demonstrated severe necrosis and mononuclear infiltrate in their gastrocnemius (Fig. 6). The 12-hour time point animals both showed mononuclear infiltrate and myofibre necrosis, however, one animal demonstrated a greater area of necrotic myofibres and mononuclear infiltrate than the other. It could only be confirmed in one 12-hour animal, by localization of the microdialysis probe within the muscle sections, that interstitial fluid was collected in an area of damage (Fig 6B). Probe localization in both animals at the 24-hour time point confirmed that interstitial fluid was collected in an area of myofibre damage.

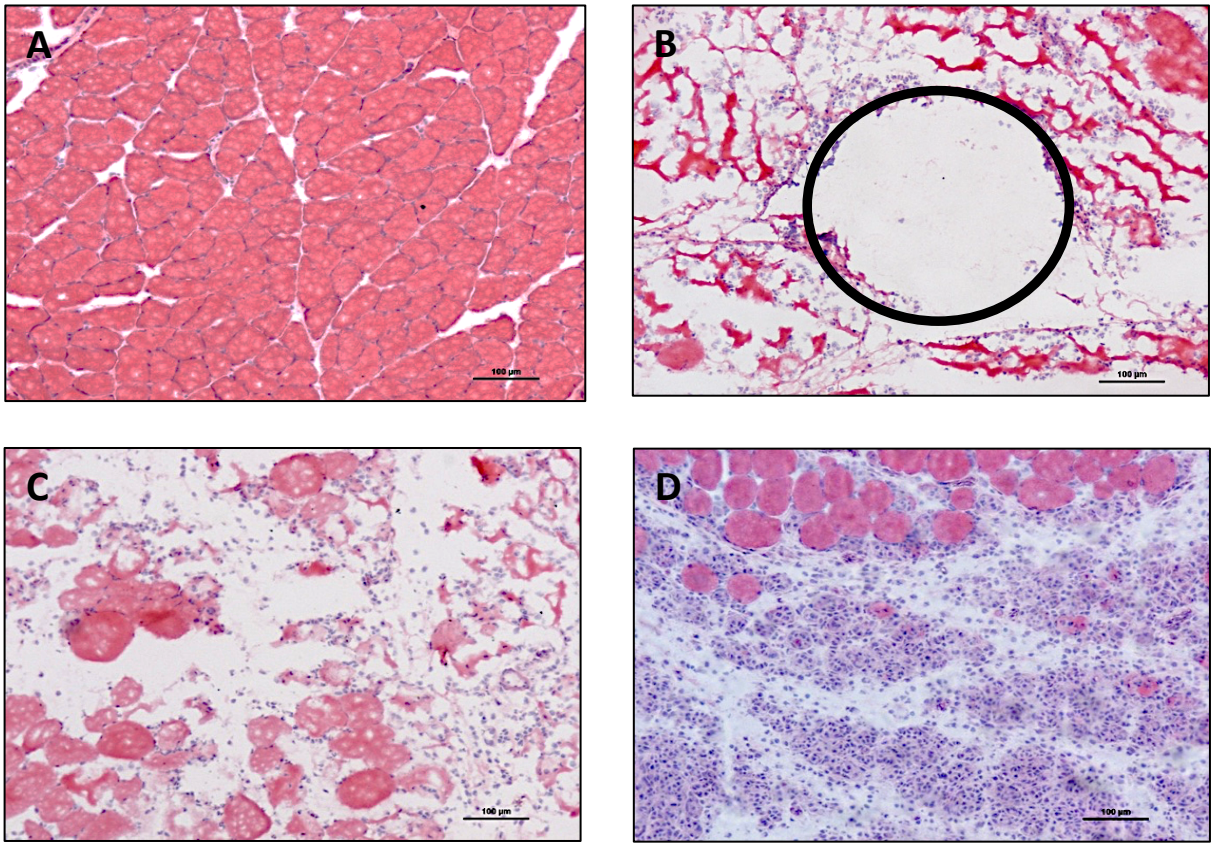

Figure 6: Visual representation of CTX-induced myofibre necrosis and mononuclear infiltrate. As demonstrated visually by H-E staining, mononuclear infiltrate and myofibre necrosis increase in severity with time post-CTX injection. (A) Uninjured leg. (B) 12-hours post-CTX injection. Black circle represents where the microdialysis probe was inserted and confirms fluid was collected in an area of damage. (C) 24-hours post-CTX injection. (D) 48-hours post-CTX injection. Images acquired with 90i Eclipse Microscope (Nikon, Inc.). Scale bars represent 100 μm.

CTX-induced myofibre injury significantly increased interstitial glutamate concentration 24-hours post-injection. Three time points were assessed to determine if glutamate was elevated following CTX injection. No significant differences in interstitial glutamate levels from uninjured legs were demonstrated at the 12- and 48-hour time points (p = 0.96 and 0.86 respectively). At 24-hours post-injection, glutamate was significantly elevated by 28% compared to control (uninjured) values (p = 0.05; Fig. 7). For a full breakdown of all metabolites measured and their respective concentrations see Appendix Table 1.

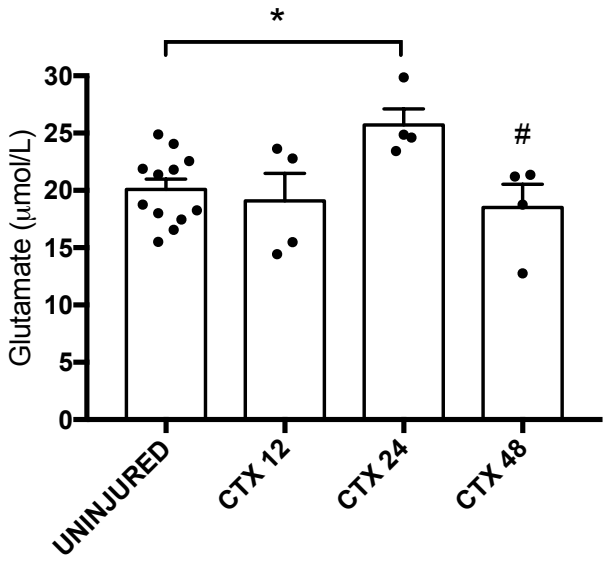

Figure 7: Interstitial glutamate concentration 12-, 24- and 48-hours post-CTX-induced myofibre injury. Glutamate was significantly 28% elevated in the skeletal muscle interstitium 24-hours post-CTX injection. All data are presented as mean ± SEM. Each data point represents sample collected from one microdialysis probe, n = 2-6 animals per group, 4 probes per animal (2 injured + 2 uninjured). * denotes statistical significance from the uninjured leg, # denotes statistical significance from the 24-hour time point. Statistical significance defined as $p \leq 0.05$.

1.4 Discussion/Conclusion

The results of this study confirm that differences in interstitial glutamate can be detected using the technique of skeletal muscle microdialysis. They also offered ~26 μmol/L as the physiological upper limit of interstitial skeletal muscle glutamate concentration (Fig. 7). Note that this number represents a fraction of the concentration of the metabolite that was in the interstitial space since skeletal muscle microdialysis does not provide 100% recovery. *In vitro* recovery rates were demonstrated at ~37%, however, the literature suggests that recovery rates for glutamate in humans at 2 μL/min is ~50% (Hutchinson et al. 2000; Karamouzis et al. 2001; Langberg et al. 1999). This puts the actual physiological upper limit between the range of ~52 and 71 μmol/L. We assume that recovery rates are constant between animals.

Interstitial glutamate was significantly greater in injured skeletal muscle than uninjured skeletal muscle 24-hours post-CTX injection (Fig. 7). We hypothesize this is the result of sarcolemma lysis and subsequent leak from the intracellular pool into the interstitial space. Interestingly, glutamate was not elevated at the 12- and 48-hour time points post-CTX injection, when sarcolemma lysis is clearly evident (Fig. 6). As glutamate is a tightly regulated molecule, we postulate that 48-hours following injury it has likely converted to the less toxic amino acid glutamine and been sequestered by surrounding tissue or cells (Julio-Pieper et al. 2011). It was more puzzling that interstitial glutamate was not elevated 12-hours post-injection, as this is when sarcolemma lysis is in its earliest stages. We suggest the lack of statistical significance at this time point to be the result of methodological error. One of the 12-hour time point animals appeared to have less mononuclear infiltrate and muscle necrosis than the other, and this

animal's interstitial glutamate levels corresponded to the two lowest data points. Therefore, it is likely that interstitial fluid was collected in an area with little myofibre injury, and an underestimation of glutamate concentration was provided. Probe localization was possible in the 12-hour time point animal with elevated interstitial glutamate and it was confirmed that this animal's sample was collected in an area of myofibre injury (Fig. 6B).

The time course design of this experiment strengthens the statement that glutamate is a tightly regulated molecule and further supports the notion that high concentrations in the interstitium are pathological. This study was also the first of its kind, to our knowledge, that assessed skeletal muscle interstitial glutamate levels following CTX-induced damage in a rodent model and provided valuable insight and comparative data for future analyses. A limitation of the current study was that localization of the microdialysis probe within the tissue sample was not always possible, making it impossible to confirm that interstitial fluid was collected in an area of damage in all samples. Additionally, since we did complete an *in vivo* microdialysis probe recovery trial, the true glutamate maximum can only be estimated from assumptions from previous work.

In conclusion, our data demonstrated that differences in glutamate can be captured and measured in the interstitial fluid of rat skeletal muscle and provided a likely physiological upper limit for interstitial glutamate concentration. These data support the use of skeletal muscle microdialysis in a rodent model for statin myalgia.

Section 2

Study Two – Statin Treatment *in vivo* (Nutella)

2.1 Rationale

Myalgia is the most common negative muscular side effect of statin treatment (Ramkumar et al. 2016) but current research offers little explanation for what causes this muscle pain in the absence of damage. Recent investigations *in vitro* by Rebalka et al. (2019) demonstrated that glutamate, a neurotransmitter involved in pain perception, may be implicated in statin myalgia. The authors demonstrated that glutamate is elevated in the extracellular space of human and murine myotubes following statin treatment. It is in this environment surrounding the myofibres that high levels of glutamate can lead to peripheral nociceptor activation and sensitization. The current study was undertaken to translate Rebalka et al.'s (2019) *in vitro* model of statin myalgia (Fig. 2) to an *in vivo* rodent model. Previous studies demonstrated that elevations in skeletal muscle interstitial glutamate can be measured *in vivo* through skeletal muscle microdialysis (Section 1, pages 30-39). As this technique allows for the collection of metabolites in the skeletal muscle interstitium, it was used in the current experiments. There is currently no validated rodent model of statin myalgia that we are aware of. Therefore, rodent strain, statin type and dose and treatment length were tested in this experiment. This experiment aimed to investigate the effects of statin (ATV40), or combination statin and sulfasalazine treatment (SSZ) on interstitial glutamate and xCT transporter content *in vivo*. Based on results from *in vitro* experiments (Rebalka et al. 2019) we hypothesized that interstitial glutamate concentrations would be elevated following statin treatment and that co-treatment with sulfasalazine would attenuate these increases. We also postulated that xCT

transporter content would increase in the skeletal muscle of statin-treated animals to compensate for statin-induced increases in oxidative stress.

2.2 Methods

Pre-Experimental Procedures

Animals

Male, Sprague-Dawley rats (450-500g) were obtained from Charles Rivers Laboratories, housed in pairs, provided enrichment material and fed a 22/5 (Envigo, Teklad 8640) rodent diet *ad libitum*. Animal housing conditions were maintained at 21°C, 50% humidity and a 12h/12h light/dark cycle. Experimentation was approved by the McMaster University Animal Research Ethics Board in accordance with the Canadian Council for Animal Care guidelines (AUP# 18-02-10). Experiments began following a one-week acclimation period after import.

Microdialysis Probe Construction

See Section 1, page 32.

Experimental Procedures

Animals

Male Sprague-Dawley rats were randomly assigned to one of three groups: control, statin treatment (ATV40) or combination statin and sulfasalazine treatment (SSZ). Control animals (n = 5 animals, 4 probes per animal) were fed four grams of Nutella (Fererro S.p.A., Canada). ATV40 animals (n = 5 animals, 4 probes per animal) were fed 40 mg/kg atorvastatin (Jamp Pharma Corporation, Boucherville, QC) mixed into four grams of Nutella. SSZ animals (n = 5 animals, 4

probes per animal) were fed 40 mg/kg atorvastatin (Jamp Pharma Corporation) plus 200 mg/kg sulfasalazine (Salazopyrin; Pfizer Canada, North York, ON) mixed into four grams of Nutella. All animals were fed their respective treatment once per day, for a total of 10 days. On day 10, while anesthetized, interstitial fluid was collected from both gastrocnemius muscles using the skeletal muscle microdialysis technique. Following collection, rats were euthanized, and blood and skeletal muscle were collected and stored appropriately for analysis.

Microdialysis Probe Insertion

Approximately three hours before interstitial fluid collection animals were given their final dose of the appropriate treatment.

For additional microdialysis probe insertion procedures see Section 1, pages 32-33.

Experimental Protocol

See Section 1, page 33.

Sample Analysis

Body Weight

All rats were weighed on a digital scale before treatment commencement and at four time points throughout their treatment.

Skeletal Muscle Interstitial Fluid Metabolite Quantification

Skeletal muscle interstitial metabolites were quantified in the Core Facility at McMaster University through ultra-performance liquid chromatography (UPLC; UPLC Amino Acid Analysis (AAA) Solution, Waters Ltd., ON, Canada)(Waters 2007). Briefly, metabolites within the interstitial fluid samples were separated with the AccQTag Ultra UPLC column and quantified through UV detection.

Western Immunoblotting

OCT was removed from the GPS muscle complex and muscle lysates were prepared as per standard protocols. Briefly, frozen GPS muscle pieces were homogenized with a mortar and pestle and 10 μL of lysis buffer was added per 1.0 mg of tissue. Following low-level sonification for a total of 30 seconds (10 seconds on, 10 seconds off), samples were placed on an orbital shaker at 4°C for one hour. Samples were then centrifuged at 4°C at 12000 rpm for 10 minutes, the supernatant was removed, aliquoted and stored at -80°C for future analysis. A bicinchoninic acid assay (BCA) was run to determine total protein concentration in lysates as per standard protocol.

xCT protein content was quantified following standard SDS-page protocols. Briefly, 10 μL of GPS muscle lysate (preparation described above) containing 10 μg of protein was loaded on a 12% acrylamide gel, transferred to a PVDF membrane (Bio-Rad), blocked with 5% BSA in TBS-T for one hour at room temperature, and incubated with xCT primary antibody (diluted 1:1000 in 5% BSA, Novus Biologicals, Centennial, CO) overnight at 4°C. The appropriate horseradish

peroxidase-conjugated secondary antibody (1:10000, Abcam, cat. No. ab-6721) was incubated for one hour at room temperature and the blot was visualised using Clarity Western ECL solution (Bio-Rad, Mississauga, ON, Canada). Band density was quantified using ImageJ software (National Institutes of Health, MD).

Statistics

All statistics were performed using Prism 7 (GraphPad Software). Statistical significance was determined using a one-way ANOVA followed by Tukey's multiple comparison post hoc test for all data except F-CON and U-CON comparisons. Statistical significance between F-CON and U-CON groups were determined using an unpaired t-test (Fig. 11A). Data presented are mean $\pm$ SEM. Individual points are included for transparency. Statistical significance was defined as $p \leq 0.05$.

2.3 Results

Statin treatment alone did not alter body weight gain. No differences in body weight gain were demonstrated between ATV40 and control animals ($p = 0.33$) from treatment day one to treatment day 10. Control animals gained 37% more weight than SSZ-treated animals ($p = 0.001$), suggesting that in combination, statins and sulfasalazine have a more toxic effect (Fig. 8).

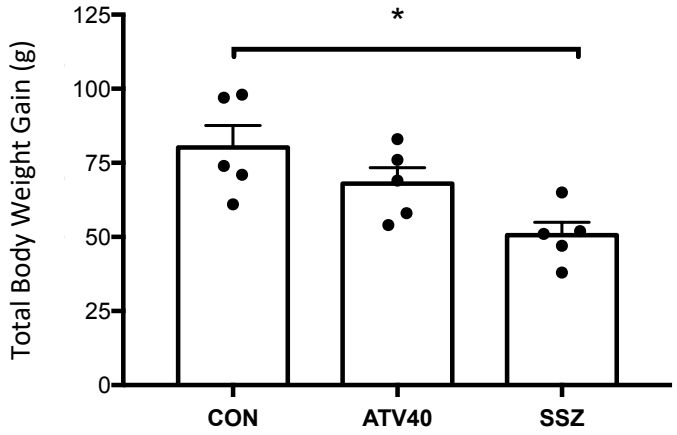

Figure 8: Total body weight gain following 10 days of control, statin or combination statin and sulfasalazine treatment. In rats, combined statin and sulfasalazine (SSZ) treatment caused significantly less weight gain than control treatment. No other significant differences were demonstrated between groups. All data are presented as mean ± SEM. n = 5 animals per group. Control treatment (CON), 40 mg/kg/day atorvastatin treatment (ATV40), 40 mg/kg/day atorvastatin + 200 mg/kg/day sulfasalazine treatment (SSZ). Statistical significance defined as $p \leq 0.05$.

Statin and combination statin and sulfasalazine treatment had no effect on interstitial glutamate concentration in vivo. Following 10 days of control, ATV40 or SSZ treatment, no differences were demonstrated in mean interstitial glutamate concentration between groups ($p = 0.97$; Fig. 9).

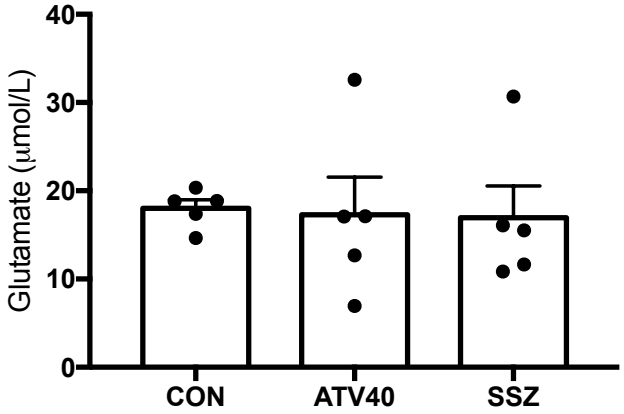

Figure 9: Interstitial glutamate concentrations following 10 days of control, statin or combination statin and sulfasalazine treatment. No significant differences were demonstrated in skeletal muscle interstitial glutamate between treatment groups. All data are presented as mean ± SEM. n = 5 animals per group, average value of all probes. Control treatment (CON), 40 mg/kg/day atorvastatin treatment (ATV40), 40 mg/kg/day atorvastatin + 200 mg/kg/day sulfasalazine treatment (SSZ). Statistical significance defined as $p \leq 0.05$.

Statin and combination statin and sulfasalazine treatment did not affect skeletal muscle xCT transporter content. Following 10 days of control, statin or SSZ treatment, no differences in mean GPS xCT transporter content were demonstrated between treatment groups (p = 0.87; Fig. 10).

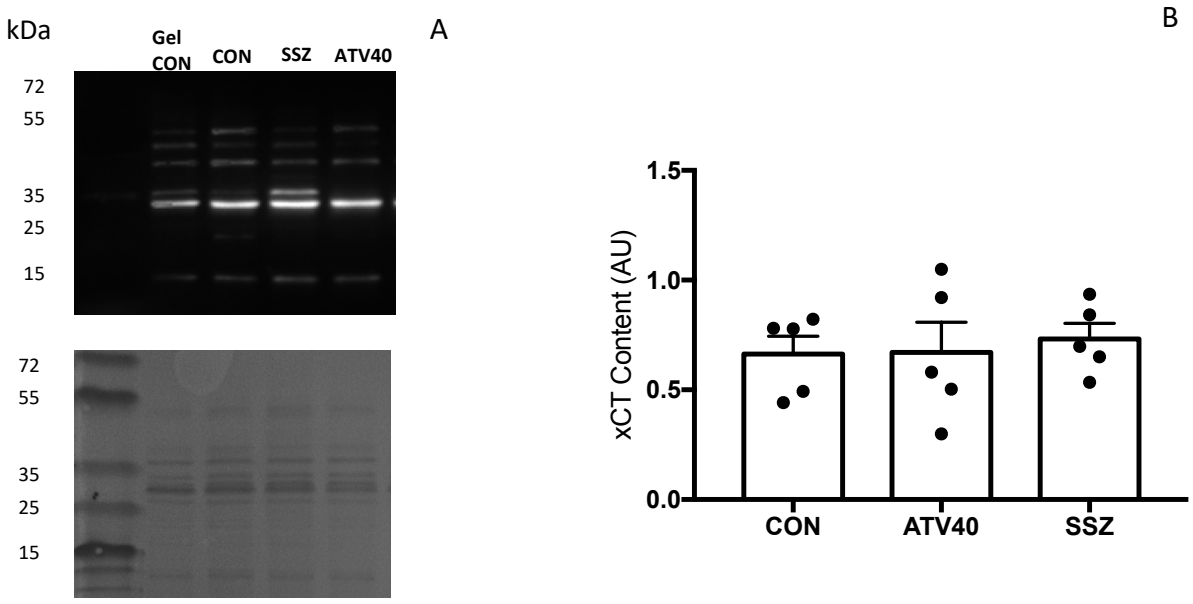

Figure 10: Skeletal muscle xCT transporter content between treatment groups. (A) representative blot (top) and corresponding Amido black loading control (bottom). (B) No significant differences in GPS xCT transporter content were demonstrated between treatment groups. All data are presented as mean ± SEM. n = 5 animals per group. Between gel control sample (Gel CON), control treatment (CON), 40 mg/kg/day atorvastatin treatment (ATV40), 40 mg/kg/day atorvastatin + 200 mg/kg/day sulfasalazine treatment (SSZ).

2.4 Discussion/Conclusion

The findings from the current experiment did not support our hypothesis that statins would elevate interstitial glutamate concentration. A large increase in variability was demonstrated in the ATV40- and SSZ-treated animals compared to control animals. This may be the result of differences in drug metabolism between animals caused by alterations in the

animal's activity, how fast the treatment was consumed and how much food the animal had consumed prior to consuming their drug treatment. All of these factors are more likely to be variable in the treated animals if the drug's side effects are negative (as is anticipated with statin treatment).

Interestingly, when interstitial glutamate levels between control animals fed Nutella and control animals not fed Nutella were compared, significant differences were demonstrated (Fig. 11A). Nutella-fed control animal (F-CON) values were obtained from the current experiment. Unfed control animal (U-CON) values were obtained from a previous CTX pilot experiment. This CTX experiment also offered comparative 24-hour post-CTX injection (CTX24) skeletal muscle interstitial glutamate data for comparison. The control animals from the CTX experiment differed from the control animals from the current experiment by only the fact that they did not receive 10 days of Nutella treatment. F-CON animals had significantly higher skeletal muscle interstitial glutamate levels than U-CON animals (Fig. 11A; $p = 0.005$). Additionally, when F-CON, U-CON and CTX24 interstitial glutamate levels were compared, CTX24 values were significantly greater than U-CON ($p = 0.03$), but not F-CON animals (Fig. 11B; $p = 0.3$). Collectively, these findings suggest that Nutella treatment elevates skeletal muscle interstitial glutamate concentrations.

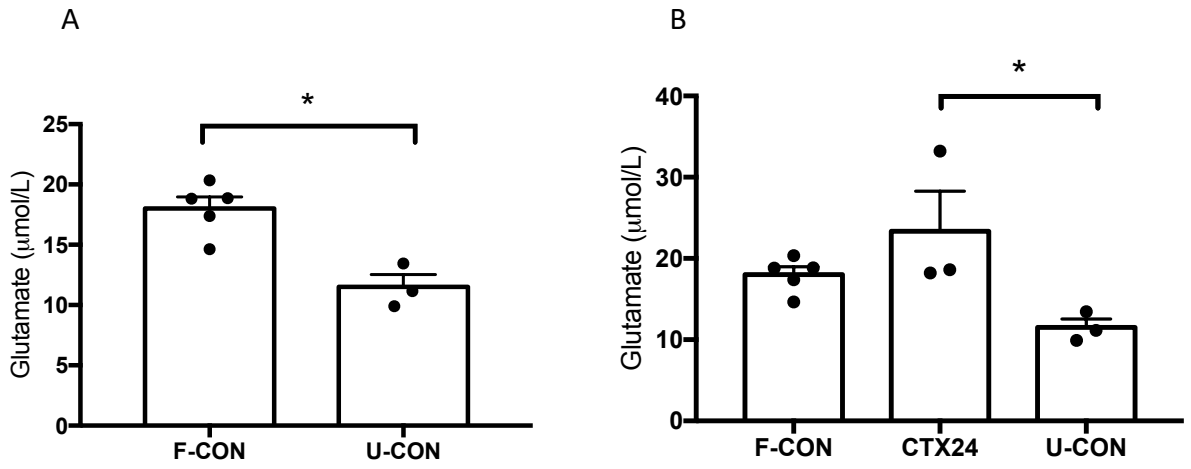

Figure 11: Skeletal muscle interstitial glutamate concentrations between experimental conditions. (A) Nutella-fed control animals (F-CON) had significantly greater interstitial glutamate levels than control animals that did not receive Nutella treatment (U-CON). (B) Interstitial glutamate of CTX injured animals (CTX24) did not significantly differ from F-CON animals but did from U-CON animals. n = 2-5 animals, 1-2 probes per animal. Statistical significance defined at $p \leq 0.05$.

Nutella was chosen as the vehicle to deliver statin treatment to reduce stress and handling that may have been caused by oral gavage treatment. This sweet treat is also completely devoured by rats, which ensured each animal received its entire dose of treatment. The current findings, however, led to further investigation into why Nutella caused elevations in skeletal muscle interstitial glutamate. It was determined that the high sugar content in Nutella may have induced oxidative stress in the skeletal muscle and been responsible for the elevations. Diets containing high sugar content have been demonstrated to increase ROS and

alter redox capacities in both rats and humans (Breinholt et al. 2003; Young et al. 1999). If this is true in our model, Nutella-induced skeletal muscle oxidative stress might have increased xCT transporter activity (Banjac et al. 2008; Sato et al. 2005; Siska et al. 2016; Sleire et al. 2015) and led to elevations in interstitial glutamate. This may also explain why no differences were seen in xCT transporter content between treatment groups (Fig. 10). If Nutella caused oxidative stress and all animals received Nutella regardless of their treatment group, xCT transporter content may be elevated in all groups. Comparative data between fed and unfed xCT transporter content would yield further insight into this hypothesis.

A major limitation of the current study was the small sample size used to compare fed and unfed control animals. Each animal had a total of four microdialysis probes inserted (two per gastrocnemius), and comparison of values within the same animal as well as comparison of values between animals were possible. Between-animal variability tends to be greater than within-animal variability. As data was only available from two unfed control animals, results may be biased.

Given the confounding effects Nutella was found to have, the results of this experiment cannot conclusively answer our research question. They did, however, provide valuable insight on how to alter the model in future experiments, in particular changing the drug delivery vehicle. Another important realization that was made through these experiments was that the Amplex Red Assay kit (A12221, Invitrogen) was not sensitive enough to provide reliable quantification of skeletal muscle interstitial glutamate. This was concluded following the comparison of Amplex Red and UPLC quantified data sets. The control values from the Amplex red data had much more variability than the control values obtained through UPLC (coefficients

of variation of 59% compared to 12% respectively; Fig. 12). Therefore, we decided that all future analysis would be completed using a more sensitive measure.

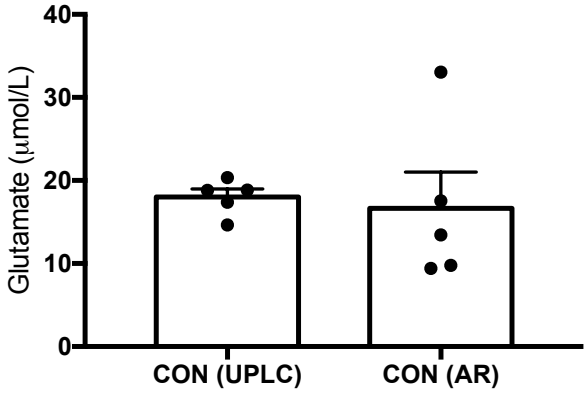

Figure 12: Comparison of UPLC and Amplex Red skeletal muscle interstitial glutamate quantification. Skeletal muscle interstitial fluid samples obtained from the same control animal were analyzed for glutamate with UPLC (CON (UPLC)) or Amplex Red assay kits (CON (AR)). Samples quantified with UPLC presented reduced variability between samples (coefficient of variation of 12%) compared to Amplex Red quantified samples (coefficient of variation 59%). n = 5 animals, average value of all probes.

Section 3

Study Three – Statin Dosing (All-Natural Peanut Butter)

3.1 Rationale

This experiment aimed to elucidate the maximal statin dose that will elicit measurable metabolic changes without inducing myopathy. Doses of 40, 60 and 80 mg/kg/day atorvastatin were chosen, and a treatment length of 10 days remained constant. We hypothesized that 40 mg/kg/day atorvastatin treatment would cause few metabolic changes based on previous data and that 60 mg/kg/day would have larger metabolic effects. We postulated that even with our short treatment length, 80 mg/kg/day of atorvastatin would elicit myopathy in our model as this has been demonstrated in animals treated with similar doses (Bouitbir et al. 2016; Ghalwash, Elmasry, and El-Adeeb 2018; Pierno et al. 2006; Zala, Bhatt, and Rajput 2019).

Results from previous experiments demonstrated that animals fed four grams of Nutella had significantly elevated skeletal muscle interstitial glutamate when compared to animals not fed Nutella (Section 2, page 49). For the current experiment, we chose drug delivery via feeding to reduce the stress and handling experienced by our animals but acknowledged that the confounding factor of Nutella must be removed, therefore, all-natural peanut butter was chosen as the statin vehicle. All-natural peanut butter was chosen due to the simplicity of its ingredients, low sugar content and desirability to be fully consumed by our animals. Additionally, since glutamate must be in very high dietary concentrations to make it past first pass clearance and into the circulation (Julio-Pieper et al. 2011), we believed high protein/amino acid content would not confound our results.

Female rats were used because the literature demonstrates that they are more susceptible to statin myotoxicity (Schaefer et al. 2004). It has also been demonstrated that females have a greater pain response and are more sensitized to elevations in interstitial glutamate in both human and rat models (Cairns et al., 2002; Cairns, Hu, Arendt-Nielsen, Sessle, & Svensson, 2001; Castrillon et al., 2012). Furthermore, the female sex is a well-documented risk factor for SAMS (Mancini et al. 2011). Therefore, we decided a female rodent model would be a better representation of statin myalgia.

3.2 Methods

Pre-experimental Procedures

Animals/Microdialysis Probe Construction

See Section 1, page 32.

Experimental Procedures

Animals

Rats were randomly assigned to one of four treatment groups and fed three grams of all-natural peanut butter (The Kraft Heinz Company, North York, ON) containing their respective treatments. All animals were fed a total of 10 doses over the course of 10 days (one dose per day). Animals treated with statins received 40 (ATV40, n = 1 animal, 4 probes per animal), 60 (ATV60, n = 1 animal, 4 probes per animal) or 80 mg/kg (ATV80, n = 1 animal, 4 probes per animal) of atorvastatin (Jamp Pharma Corporation) mixed into three grams of all-natural peanut butter. Control animals (CON, n = 2 animals, 4 probes per animal) received only three grams of

all-natural peanut butter. On day 10, while anesthetized, interstitial fluid was collected from both gastrocnemius muscles using the skeletal muscle microdialysis technique. Following collection rats were euthanized and blood and skeletal muscle were collected for analysis. Given the extensive time spent under anaesthetic, a heating pad was placed under the body of the rat to minimize heat loss during the procedure.

Microdialysis Probe Insertion

Approximately three hours prior anesthetization, rats were fed their final treatment. Rats remained anaesthetized for the duration of the experiment. For additional microdialysis probe insertion procedures see Section 1, pages 32-33.

Experimental Protocol

See Section 1, page 33, for microdialysis probe insertion and interstitial fluid sample collection/preparation protocol.

Once interstitial fluid collection was complete, animals were euthanized. Left and right GPS muscle complexes were harvested, the soleus was separated, and the gastrocnemius-plantaris complex was cut longitudinally so that each piece of muscle contained one microdialysis probe. Tibialis anterior (TA) and extensor digitorum longus (EDL) were also harvested. Muscles were embedded in OCT, frozen in isopentane cooled by liquid nitrogen and stored at -80°C for future analysis.

Sample Analysis

Body Weight

All rats were weighed on a digital scale before treatment commencement and at four time points throughout their treatment.

Skeletal Muscle Interstitial Fluid Metabolite Quantification

See Section 1, page 34.

Histology

Muscles (gastrocnemius-plantaris, soleus, TA and EDL) were sectioned into 6 μm cryosections and air-dried for 30 minutes. H-E staining was performed using a standard protocol. All images were obtained with a 90i Eclipse Microscope (Nikon, Inc.). Indication of altered myofibre morphology was assessed visually by presence of mononuclear infiltrate and necrotic myofibres.

Statistics

All statistics were performed using Prism 7 (GraphPad Software). Statistical significance was determined using a one-way ANOVA followed by Tukey's multiple comparison post hoc test. Data presented are mean $\pm$ SEM. Individual points are included for transparency. Statistical significance was defined as $p \leq 0.05$.

3.3 Results

Consumption of statin treatment. Control, ATV40- and ATV60-treated animals finished their entire dose of all-natural peanut butter and respective treatments every day. The ATV80-treated animal consumed treatments in full until day seven, in which approximately 75% of the three-gram bolus of all-natural peanut butter with the statin mixed in was consumed. For the duration of treatment (days 8-10) approximately 50% was consumed.

Body weight. All animals gained weight throughout the duration of treatment (Fig. 13).

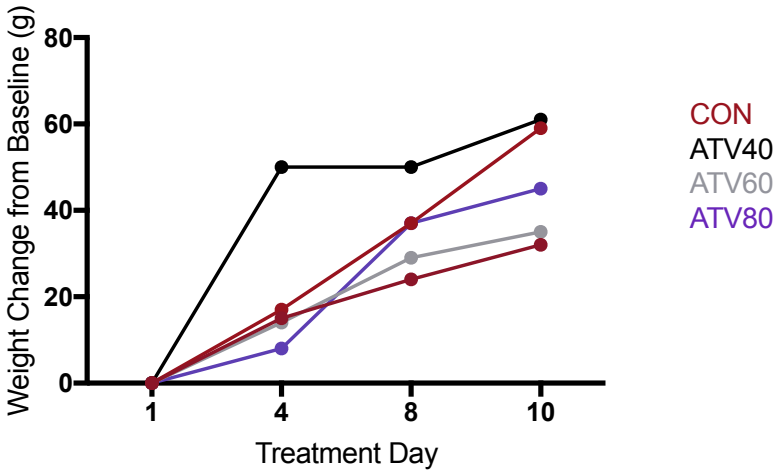

Figure 13: Total body weight gain at days 1, 4, 8 and 10 of control and statin treatment. All animals gained weight throughout the duration of treatment. Control treatment (CON), 40 mg/kg/day atorvastatin treatment (ATV40), 60 mg/kg/day atorvastatin treatment (ATV60), 80 mg/kg/day atorvastatin treatment (ATV80). Each line represents a different animal. Statistical tests were not possible given the small sample size.

Statin treatment did not elevate skeletal muscle interstitial glutamate concentration. No significant differences in interstitial glutamate were demonstrated between treatment groups (Fig. 14). For a full breakdown of all metabolites measured and their respective concentrations see Appendix Table 2.

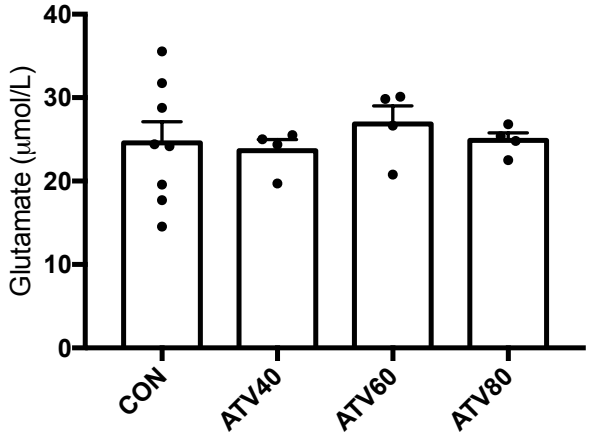

Figure 14: Skeletal muscle interstitial glutamate in control and statin-treated animals. No significant differences were demonstrated in interstitial glutamate between treatment groups ($p = 0.8$). All data are presented as mean $\pm$ SEM. n = 1-2 animals per group, 4 probes per animal. Control treatment (CON), 40 mg/kg/day atorvastatin treatment (ATV40), 60 mg/kg/day atorvastatin treatment (ATV60), 80 mg/kg/day atorvastatin treatment (ATV80).

High dose statin treatment caused mononuclear infiltration in the soleus muscle only. Following 10 days of statin treatment, visual analysis of H-E stained muscle sections showed no mononuclear infiltrate, centrally located nuclei or muscle necrosis in the gastrocnemius-plantaris (Fig. 15), TA (data not shown) or EDL (data not shown) muscle sections in any

treatment group. CON, ATV40 and ATV60 soleus muscle sections elicited no signs of myopathy, but ATV80 soleus sections demonstrated mononuclear infiltrate in both hindlimbs (Fig. 16).

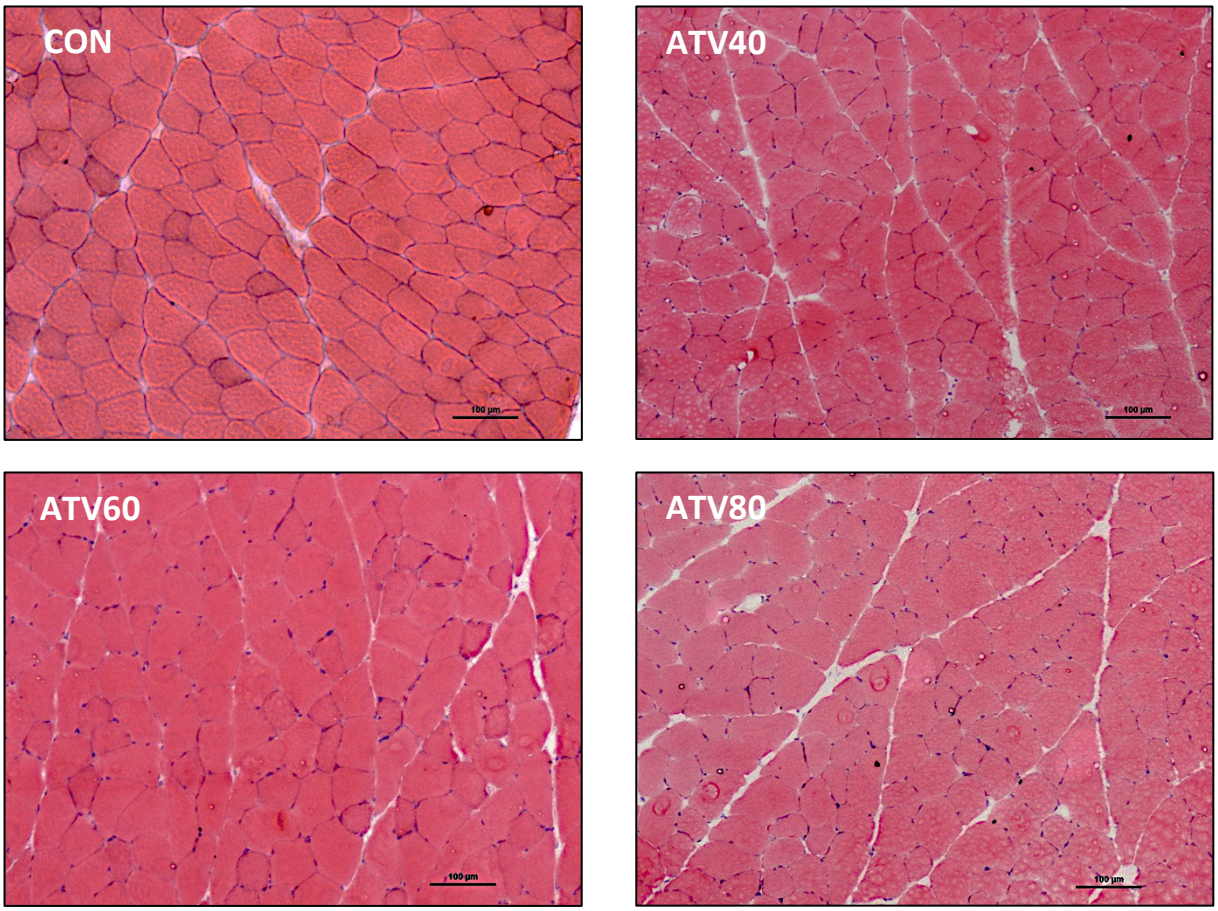

Figure 15: Representative H-E stained gastrocnemius-plantaris muscle sections of control and statin-treated animals. No obvious visual signs of muscle necrosis, mononuclear infiltrate or centrally located nuclei were demonstrated in the gastrocnemius-plantaris muscle of any animal. Control treatment (CON), 40 mg/kg/day atorvastatin treatment (ATV40), 60 mg/kg/day atorvastatin treatment (ATV60), 80 mg/kg/day atorvastatin treatment (ATV80). Scale bars represent 100 μm.

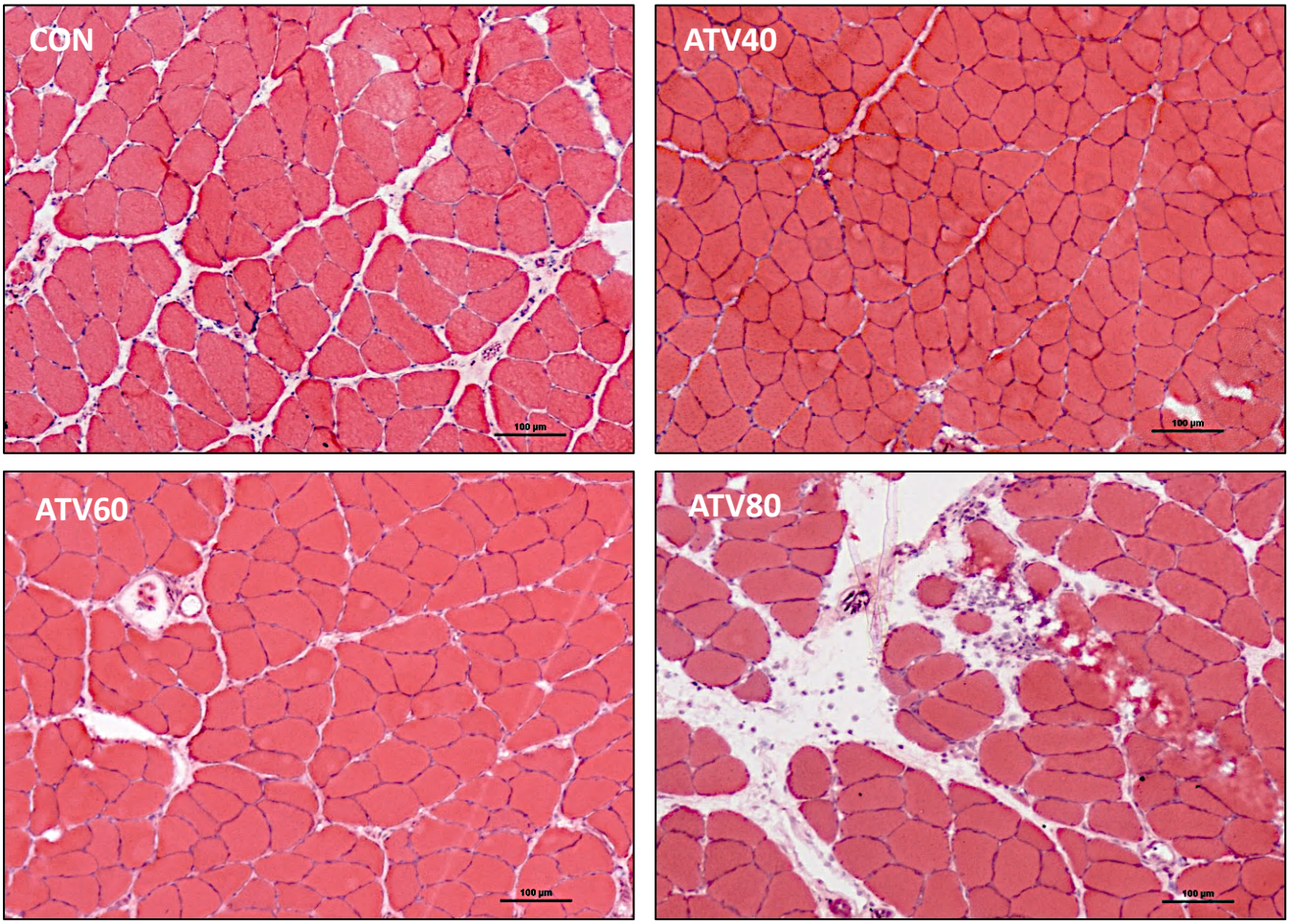

Figure 16: Representative H-E stained soleus sections of control and statin-treated animals.

No obvious visual signs of muscle necrosis, mononuclear infiltrate or centrally located nuclei are demonstrated in the soleus muscle of CON, ATV40- or ATV60-treated animals. Mononuclear infiltrate is evident in the soleus of the ATV80-treated animal. Control treatment (CON), 40 mg/kg/day atorvastatin treatment (ATV40), 60 mg/kg/day atorvastatin treatment (ATV60), 80 mg/kg/day atorvastatin treatment (ATV80). Scale bars represent 100 μm.

3.4 Discussion/Conclusion

This experiment aimed to determine the maximum statin dose that could be administered to rats for 10 days to elicit changes in interstitial glutamate content without eliciting myopathy. Results indicated that regardless of dose, statin treatment did not alter skeletal muscle interstitial glutamate concentration (Fig. 14).

Given that we did not see what was expected and that Nutella had been previously demonstrated to have large confounding effects (Section 2, page 49), the potential confounding effects that all-natural peanut butter could have were investigated. Control female rat interstitial glutamate values from the CTX experiment (Section 1, pages 30-39) were compared to control values from the current experiment. The only difference between these two groups was that the animals from the CTX experiment did not receive all-natural peanut butter and the animals from the current experiment received three grams of all-natural peanut butter for 10 days. Comparison of fed and unfed groups shows a trend towards elevated interstitial glutamate in the fed animals (Fig. 17), suggesting that all-natural peanut butter and Nutella elevated interstitial glutamate to a similar extent.

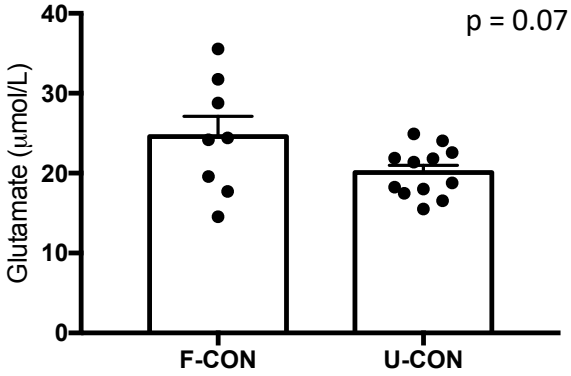

Figure 17: Comparison of fed and unfed animal skeletal muscle interstitial glutamate. Unfed control animals (U-CON) trended towards having reduced interstitial glutamate levels (p = 0.07) than control animals fed all-natural peanut butter (F-CON). All data are presented as mean ± SEM. n = 2-6 animals per group, 2-4 probes per animal. Statistical significance defined as $p \leq 0.05$.

Glutamate must be in very high concentrations in food to make it past first pass clearance in the gut and into circulation (Julio-Pieper et al. 2011). As such, we did not suspect that that the high protein content in all-natural peanut butter was responsible for the elevations demonstrated in interstitial glutamate. When caloric density and fat content were assessed, all-natural peanut butter was found to contain 18 kcal/3 g. On average, Sprague-Dawley rats eat 15-20 g of standard chow per day, which amounts to approximately 45-60 kcal/day (Laaksonen et al. 2013; Vento et al. 2008). Given the size and sex of our animals, they are likely on the lower end of this spectrum, thus, the bolus of all-natural peanut butter that the animal received represented approximately 44 percent of its daily caloric intake. Animals

did, in fact, gain weight at a greater rate than is typical for adult, female Sprague-Dawley rats (Janvier 2017). We propose that consuming this energy-dense bolus of all-natural peanut butter induced substrate overload and ROS production in the animal's skeletal muscle. If this is the case, endogenous antioxidant need and production would have also increased, resulting in increased xCT transporter activity and interstitial glutamate.

This study once again highlighted the confounding effects that food vehicles can have on outcomes, highlighting important changes that must be made in future experiments. In addition, this experiment was successful in demonstrating that 80 mg/kg/day atorvastatin treatment has the capacity to cause myopathy and thus is not a suitable dose for our model of statin myalgia.

Section 4

Study Four – Statin Treatment *in vivo* (Gavage)

4.1 Rationale

Previously, Nutella or all-natural peanut butter was used as a vehicle to deliver statin treatment to our animals. These options were chosen with the intent to reduce the amount of stress and handling experienced by our animals which may be caused by oral gavage treatment. The confounding effects that Nutella and all-natural peanut butter were demonstrated to have on interstitial glutamate concentrations (Section 2, page 49, and Section 3, page 61), however, deemed treating our animals by oral gavage a necessity. Data from the statin dosing study indicated that 80 mg/kg/day atorvastatin treatment for 10 days caused signs of myopathy (mononuclear infiltrate) in the soleus muscle (Section 3, page 59). Atorvastatin treatment was dosed at 60 mg/kg/day in the current study since animals treated with this dose previously elicited no signs of myopathy (Section 3, pages 58-59). Two animals were treated with 80 mg/kg/day atorvastatin to act as a positive control, with the expectation that they would demonstrate signs of myopathy. The purpose of the current experiment was to replicate the model for statin myalgia, as demonstrated *in vitro* by Rebalka et al. (2019), to an *in vivo* model. We aspired to elucidate if skeletal muscle interstitial glutamate is elevated following statin treatment. We hypothesized that following 10 days of statin treatment animals would demonstrate elevated skeletal muscle interstitial glutamate as a result of elevated xCT transporter activity.

4.2 Methods

Pre-experimental Procedures

Animals/Microdialysis Probe Construction

See Section 1, page 32.

Animals

All animals received their treatment dissolved in 1.5 mL of drinking water through oral gavage once per day for a total of 10 days. CON animals received 1.5 mL drinking water (n = 5 animals, 4 probes per animal), ATV60 animals received 60 mg/kg atorvastatin (Jamp Pharma Corporation) dissolved into 1.5 mL drinking water (n = 5 animals, 4 probes per animal) and ATV80 animals received 80 mg/kg atorvastatin (Jamp Pharma Corporation) dissolved in 1.5 mL drinking water (n = 2 animals, 4 probes per animal). On day 10, while anesthetized, interstitial fluid was collected from both gastrocnemius muscles using the skeletal muscle microdialysis technique. Following collection, rats were euthanized and blood and skeletal muscle were collected for analysis. Given the extensive time spent under anaesthetic, a heating pad was placed under the body of the rat to minimize heat loss during the procedure.

Experimental Procedures

Microdialysis Probe Insertion

All animals received their final statin treatment on treatment day 10 at 7:00am; three to eight hours prior to the skeletal muscle microdialysis procedure. For additional microdialysis probe insertion procedures see Section 1, pages 32-33.

Experimental Protocol

See Section 1, page 33, for microdialysis probe insertion and interstitial fluid sample collection/preparation protocol.

Once the interstitial fluid collection was complete animals were euthanized. Blood was collected from the chest cavity. Left and right GPS muscle complexes were harvested, the soleus was separated, and the gastrocnemius-plantaris complex was bisected longitudinally so that each piece of muscle contained one microdialysis probe. Following the bisection, muscle was embedded in OCT, frozen in isopentane cooled by liquid nitrogen and stored at -80°C for future analysis.

Sample Analysis

Endpoint Monitoring

Rats were monitored daily for endpoints that would suggest statin toxicity including weight loss greater than 20% of body weight, labored breathing, piloerection, ruffled coat, porphyrin staining, closed/sunken eyes and hunched posture (Ghalwash et al. 2018; Sidaway et al. 2009; Westwood et al. 2005).

Body Weight

All rats were weighed on a digital scale prior to treatment commencement and at four time points throughout their treatment.

Serum

Following euthanization blood was collected from the chest cavity and kept on ice for the duration of the experiments. At the end of the experiments blood was centrifuged at 2000 g for 15 minutes and supernatant was collected, aliquoted and stored at -21°C for future analysis.

Serum Preparation for Metabolite Quantification

2 μL of internal standard solution was mixed with 18 μL of serum for a final internal standard concentration of 20 μM 4-fluoro-D-phenylalanine, 20 μM 3-chloro-L-tyrosine, 20 μM naphthalenesulfonate and 2 mM 13C-glucose.

Skeletal Muscle Interstitial Fluid and Serum Metabolite Quantification

See Section 1, page 34.

Serum Statin Concentration Quantification

Analysis was performed on an Agilent 7100 capillary electrophoresis (CE) instrument (Agilent Technologies Inc.) coupled to an Agilent 6230 Time-of-Flight Mass Spectrometer (TOF-MS).

Serum samples were prepared following a slightly modified protocol (Azab, Ly, and Britz-Mckibbin 2019). Briefly, 100 μL of 0.01% v/v butylated hydroxytoluene in methanol was mixed with a 100 μL aliquot of serum. 250 μL of 4 μmol/L fluoro-phenylalanine (recovery standard) in methyl-tert-butyl ether and 25 μL of 1M HCl were then added to the mixture by vigorous shaking for 30 minutes at room temperature. Phase separation was induced by the addition of

100 μL deionized water. Samples were then centrifuged at 3000 g for 30 minutes at 4°C. Extracts were stored at -80°C before analysis when they were reconstituted in 25 μL of methanol: water (30:70) and 40 μM Cl-tyrosine. Background electrolyte consisted of 50 mmol/L ammonium bicarbonate (pH 8.5). Serial sample injection sequence consisted of 13 discrete samples injected hydrodynamically interspaced with background electrolyte spacers injected electrokinetically at 30 kV for 75 seconds. Separations were performed with an applied voltage of 30 kV at 25°C. Data acquisition was performed in full-scan mode on the TOF-MS spanning a mass range of 50-1700 m/z.

Histology

Muscle (gastrocnemius-plantaris and soleus) was sectioned into 6 μm cryosections and air-dried for 30 minutes. H-E staining was performed following a standard protocol. All images were obtained with a 90i Eclipse Microscope (Nikon, Inc.). Indication of altered myofibre morphology was assessed visually by the presence of mononuclear infiltrate and necrotic myofibres.

Statistics

All statistics were performed using Prism 7 (GraphPad Software). Statistical significance between interstitial fluid values was determined using a one-way ANOVA followed by Tukey's multiple comparison post hoc test. Statistical significance between serum values was determined with an unpaired t-test. Data presented are mean $\pm$ SEM. Individual points are included for transparency. Statistical significance was defined as $p \leq 0.05$.

4.3 Results

Endpoint monitoring. No animals exhibited any of the monitored endpoints at any time point throughout treatment.

Animal exclusion. One control animal was excluded from interstitial fluid analysis following microdialysis probe localization and determination that excess damage occurred in the area of probe insertion (Fig. 18). Previous experiments demonstrated that interstitial glutamate is elevated following myofibre injury (Section 1, pages 30-39).

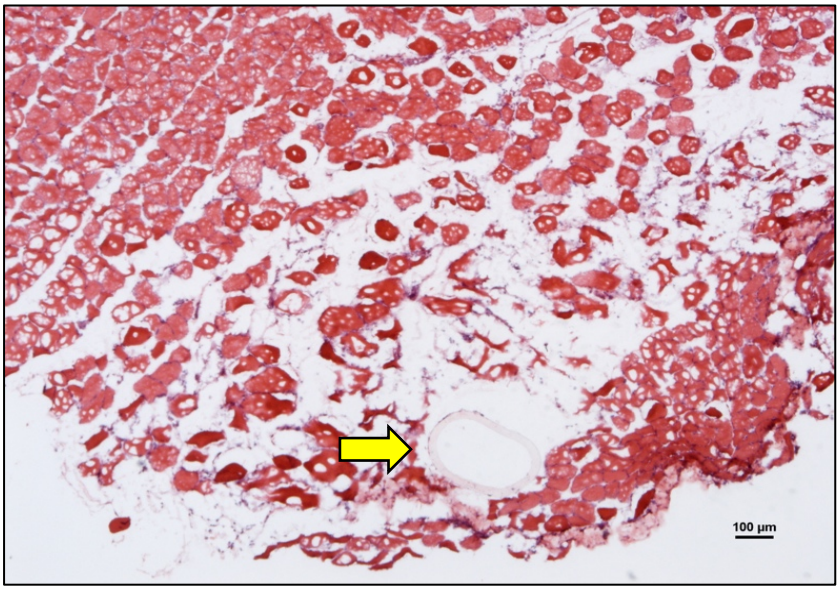

Figure 18: Representative image of probe insertion that caused damage to the myofibre environment. Altered myofibre morphology and mononuclear infiltrate were evident in the environment surrounding the microdialysis probe (yellow arrow) suggesting that interstitial fluid was collected in an area of myofibre injury. Myofibre injury has previously been demonstrated to cause elevations in interstitial glutamate. Scale bars represent 100 μm.

Body weight. All animals gained weight by the tenth day of treatment at a trajectory typical to their age and sex (Fig. 19).

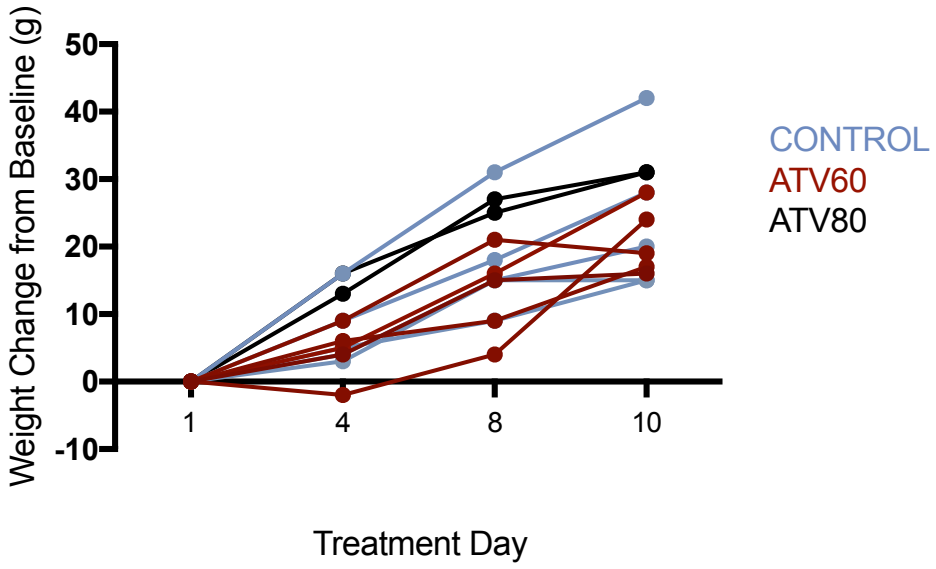

Figure 19: Total body weight gain at days 1, 4, 8 and 10 of control and statin-treated animals. All animals gained weight at a trajectory typical to their age and sex by day 10 of treatment. Unpaired t-test between CON and ATV60 animals demonstrated no significant differences. Control treatment (CON), 60 mg/kg atorvastatin dissolved in 1.5 mL drinking water (ATV60), 80 mg/kg atorvastatin dissolved in 1.5 mL drinking water (ATV80). All animals treated through oral gavage for 10 days. Each line represents a different animal.

Statin treatment did not elicit signs of myopathy in the gastrocnemius or soleus muscle. H-E stained gastrocnemius and soleus muscle sections demonstrated no centrally located nuclei, myofibre necrosis or mononuclear infiltrate following 10 days of 60 or 80 mg/kg/day statin treatment (Fig. 20).

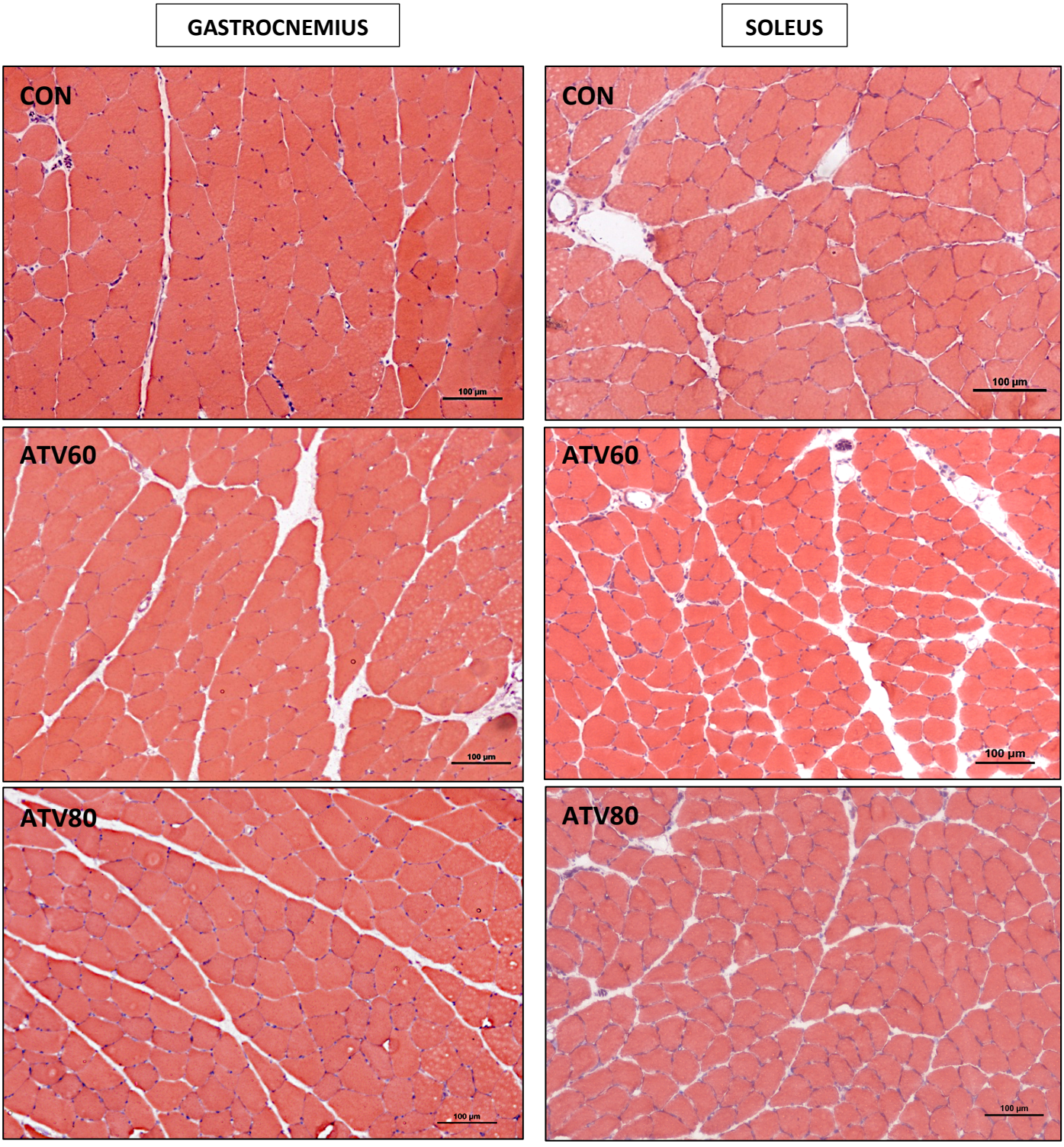
GASTROCNEMIUS
SOLEUS
CON
CON
ATV60
ATV60
ATV80
ATV80
100 µm
100 µm
100 µm
100 µm
100 µm
100 µm

Figure 20: Representative H-E stained gastrocnemius-plantaris and soleus muscle. No obvious visual signs of muscle necrosis, mononuclear infiltrate or centrally located nuclei were demonstrated in the gastrocnemius-plantaris or soleus muscle of any animal following 10 days of their respective treatment. Control treatment (CON), 60 mg/kg/day atorvastatin treatment (ATV60), 80 mg/kg/day atorvastatin treatment (ATV80). Images acquired with 90i Eclipse Microscope (Nikon, Inc.). Scale bars represent 100 μm.

Interstitial glutamate did not change following 10 days of 60 mg/kg/day statin treatment but was reduced following 10 days of 80 mg/kg/day statin treatment. Following 10 days of statin treatment by oral gavage no differences in interstitial glutamate were demonstrated between CON and ATV60-treated animals, however, glutamate was reduced in the ATV80-treated animals (Fig. 21A). No differences in interstitial cystine concentrations were demonstrated between groups (Fig. 21B). No differences in serum glutamate or cystine concentration were demonstrated between groups (Fig. 21C/D). For a full breakdown of all metabolites measured and their respective concentrations see Appendix Table 3.

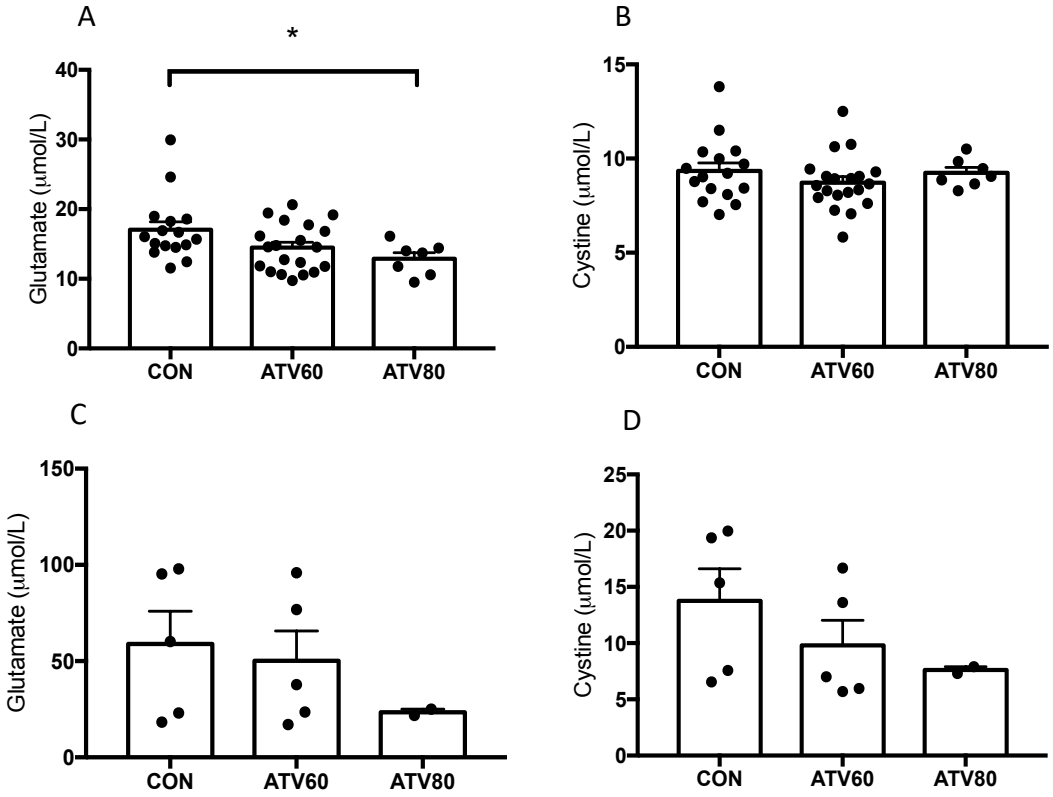

Figure 21: Skeletal muscle interstitial glutamate/cystine and serum glutamate/cystine concentrations in control, ATV60- and ATV80-treated animals. (A) Skeletal muscle interstitial glutamate was significantly reduced in ATV80-treated animals. (B) No significant differences were demonstrated in skeletal muscle interstitial cystine concentrations between treatment groups. (C)(D) No significant differences were demonstrated in serum glutamate or cystine between treatment groups. All data are presented as mean ± SEM. n = 4-5 animals per group, 3-4 probes per animal (interstitial fluid). n = 5 animals per group (serum). Control treatment (CON), 60 mg/kg/day atorvastatin treatment (ATV60), 80 mg/kg/day atorvastatin treatment (ATV80). Statistical significance defined as $p \leq 0.05$.

Muscle statin concentration. The concentration of atorvastatin in the GPS muscle complex, quantified by MSI-CE-MS, was below the instrument's limit of detection of 1 μmol/L.

Serum statin concentration. Atorvastatin was detectable in the serum of three of five statin-treated animals, through MSI-CE-MS, at a detection limit of 100 nmol/L (Table 1).

Table 1: Concentration of atorvastatin in the serum of control and statin-treated animals. Atorvastatin was detectable in the serum of three of five statin-treated animals. Control treatment (CON), 60 mg/kg/day atorvastatin treatment (ATV60), 80 mg/kg/day atorvastatin treatment (ATV80). <DL denotes lower than the detection limit of MSI-CE-MS quantification. Detection limit = 100 nmol/L.

Treatment Group	**Serum Atorvastatin Concentration (nmol/L)**
CON	<DL
ATV60	350
ATV60	900
ATV60	<DL
ATV60	<DL
ATV80	120

4.4 Discussion/Conclusion

The current experiment aimed to elucidate if glutamate is elevated in the interstitial space of skeletal muscle following statin treatment *in vivo,* without the confounding factors of Nutella or all-natural peanut butter. We hypothesized that skeletal muscle interstitial glutamate would be elevated following statin treatment, however, this was not demonstrated in our model. In fact, interstitial glutamate was reduced in the ATV80-treated animals (Fig. 21A).

Our hypothesis that glutamate would be elevated in the interstitial space is based on the assumption that statins induce oxidative stress in rodent skeletal muscle, a finding that has been repeatedly demonstrated in the literature (Bouitbir et al. 2011, 2012, 2016; La Guardia et al. 2013; Kaufmann et al. 2006; Rebalka et al. 2019; Sirvent et al. 2005). It is possible, however, that the alterations made to our model with the attempt at mimicking statin myalgia rather than myopathy, have resulted in an inadequate oxidative stress response to elicit changes in interstitial glutamate. These alterations include the statin dose and length of treatment. The literature shows that statin-induced myopathy presents at approximately the twelfth day of treatment in rats (Sidaway et al., 2009; Westwood, Bigley, Randall, Marsden, & Scott, 2005; Westwood, Scott, Marsden, Bigley, & Randall, 2008). These studies demonstrated that treatment length is more important than dose in terms of when myopathy will present. Therefore, we treated our animals for a reduced period (10 days) but increased the statin dose with the intention of causing a large oxidative stress in the skeletal muscle without causing myopathy. We cannot be certain to what extent oxidative stress was induced to the skeletal muscle in our model and whether it was large enough to alter glutamate homeostasis. We postulate that the lack of change to interstitial glutamate levels in the ATV60-treated animals is

the result of an inadequate oxidative stress response. Unfortunately, due to sample preparation at the time of harvest, oxidative stress measures such as GSH/GSSG ratios and SOD quantification could not be confidently tested in our tissue samples.

Interestingly, the ATV80-treated animals showed the opposite of what was expected. This group demonstrated reduced skeletal muscle interstitial glutamate levels (Fig. 21A). This group of animals was added as a positive control with the expectation, based on previous experiments, that they would elicit signs of myopathy. Contrastingly, these animals showed no signs of myopathy to any muscle (Fig. 20). It is important to note that the sample size of these animals was very small (n = 2 animals, 3-4 probes per animal) because indications of myopathy were expected. The within-animal variability (between probes) in microdialysis experiments is typically lower than the between-animal variability. While it is hypothesized that increasing the ATV-80 sample size would remove the differences demonstrated between treatment groups, further investigation is required before firm conclusions can be drawn.

We also called in question whether enough statin was physically getting into the muscle of the animals to induce an oxidative stress. It is assumed in the literature that statins enter skeletal muscle because downstream responses, such as altered mitochondrial bioenergetics and elevations in oxidative stress markers, result from treatment (Bouitbir et al. 2011, 2012, 2016; La Guardia et al. 2013; Kaufmann et al. 2006; Rebalka et al. 2019; Sirvent et al. 2005). Only very recently was statin concentration directly measured in mouse muscle (Singh et al. 2019). Although statins were undetectable with our MSI-CE-MS method (detection limit of 1 μmol/kg), Singh et al. (2019) saw median intramuscular statin levels of 3.2 nmol/kg. This

suggests that statins may have entered the myofibre in our model, but our method of quantification was not sensitive enough to detect such low concentrations.

Since statins were not measurable in the muscle, we next confirmed their presence in the serum. Atorvastatin was detectable in three of the five statin-treated samples that were tested, with the detection limit of 100 nmol/L (Table 1). Singh et al. (2019) demonstrated that mice treated with 10 mg/kg atorvastatin have serum statin concentrations of median 15.7 nmol/L, but the values ranged from 9.1-32.6 nmol/L. As our animals were treated with much higher doses of atorvastatin (60 and 80 mg/kg), it was expected that atorvastatin would be present in the serum above the 100 nmol/L detection limit. It is possible that the two animals that presented below the detection limit had values in the lower range and were not detectable with our method. Factors including differences in harvest time following final treatment, blood collection/preparation and metabolism (since animals were not fasted prior to final treatment) may also explain the large differences that were demonstrated in serum atorvastatin levels.

Though current findings did not support our hypothesis, a major limitation of our study was the we did not measure oxidative stress. We created this model with the assumption that statins would elicit a large enough oxidative stress in the muscle to increase xCT transporter activity. Elevated xCT transporter activity has been demonstrated during periods of oxidative stress as a way to increase GSH synthesis (Banjac et al. 2008). The assumption that statins would elevate xCT transporter activity in our model was based on our findings *in vitro,* in that xCT protein content and extracellular glutamate were elevated following statin treatment (Rebalka et al. 2019). Additionally, *in vitro* and *in vivo* models within the literature have repeatedly shown that statins cause oxidative stress in skeletal muscle (Bouitbir et al. 2011,

2012, 2016; La Guardia et al. 2013; Kaufmann et al. 2006; Schaefer et al. 2004; Sirvent et al. 2005). Since we did not see signs of myopathy in our animals treated 80 mg/kg/day atorvastatin as well as no demonstrated change in xCT transporter activity, we hypothesized the oxidative stress in our model was insufficient. We are limited by firmly stating this because of our lack of measure for oxidative stress. Indication of oxidative stress (i.e. GSH/GSSG, SOD activity or lipid peroxidation) and altered mitochondrial bioenergetics in our model would allow firmer conclusions to be drawn on why xCT transporter activity, and thus interstitial glutamate, does or does not change. Including these measurements would provide insight to if a rodent model for statin myalgia is appropriate and to what extent glutamate plays a role in the pathology.

Section 5
Consolidating Discussion and Conclusions

This set of studies was the first attempt at determining a rodent model to investigate glutamate as an underlying mechanism for statin myalgia. It attempted to bridge the knowledge gap that exists in the literature for rodent models of statin myalgia – the most common SAMS. This set of studies successfully identified an appropriate method to assess skeletal muscle interstitial glutamate levels in rats, challenged commonly made assumptions surrounding SAMS and identified confounding factors that led to the discovery of some interesting nutritional data.

Skeletal muscle microdialysis was employed and deemed a valid technique to collect and assess differences in rat skeletal muscle interstitial glutamate. While differences between statin-treated and untreated animals were not apparent, differences in skeletal muscle interstitial glutamate were quantifiable between uninjured and CTX-injured legs, as well as between fed and unfed animals. We are confident, therefore, that the lack of differences demonstrated between statin-treated and untreated animals is not the result of our collection technique.

This set of studies also discovered that treating rats by mixing therapeutics into Nutella and all-natural peanut had large confounding effects. Initially, we decided to treat our animals via this method to reduce the stress and handling that is caused by oral gavage. It was discovered, however, that feeding our animals a bolus of high-sugar or high-fat food increased xCT transporter activity and thus skeletal muscle interstitial glutamate levels. Our model relies on the assumption that statins cause oxidative stress, therefore, finding that feeding our

animals Nutella and all-natural peanut butter also caused large oxidative stress was critical. This discovery was important for both our model and all rodent models that focus on oxidative stress in skeletal muscle.

Finally, this set of studies challenged commonly made assumptions surrounding SAMS and brought awareness to the large differences that exist in rat and human statin metabolism. Though these discoveries did not favour our model, they provided insight and certainly contributed valuable knowledge to the vast body of literature that exists for SAMS. Overall, our rodent model in its current state is not an ideal representation of statin myalgia and more experiments are required before the model can be validated. Firm conclusions cannot be drawn on the implications of glutamate in statin myalgia without the limitations of the current experiments addressed first.

The foundations of the above thesis arose from the many assumptions that were taken from the literature during its creation. These assumptions included: 1) statins enter the myofibre and cause oxidative stress; and 2) that statins act and are metabolized similarly in rats as they are in humans. Upon further investigation, our studies demonstrated that these assumptions may not be as simple as the literature has made them out to be. Our studies also brought awareness to disparity that exists in the literature for models of statin myopathy (Table 2) and highlighted the importance of having a standardized model.

The current rodent model was created based on a human phenomenon: statin associated muscle pain, or myalgia. We attempted to translate what was demonstrated *in vitro* (Rebalka et al. 2019)*, in vivo*, with the hopes of paving the way for identifying the mechanisms behind statin myalgia in humans.

Statins are prescribed because of their ability to reduce blood lipid and cholesterol concentrations and have been demonstrated to reduce risk of all-cause and cardiovascular mortality (De Backer et al. 2004; Descamps et al. 2012; Ong 2005; Stone et al. 2014), however, we were not able to demonstrate that statin treatment had any effect on blood cholesterol in our rats. While differences in blood cholesterol concentrations between young and aged rats were demonstrated (Fig. 22A), no differences in blood cholesterol occurred as a result of statin treatment in either age group (Fig. 22B). Aged statin-treated rats were treated with atorvastatin or rosuvastatin for 30 days. Young statin-treated rats were treated with atorvastatin for 10 days. Regardless of age, treatment length or type, statins had no effect on blood cholesterol. These findings establish that statins do not have the same effect in rats as they do in humans.

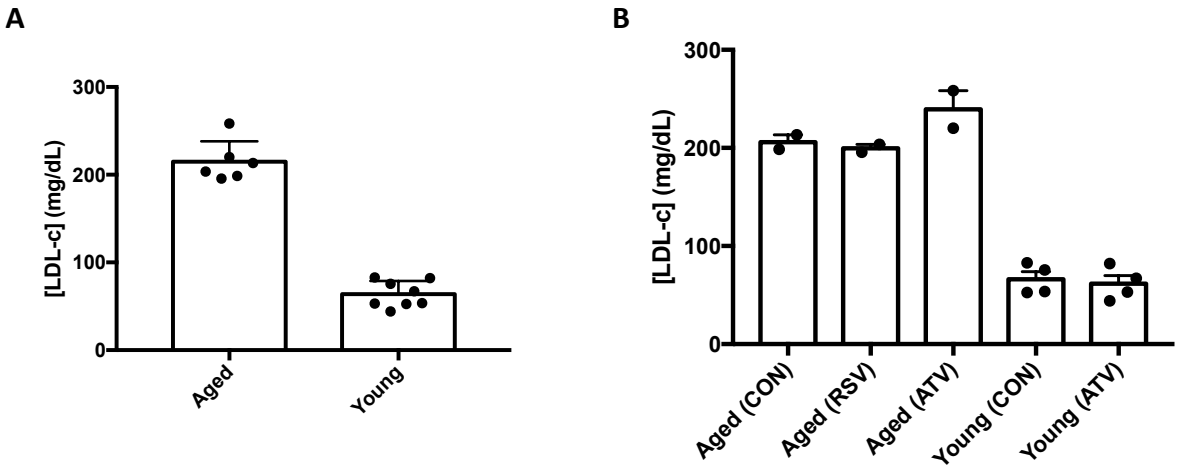

Figure 22: LDL-cholesterol quantification in aged and young rats treated with and without statins. (A) Aged rats have elevated serum LDL-cholesterol concentration [LDL-c] compared to young rats. (B) No differences in serum LDL-cholesterol concentration [LDL-c] are demonstrated between rats treated with and without statins in their respective age groups. Aged control rats (Aged CON), aged rats treated with rosuvastatin (Aged RSV), aged rats treated with atorvastatin (Aged ATV), young control rats (Young CON), young rats treated with atorvastatin (Young ATV). Data collected with LDL-cholesterol assay kit (Crystal Chem, Elk Grove Village, IL).

Statins reduce blood cholesterol concentrations in humans by inhibiting cholesterol biosynthesis in the liver and reducing secretion into the bloodstream, but also through transcriptional upregulation of hepatic and peripheral LDL-cholesterol receptors leading to increased LDL-cholesterol clearance (Berglund et al. 1998; Huff and Burnett 1997). Rats carry the majority of their cholesterol in the high-density lipoprotein (HDL) fraction (Krause and Newton 1995), however, which may explain why statins are ineffective at reducing their blood

cholesterol. This raises doubts that in a rat, statins would cause other human side effects, including statin myalgia.

Another assumption that our model heavily relied on was that statins enter the myofibre and induce an oxidative stress response. When skeletal muscle statin concentrations within our animals were analyzed, they could not be detected. The detection limit of our method of analysis was likely too high (1 μmol/L) to detect statins, but it did provoke further investigation into why it is so often assumed that statins enter the myofibre. Intriguingly, not many investigators have directly measured muscle statin concentrations and instead use downstream measures such as myopathy and oxidative stress as an indication that statins have entered the muscle. When statin concentration was measured in the serum of our animals, results were extremely variable (Table 1).

The next assumption we made based on the literature was that statins cause oxidative stress in the myofibre. Given numerous demonstrations that statin-treated rats will present with myopathy (Table 2), we believed this oxidative response would be large enough to reduce intracellular GSH content and initiate increased xCT transporter activity. As our model intended to mimic myalgia and not myopathy, we reduced our treatment length to 10 days as it has been repeatedly demonstrated that rats elicit signs of myopathy at approximately day 12 of treatment (Schaefer et al. 2004; Sidaway et al. 2009; Westwood et al. 2005, 2008). We hypothesized that at day 10 of treatment, oxidative stress would be at its non-myopathic peak. Our data give the indication, however, that the oxidative stress following 10 days of treatment was insufficient to increase xCT transporter activity.

Our animals were treated with very high statin doses that should, in theory, elicit a large oxidative stress response. Atorvastatin is typically prescribed to humans between the doses of 10-80 mg per day (Lennernäs 2003). We treated our animals with doses up to 80 mg/kg per day. If we extrapolate this to the average American man weighing approximately 90 kg, it would equate to 7200 mg of atorvastatin per day. The fact that our rats were able to endure this dose for 10 days without any signs of toxicity clearly demonstrates that statins are not metabolized the same in rats as they are in humans. Since we did not measure oxidative stress in our model, we do not know the extent to which statins actually caused an oxidative response and cannot conclude whether our mechanism was unsupported or if the oxidative stress was simply not enough to activate it.

These findings once again highlight the differences that exist in human and rat statin metabolism. These differences may be explained in part by variations in metabolic enzymes. In humans, activity of the cytochrome P450 enzyme family (CYP) is the most important for statin metabolism (Corsini et al. 1999). These enzymes are expressed in almost all organs, but they are found for the majority in hepatocytes and the intestinal epithelia (Martignoni, Groothuis, and de Kanter 2006; Shakunthala 2010). These enzymes account for approximately 70-80 percent of all enzymes involved in drug metabolism (Shakunthala 2010). Atorvastatin is primarily transformed and metabolized by CYP3A4 (Stern, Gibson, and Whitfield 1998). The small differences in the primary amino acid sequence of the CYPs across species can alter substrate specificity and catalytic activity, largely altering metabolism (Martignoni et al. 2006). While rats have a number of CYP3A genes, they do not possess CYP3A4. Rats possess CYP3A62 and CYP3A9 which have been demonstrated to have similar expression profiles to the human

CYP3A4 (Matsubara et al. 2004) but Martignoni, Groothuis, and de Kanter (2006) state that "the various CYP3A isoforms expressed in different species show different substrate specificities, making the extrapolation from animal to man quite hazardous." The elimination half-life of atorvastatin is approximately seven hours in humans (Lennernäs 2003) and approximately one hour in rats (Lin et al. 2017). Collectively, this information demonstrates large differences in human and rat statin metabolism, again raising concern regarding rat models for statin myalgia and also SAMS in general.

Another factor that makes addressing statin myalgia in a rat model difficult is that statin myalgia presents in approximately 29 percent of human statin users (Rosenson et al. 2014). As is evident in the literature, rodent models of statin myopathy can ensure that animals develop myopathy. We cannot, however, force our animal to develop myalgia, since we do not know exactly what causes it. In a sample of five animals, based on the prevalence of statin myalgia in a human population, it would be expected that only one of these animals would develop myalgia. Thus, data from the singular animal with symptoms may be washed out by the other four animals that do not display symptoms. To remove this limitation, a valid indication of pain must be included in future models. Non-invasive techniques that could be employed include measuring withdrawal reflexes or time to failure on physical tasks (Kniffki, Mense, and Schmidt 1978; Zala et al. 2019). These techniques do not give a direct measure of pain and results would need to be interpreted with caution.

An additional approach to increase the prevalence of statin myalgia in rats could be to introduce another stressor. Risk factors for SAMS in humans have already been identified, and include female sex, elderly age and combination pharmaceutical treatment (Mancini et al.

2011; Marot et al. 2011; Ozdemir et al. 2000; Yeter et al. 2007). Our data does support that a secondary stressor or a 'double-hit' may be necessary for SAMS to present. This is demonstrated by comparing data from study three (Section 3, page 59) to data from study four (Section 4, page 70). The animal treated with 80 mg/kg/day atorvastatin from study three demonstrated signs of myopathy in its soleus muscle. This animal also refused to finish its entire dose of treatment from treatment days 7-10. As such, we hypothesized that the animal treated with 80 mg/kg/day atorvastatin in study four would also demonstrate signs of myopathy. We expected this in particular because the animals in study four were treated through oral gavage and therefore would be receiving their treatments in full. The change in means of statin administration was the only difference between studies. Contrary to our hypothesis, no animal from study four demonstrated any signs of drug toxicity, including myopathy to the soleus. We suggest that the animal from study three showed signs of myopathy as a result of the added dietary stress of all-natural peanut butter. Similar to Nutella treatment in study two, all-natural peanut butter treatment alone caused elevations in interstitial glutamate, suggesting that oxidative stress was high and xCT transporter activity was elevated. The oversupply of substrates (substrate overload) in the myofibre impacts its functioning. In the instance of excess fat, the TCA cycle/β-oxidation pathway becomes overwhelmed and produces excess metabolic intermediates. This, in turn, increases the redox state of complex I, increasing O_2^- and H_2O_2 production (Anderson et al. 2009). It has been demonstrated that within four hours of consuming a high-fat meal, H_2O_2 production is elevated in permeabilized muscle fibres and by 12-hours post-feeding, rodents fed a high-fat diet had reduced GSH/GSSG compared to animals fed standard chow (Anderson et al. 2009).

Adding an additional stressor when creating a model for statin myalgia becomes problematic for two reasons. First, the additional stressor must be strong enough to increase oxidative stress, but not to the point to which the rat develops myopathy since statin myalgia presents in the absence of myofibre injury in humans. Introducing another stress increases the chance of increasing xCT transporter activity but dangerously increases the chance of the rat developing myopathy. Secondly, the introduction of another stressor to the model may washout the effects of the statin. Too strong of a stressor may make it difficult to decipher whether results are due to statin treatment or the additional stressor. The 'double-hit' must be meticulously chosen as strong enough to elicit oxidative changes without causing myopathy or masking the effects of the statins.

Evidently, many questions regarding the optimal rat model for statin myalgia must still be answered. The following experimental design is proposed as a means to continue building the optimal model.

Animals should be treated for a total of 10 days to avoid myopathy (Schaefer et al. 2004; Sidaway et al. 2009; Westwood et al. 2005, 2008). The rat model should remain in female rats since the female sex is a well-documented risk factor of statin myopathy and female rats are more susceptible to nociceptor sensitization and activation (Cairns et al. 2001, 2002; Castrillon et al. 2012; Mancini et al. 2011; Schaefer et al. 2004). Animals should receive 60 mg/kg/day atorvastatin treatment through oral gavage. A baseline surrogate measure of pain should be recorded. This measure could be a withdrawal reflex or time to exhaustion on a physical task. Follow-up measurements should be taken mid-treatment and on day nine of treatment. At approximately day five of treatment, one hour following statin treatment, a blood draw should

be completed to measure serum statin levels. Rats should be anaesthetized immediately following their final dose of statin treatment to undergo skeletal muscle microdialysis and interstitial fluid collection. Instead of a one-hour equilibration period and three 30-minute interstitial fluid sample collection periods, the microdialysis equilibration period should be reduced to 45 minutes followed by one 30-minute interstitial fluid sample collection. This will reduce the amount of time the animal is under anesthesia. Immediately following the 30-minute interstitial collection period, one gastrocnemius should be frozen for GSH/GSSG, xCT protein content, lipid peroxidation and muscle statin concentration analyses. The other gastrocnemius should have the soleus separated. A piece of the gastrocnemius should be prepared for fresh tissue SOD assays and another piece should be prepared to undergo mitochondrial respiration analysis. The remaining gastrocnemius and soleus should both be embedded in OCT and frozen in liquid nitrogen for histological analysis. Blood should be collected from the chest cavity once the animal is euthanized and spun down as soon as possible following harvest. This experiment addresses the assumptions that were made from the literature and in previous experiments and should provide answers to their validity (Fig. 23). This experimental design would also provide firm evidence for the efficacy of a rat model of statin myalgia. Indication of oxidative stress in this model would validate the previously proposed xCT transporter activity/interstitial glutamate hypothesis for statin myalgia.

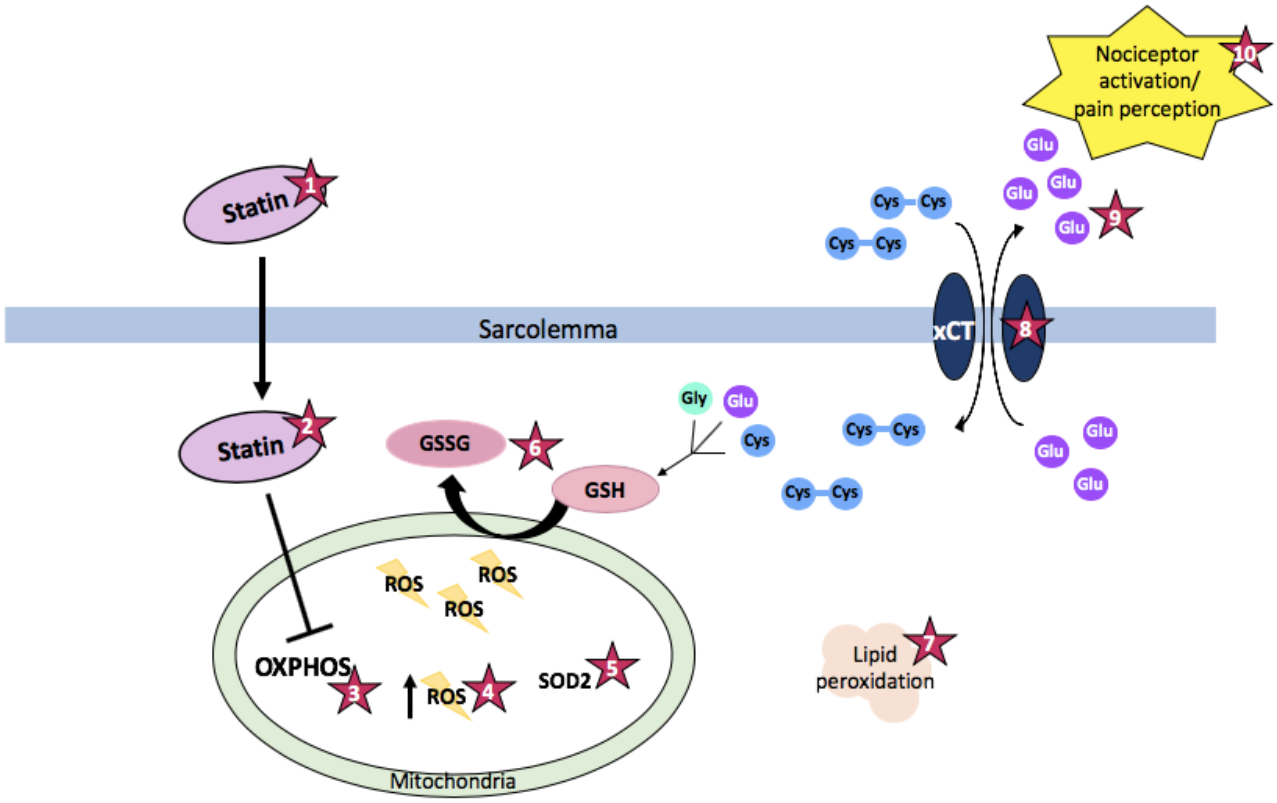

Figure 23: Schematic of the proposed model for statin myalgia and how each portion would be quantified. (1) Statins are present in the serum (MSI-CE-MS). (2) Statins enter the myofibre from circulation (liquid chromatography-mass spectrometry). (3) Statins inhibit OXPHOS and reduce mitochondrial respiration (high resolution respirometry). (4) Statins increase ROS production (high resolution respirometry). (5) SOD2 activity will give an indication of redox state within the mitochondria (fresh muscle tissue SOD assay). (6) GSH reduces ROS through its subsequent oxidation to GSSG (GSH/GSSG ratio, high performance liquid chromatography). (7) Lipid peroxidation will give an indication of oxidative stress (4HNE western blot). (8) xCT transporter content and activity increase as a result of elevated oxidative stress and need for glutathione synthesis (xCT protein content western blots). (9) Glutamate is elevated in the interstitium as a result of increased xCT transporter activity (skeletal muscle microdialysis, MSI-CE-MS). (10) Excess glutamate in the interstitium causes nociceptor sensitization and activation (behavioural measure of pain). OXPHOS = oxidative phosphorylation, ROS = reactive oxygen species, SOD2 = superoxide dismutase 2, GSH = reduced glutathione, GSSG = oxidized glutathione, Glu = glutamate, Cys = cysteine, Gly = glycine, Cys-Cys = cystine.

In conclusion, results from the current experiments in conjunction with the discrepancies between human and rat statin metabolism indicate a rat model for statin myalgia to be inappropriate. Numerous limitations still need to be addressed, however, before this can be conclusively stated. It is of utmost importance that a valid measure of oxidative stress is included in future models of statin myalgia. Additionally, including a measurement for pain would provide integral insight into the development of statin myalgia in a rat. If the "double-hit" strategy is to be employed, extreme caution should be taken to ensure myopathy does not present, and the additional stressor does not wash out the effects of the statin treatment. This set of experiments was the first step in determining a rat model of statin myalgia and lays the foundation for a standardized model if deemed valid and appropriate. These studies were successful in many aspects. They identified an appropriate method to assess rat skeletal muscle interstitial glutamate and identified key confounding factors of skeletal muscle oxidative stress. They also brought awareness to the disparities that exist in the literature in terms of rat models for statin myopathy, raised concern around their validity and highlighted the importance of having standardized models. Though our model in its current state is not supported, the results of these studies challenge commonly held beliefs surrounding SAMS and contribute valuable knowledge to the literature.

Table 2: Summary of select rat models of statin myopathy. While statin myopathy has been demonstrated robustly in rats in the literature, a huge disparity exists between models. There is a lack of consistency in dose, type and length of statin treatment, as well as in how myopathy presents, making it very difficult to draw conclusions and extrapolate data. Results in column seven compare control animals (treated with placebo) to animals treated with statins only.

Study	**Study Design**	**Rodent Model**	**Drug Delivery**	**Statin Type and Dose**	**Treatment Length**	**Evidence for/against Myopathy** ***(Statin-treated animals compared to control animals)***
Statins with different lipophilic indices exert distinct effects on skeletal, cardiac and smooth muscle (Irwin et al. 2020)	Animals treated with placebo or statins	Female, Wistar	Oral gavage	Simvastatin (80 mg/kg/day) OR Pravastatin (160mg/kg/day)	Two weeks	No differences in muscle mass Muscle force production reduced by simvastatin but increased by pravastatin
Evaluation of efficacy of formoterol fumarate on simvastatin induced myopathy in rats (Zala et al. 2019)	Animals treated with placebo, statins, formoterol fumarate or statins + formoterol fumarate	Male and female, Wistar	Oral gavage	Simvastatin (80 mg/kg/day)	Two weeks	No differences in body weight Elevated serum creatine kinase Reduced Rotarod activity time Central nuclei, enlarged edematous muscle fibres, separation of myofibrils in biceps femoris
Effect of L-carnitine on the skeletal muscle contractility in simvastatin-induced myopathy in rat (Ghalwash et al. 2018)	Animals treated with placebo, statins or statins + L-carnitine	Female, Sprague-Dawley	Oral gavage	Simvastatin (88 mg/kg/day)	Three weeks	Reduced muscle weight Reduced body weight Elevated serum creatine kinase Elevated malondialdehyde

Validation of a clinically-relevant rodent model of statin-associated muscle symptoms for use in pharmacological studies (Irwin et al. 2018)	Animals treated with placebo or statins	Female, Wistar	Dissolved in drinking water	Simvastatin (80 mg/kg/day)	Two weeks	Peak force reduced in gastrocnemius No differences in serum creatine kinase No differences in muscle mass Reduced body weight
Statins trigger mitochondrial reactive oxygen species-induced apoptosis in glycolytic skeletal muscle (Bouitbir et al. 2016)	Animals treated with placebo, statins, quercetin or statins + quercetin	Male, Wistar	Oral gavage	Atorvastatin (10 mg/kg/day)	Two weeks	Central nuclei, fibrosis and fibre size variability in plantaris but not soleus Elevated H_2O_2 production in plantaris but not soleus Reduced GSH/GSSG in plantaris but not soleus
Statin-induced myotoxicity is exacerbated by aging: a biophysical and molecular biology study in rats treated with atorvastatin (Camerino et al. 2016)	Adult and aged rats treated with placebo or statins	Male, Wistar	Oral gavage	Atorvastatin (10 mg/kg/day)	Four-five weeks	No differences in muscle weight No differences in serum creatine kinase Specific vacuolation in TA
Rosuvastatin: characterization of induced myopathy in the rat (Westwood et al. 2008)	Animals treated with placebo or statins	Female, Wistar	Oral gavage	Rosuvastatin (150 mg/kg/day)	5, 8, 10, 12, 14 or 16 days	Necrosis presents at day 10 and is variable between animals Soleus muscle generally spared Elevated serum creatine kinase by day 10 but returned to normal by day 14
Statin-induced muscle necrosis in the rat: distribution, development, and fibre selectivity	Animals treated with different types/doses of statins for varying lengths of time	Female, Wistar	Oral gavage	Simvastatin (80 mg/kg/day) OR Cerivastatin (0.5 mg/kg/day)	5, 8, 10, 12, 14 or 16 days	No muscle necrosis in animals from the 5-, 8- or 10-day time point

(Westwood et al. 2005)						Elevated creatine kinase on and after day 12 Animals in 12-, 14- and 16-day time points demonstrated differing severities in muscle necrosis (dependent on rat and muscle analyzed) Soleus spared in all animals that demonstrated muscle necrosis
Evaluation of ubiquinone concentration and mitochondrial function relative to cerivastatin-induced skeletal myopathy in rats (Schaefer et al. 2004)	Animals treated with placebo or statins for varying lengths of time	Female, Sprague-Dawley	Oral gavage	Cerivastatin (0.5 or 1.0 mg/kg/day)	5, 10 or 15 days	Muscle necrosis and inflammation presented in quadriceps by day 15 No differences in creatine kinase in 5- or 10-day treatment groups

Appendices

Appendix Table 1: Metabolite quantification in skeletal muscle interstitial fluid 12-, 24- and 48-hours post-CTX injection. Uninjured condition (CON), 12-hours post-CTX injection (CTX12), 24-hours post-CTX injection (CTX24), 48-hours post-CTX injection (CTX48). n = 2-6 animals per group, 4 probes per animal (2 uninjured + 2 injured). Metabolite concentrations are μmol/L. All values are mean ± SEM. <DL denotes concentrations lower than the detection limit of analysis. * denotes statistical significance from CON. Statistical significance accepted as $p \leq 0.05$. Interstitial fluid collected from gastrocnemius muscle. For full study see Section 1 (pages 30-39).

Metabolite	CON	CTX12	CTX24	CTX48
Adenosine	<DL	<DL	<DL	<DL
Alanine	142.50±12.81	166.70±41.26	183.00±23.74	131.30±31.31
Asparagine	13.28±1.50	15.53±3.96	19.17±2.65	12.84±3.98
ATP	<DL	<DL	<DL	<DL
Cystine	15.28±0.40	15.98±0.78	17.39±0.41*	14.70±1.09
GABA	2.8±0.59	3.34±1.21	5.2±1.96	2.44±0.82
Glutamic Acid	20.10± 0.88	19.09±2.40	25.70±1.42*	18.52±2.01
Glutamine	138.20±13.88	139.20±32.41	183.20±29.39	121.60±36.10
Glycine	78.56±7.52	80.75±24.97	97.49±16.92	74.38±17.52
Histidine	18.30±1.11	19.34±3.13	20.03±2.79	18.79±2.43
Lysine	60.56±7.18	69.59±20.06	46.23±7.08	56.84±17.62
Methionine	7.68±0.66	9.00±1.78	10.40±1.24	7.14±1.93

Phenylalanine	18.87±0.79	20.01±1.45	23.88±1.97*	17.43±2.09
Proline	45.24±3.08	49.59±7.79	58.4±3.63*	40.68±8.27
Serine	56.9±4.56	59.49±12.59	76.5±7.96*	52.00±12.51
Threonine	55.79±4.54	64.70±12.35	67.59±2.00	51.94±13.23
Tryptophan	2.98±0.19	3.47±0.51	3.86±0.47	2.84±0.52
Tyrosine	14.86±0.65	16.61±2.00	17.24±1.08	13.79±1.09
Valine	38.33±3.71	44.61±7.41	45.47±3.49	33.30±7.12

Appendix Table 2: Metabolite quantification in skeletal muscle interstitial fluid of control and statin-treated animals. Control treatment (CON), 40 mg/kg/day atorvastatin treatment (ATV40), 60 mg/kg/day atorvastatin treatment (ATV60), 80 mg/kg/day atorvastatin treatment (ATV80). n = 1-2 animals per group, 4 probes per animal. Metabolite concentrations are μmol/L. All values are mean ± SEM. <DL denotes concentrations lower than the detection limit of analysis. * denotes statistical significance from CON. Statistical significance accepted as $p \leq 0.05$. Interstitial fluid collected from gastrocnemius muscle. For full study see Section 3 (pages 52-62).

Metabolite	**CON**	**ATV40**	**ATV60**	**ATV80**
Alanine	125.5±13.80	154±8.60	208.80±23.17*	133.3±5.25
Asparagine	15.14±2.54	21.59±2.06	36.33±3.77	21.91±0.62
Aspartic Acid	<DL	<DL	<DL	<DL
Cystine	16.14±0.59	17.73±0.97	19.02±0.93*	17.31±0.45

GABA	3.803±0.40	3.835±0.88	6.085±1.42	1.923±0.45
Glutamic Acid	24.57±2.54	23.66±1.33	26.85±2.17	24.89±0.90
Glutamine	114.7±12.91	129.6±13.57	195±22.72*	137.2±4.97
Glycine	46.64±7.72	57.08±3.82	66.25±13.19	55.14±3.52
Histidine	16.62±1.04	18.57±1.34	21.77±2.54	20.98±0.47
Isoleucine	23.72±2.01	25.21±1.25	31.54±2.19	27.62±1.31
Leucine	31.43±2.59	39.43±2.92	46.15±6.62*	31.09±1.07
Lysine	58.06±6.64	63.93±6.72	98.81±10.38*	90.56±4.28*
Methionine	9.383±1.22	7.295±0.57	16.55±1.91*	12.59±0.53
Phenylalanine	21.13±1.44	20.9±0.95	28.51±2.34*	24.27±0.64
Proline	48.68±4.81	54.45±3.32	81.24±7.81*	54.91±1.06
Serine	58.39±6.17	61.08±8.78	151.5±14.57*	71.89±3.214
Serotonin	<DL	<DL	<DL	<DL
Threonine	61.14±7.71	97.28±6.22	167.9±16.85*	115.2±2.84*
Tryptophan	4.509±0.43	3.529±0.18	6.078±0.69	5.535±0.19
Tyrosine	16.15±0.91	14.59±0.42	20.52±1.25*	17.15±0.44

Appendix Table 3: Metabolite quantification in skeletal muscle interstitial fluid of control and statin-treated animals. Control treatment (CON), 40 mg/kg/day atorvastatin treatment (ATV40), 60 mg/kg/day atorvastatin treatment (ATV60), 80 mg/kg/day atorvastatin treatment (ATV80). n = 4-5 animals per group, 3-4 probes per animal. Metabolite concentrations are μmol/L. All values are mean ± SEM. <DL denotes concentrations lower than the detection limit of analysis.

* denotes statistical significance from CON. Statistical significance accepted as $p \leq 0.05$.

Interstitial fluid collected from gastrocnemius muscle. For full study see Section 4 (pages 63-77).

Metabolite	CON	ATV60	ATV80
Alanine	121.5±5.61	116.6±8.53	128.6±9.68
Asparagine	23.04±1.30	22.74±1.21	23.73±1.43
Cystine	9.34±0.42	8.72±0.32	9.24±0.29
Glutamate	17.04±1.15	14.17±0.76	12.88±0.88*
Glutamine	149.90±7.00	152.20±7.17	164.90±7.92
Glycine	58.21±4.85	68.50±2.87	76.09±6.07*
Lysine	45.73±2.53	49.04±4.24	80.99±10.02*
Methionine	11.90±0.67	10.12±0.56	10.03±0.67
Phenylalanine	14.68±0.64	12.98±0.59	12.86±0.51
Proline	47.27±2.06	41.14±1.81	39.45±2.06
Serine	58.81±2.70	59.81±2.93	60.69±2.70
Threonine	63.97±2.52	61.97±3.59	59.78±6.59
Tryptophan	5.03±0.36	4.23±0.27	4.18±0.23
Tyrosine	12.29±0.84	10.75±0.69	11.03±0.30
Valine	32.52±1.61	33.75±2.07	30.30±1.77

References

Adam-Vizi, Vera and Christos Chinopoulos. 2006. “Bioenergetics and the Formation of Mitochondrial Reactive Oxygen Species.” *Trends in Pharmacological Sciences* 27(12):639–45.

Alfredson, H., K. Thorsen, and R. Lorentzon. 1999. “In Situ Microdialysis in Tendon Tissue: High Levels of Glutamate, but Not Prostaglandin E2 in Chronic Achilles Tendon Pain.” *Knee Surgery, Sports Traumatology, Arthroscopy* 7(6):378–81.

Allard, Neeltje A. E., Tom J. J. Schirris, Rebecca J. Verheggen, Frans G. M. Russel, Richard J. Rodenburg, Jan A. M. Smeitink, Paul D. Thompson, Maria T. E. Hopman, and Silvie Timmers. 2018. “Statins Affect Skeletal Muscle Performance: Evidence for Disturbances in Energy Metabolism.” *Journal of Clinical Endocrinology and Metabolism* 103(1):75–84.

Anderson, E. J., M. E. Lustig, K. E. Boyle, T. L. Woodlief, D. A. Kane, C. T. Lin, J. W. Price, L. Kang, P. S. Rabinovitch, H. H. Szeto, and J. A. Houmard. 2009. “Mitochondrial H2O2 Emission and Cellular Redox State Link Excess Fat Intake to Insulin Resistance in Both Rodents and Humans.” *The Journal of Clinical Investigation* 119(3):573–81.

Arriza, Jeffrey L., Wendy A. Fairman, Susan G. Amara, P. Kavanaugh, I. Wadiche, and H. Murdoch. 1994. “Functional Comparisons of Three Glutamate Cloned from Human Motor Cortex Transporter.” *The Journal of Neuroscience : The Official Journal of the Society for Neuroscience* 14(9):5559–69.

Azab, Sandi, Ritchie Ly, and Philip Britz-Mckibbin. 2019. “Robust Method for High-Throughput Screening of Fatty Acids by Multisegment Injection-Nonaqueous Capillary Electrophoresis-Mass Spectrometry with Stringent Quality Control.” *Analytical Chemistry* 91(3):2329–36.

De Backer, Guy, Ettore Ambrosioni, Knut Borch-Johnsen, Carlos Brotons, Renata Cifkova, Jean Dallongeville, Shah Ebrahim, Ole Faergeman, Ian Graham, Giuseppe Mancia, Volkert Manger Cats, Kristina Orth-Gomér, Joep Perk, Kalevi Pyörälä, José L. Rodicio, Susana Sans, Vedat Sansoy, Udo Sechtem, Sigmund Silber, Troels Thomsen, and David Wood. 2004. "European Guidelines on Cardiovascular Disease Prevention in Clinical Practice. Third Joint Task Force of European and Other Societies on Cardiovascular Disease Prevention in Clinical Practice (Constituted by Representatives of Eight Societies and by Invit." *Atherosclerosis* 173(2):381–91.

Banach, Maciej, Corina Serban, Sorin Ursoniu, Jacek Rysz, Paul Muntner, Peter P. Toth, Steven R. Jones, Manfredi Rizzo, Stephen P. Glasser, Gerald F. Watts, Roger S. Blumenthal, Gregory Y. H. Lip, Dimitri P. Mikhailidis, and Amirhossein Sahebkar. 2015. "Statin Therapy and Plasma Coenzyme Q10 Concentrations - A Systematic Review and Meta-Analysis of Placebo-Controlled Trials." *Pharmacological Research* 99:329–36.

Banjac, A., T. Perisic, H. Sato, A. Seiler, S. Bannai, N. Weiss, P. Kölle, K. Tschoep, R. D. Issels, P. T. Daniel, and M. Conrad. 2008. "The Cystine/Cysteine Cycle: A Redox Cycle Regulating Susceptibility versus Resistance to Cell Death." *Oncogene* 27(11):1618–28.

Bannai, S. 1986. "Exchange of Cystine and Glutamate across Plasma Membrane of Human Fibroblasts." *Journal of Biological Chemistry* 261(5):2256–63.

Bao, Liming, Čestmír Vlček, Václav Pačes, and Jan P. Kraus. 1998. "Identification and Tissue Distribution of Human Cystathionine β- Synthase MRNA Isoforms." *Archives of Biochemistry and Biophysics* 350(1):95–103.

Berglund, Lars, Joseph L. Witztum, Narmer F. Galeano, Andrew S. Khouw, Henry N. Ginsberg,

and Rajasekhar Ramakrishnan. 1998. “Three-Fold Effect of Lovastatin Treatment on Low Density Lipoprotein Metabolism in Subjects with Hyperlipidemia: Increase in Receptor Activity, Decrease in ApoB Production, and Decrease in Particle Affinity for the Receptor. Results from a Novel Triple-Tr.” *Journal of Lipid Research* 39(4):913–24.

Bergstrom, J., P. Furst, L. O. Noree, and E. Vinnars. 1974. “Intracellular Free Amino Acid Concentration in Human Muscle Tissue.” *Journal of Applied Physiology* 36(6):693–97.

Betts, J. Gordon, Peter Desaix, Eddie (Edward W. .. Johnson, Jody E. Johnson, Oksana Korol, Dean Kruse, Brandon Poe, James Wise, Mark D. Womble, Kelly A. Young, and OpenStax College. 2017. *Anatomy & Physiology*.

Bleakman, David, Andrew Alt, and Eric S. Nisenbaum. 2006. “Glutamate Receptors and Pain.” *Seminars in Cell and Developmental Biology* 17(5):592–604.

Bookstaver, David A., Nancy A. Burkhalter, and Christos Hatzigeorgiou. 2012. “Effect of Coenzyme Q10 Supplementation on Statin-Induced Myalgias.” *American Journal of Cardiology* 110(4):526–29.

Bouitbir, Jamal, Anne Laure Charles, Andoni Echaniz-Laguna, Michel Kindo, Frédéric Daussin, Johan Auwerx, François Piquard, Bernard Geny, and Joffrey Zoll. 2012. “Opposite Effects of Statins on Mitochondria of Cardiac and Skeletal Muscles: A ‘mitohormesis’ Mechanism Involving Reactive Oxygen Species and PGC-1.” *European Heart Journal* 33(11):1397–1407.

Bouitbir, Jamal, Anne Laure Charles, Laurence Rasseneur, Stéphane Dufour, François Piquard, Bernard Geny, and Joffrey Zoll. 2011. “Atorvastatin Treatment Reduces Exercise Capacities in Rats: Involvement of Mitochondrial Impairments and Oxidative Stress.” *Journal of Applied Physiology* 111(5):1477–83.

Bouitbir, Jamal, François Singh, Anne Laure Charles, Anna Isabel Schlagowski, Annalisa Bonifacio, Andoni Echaniz-Laguna, Bernard Geny, Stephan Krahenbuhl, and Joffrey Zoll. 2016. "Statins Trigger Mitochondrial Reactive Oxygen Species-Induced Apoptosis in Glycolytic Skeletal Muscle." *Antioxidants and Redox Signaling* 24(2):84–98.

Breinholt, Vibeke M., Salka E. Nielsen, Pia Knuthsen, Søren T. Lauridsen, Bahram Daneshvar, and Annemarie Sørensen. 2003. "Effects of Commonly Consumed Fruit Juices and Carbohydrates on Redox Status and Anticancer Biomarkers in Female Rats." *Nutrition and Cancer* 45(1):46–52.

Brigham, M. Prince, William H. Stein, and Stanford Moore. 1960. "The Concentrations of Cysteine and Cystine in Human Blood Plasma." *Journal of Clinical Investigation* 39(11):1633–38.

Bruckert, Eric, Gilles Hayem, Sylvie Dejager, Caroline Yau, and Bernard Bégaud. 2005. "Mild to Moderate Muscular Symptoms with High-Dosage Statin Therapy in Hyperlipidemic Patients - The PRIMO Study." *Cardiovascular Drugs and Therapy* 19(6):403–14.

Brunham, L. R., P. J. Lansberg, L. Zhang, F. Miao, C. Carter, G. K. Hovingh, H. Visscher, J. W. Jukema, A. F. Stalenhoef, C. J. D. Ross, B. C. Carleton, J. J. P. Kastelein, and M. R. Hayden. 2012. "Differential Effect of the Rs4149056 Variant in SLCO1B1 on Myopathy Associated with Simvastatin and Atorvastatin." *Pharmacogenomics Journal* 12(3):233–37.

Busanello, Estela N. B., Ana C. Marques, Noelia Lander, Diogo N. de Oliveira, Rodrigo R. Catharino, Helena C. F. Oliveira, and Anibal E. Vercesi. 2017. "Pravastatin Chronic Treatment Sensitizes Hypercholesterolemic Mice Muscle to Mitochondrial Permeability Transition: Protection by Creatine or Coenzyme Q 10." *Frontiers in Pharmacology*

8(APR):1–11.

Cadenas, Enrique and Kelvin J. A. Davies. 2000. “Mitochondrial Free Radical Generation, Oxidative Stress, and Aging.” *Free Radical Biology and Medicine* 29(3–4):222–30.

Cairns, B. E., G. Gambarota, P. Svensson, L. Arendt-Nielsen, and C. B. Berde. 2002. “Glutamate-Induced Sensitization of Rat Masseter Muscle Fibers.” *Neuroscience* 109(2):389–99.

Cairns, Brian E. and Xudong Dong. 2008. “The Role of Peripheral Glutamate and Glutamate Receptors in Muscle Pain.” *Journal of Musculoskeletal Pain* 16(1–2):85–91.

Cairns, Brian E., Xudong Dong, Mandeep K. Mann, Peter Svensson, Barry J. Sessle, Lars Arendt-Nielsen, and Keith M. McErlane. 2007. “Systemic Administration of Monosodium Glutamate Elevates Intramuscular Glutamate Levels and Sensitizes Rat Masseter Muscle Afferent Fibers.” *Pain* 132(1–2):33–41.

Cairns, Brian E., James W. Hu, Lars Arendt-Nielsen, Barry J. Sessle, and Peter Svensson. 2001. “Sex-Related Differences in Human Pain and Rat Afferent Discharge Evoked by Injection of Glutamate into the Masseter Muscle.” *Journal of Neurophysiology* 86(2):782–91.

Camerino, Giulia M., Olimpia Musumeci, Elena Conte, Kejla Musaraj, Adriano Fonzino, Emanuele Barca, Marco Marino, Carmelo Rodolico, Domenico Tricarico, Claudia Camerino, Maria R. Carratù, Jean François Desaphy, Annamaria De Luca, Antonio Toscano, and Sabata Pierno. 2017. “Risk of Myopathy in Patients in Therapy with Statins: Identification of Biological Markers in a Pilot Study.” *Frontiers in Pharmacology* 8(July).

Castrillon, Eduardo E., Brian E. Cairns, Kelun Wang, Lars Arendt-Nielsen, and Peter Svensson. 2012. “Comparison of Glutamate-Evoked Pain between the Temporalis and Masseter Muscles in Men and Women.” *Pain* 153(4):823–29.

Combs, Joseph A. and Gina M. Denicola. 2019. “The Non-Essential Amino Acid Cysteine Becomes Essential for Tumor Proliferation and Survival.” *Cancers* 11(5).

Conn, Jeffrey. 2003. “Physiological Roles and Therapeutic Potential of Metabotropic Glutamate Receptors.” *Annals of the New York Academy of Sciences* 1003(1):12–21.

Corsini, Alberto, Stefano Bellosta, Roberta Baetta, Remo Fumagalli, Rodolfo Paoletti, and Franco Bernini. 1999. “New Insights into the Pharmacodynamic and Pharmacokinetic Properties of Statins.” *Pharmacology and Therapeutics* 84(3):413–28.

Craig, AD and KD Kniftki. 1985. “Spinothalamic Lumbosacral Lamina I Cells Responsive to Skin and Muscle Stimulation in the Cat.” *J. Physiol.* 365:197–221.

Dale, Krista M., C. Michael White, Nickole N. Henyan, Jeffrey Kluger, and Craig I. Coleman. 2007. “Impact of Statin Dosing Intensity on Transaminase and Creatine Kinase.” *American Journal of Medicine* 120(8):706–12.

DeGorter, M. K., R. G. Tirona, U. I. Schwarz, Y. H. Choi, G. K. Dresser, N. Susken, K. Myers, G. Zho, O. Iwuchukwu, W. Wei, R. A. Wilke, R. A. Hegele, and R. .. Kim. 2013. “Clinical and Pharmacogenetic Predictors of Circulating Atorvastatin and Rosuvastatin Concentrations in Routine Clinical Care.” *Circulation: Cardiovascular Genetics* 6(4):400–408.

Deminice, Rafael and Alceu Afonso Jordao. 2012. “Creatine Supplementation Reduces Oxidative Stress Biomarkers after Acute Exercise in Rats.” *Amino Acids* 43(2):709–15.

Descamps, O. S., G. B. De, L. Annemans, E. Muls, and A. J. Scheen. 2012. “New European Guidelines for the Management of Dyslipidaemia in Cardiovascular Prevention.” *Revue Medicale de Liege* 67(3):118–27.

Dohlmann, Tine Lovsø, Thomas Morville, Anja Birk Kuhlman, Karoline Maise Chrøis, Jørn Wulff

Helge, Flemming Dela, and Steen Larsen. 2019. “Statin Treatment Decreases Mitochondrial Respiration but Muscle Coenzyme Q10 Levels Are Unaltered: The LIFESTAT Study.” *Journal of Clinical Endocrinology and Metabolism* 104(7):2501–8.

Dreyer, Evan B., David Zurakowski, Robert A, Steven M. Podos, and Stuart a Lipton. 1996. “Elevated Glutamate Levels in the Vitreous Body of Humans and Monkeys with Glaucoma.” *Archives of Opthamology* 3(114):299–305.

Dröge, W., H. P. Eck, M. Betzler, P. Schlag, P. Drings, and W. Ebert. 1988. “Plasma Glutamate Concentration and Lymphocyte Activity.” *Journal of Cancer Research and Clinical Oncology* 114(2):124–28.

Du, Jian Tong, Wei Li, Jin Yan Yang, Chao Shu Tang, Qi Li, and Hong Fang Jin. 2013. “Hydrogen Sulfide Is Endogenously Generated in Rat Skeletal Muscle and Exerts a Protective Effect against Oxidative Stress.” *Chinese Medical Journal* 126(5):930–36.

Dykens, James and Yvonne Will. 2008. *Drug-Induced Mitochondrial Dysfunction*. John Wiley & Sons.

Eisen, Alon, Eli Lev, Zaza Iakobishvilli, Avital Porter, David Brosh, David Hasdai, and Aviv Mager. 2014. “Low Plasma Vitamin D Levels and Muscle-Related Adverse Effects in Statin Users.” *Israel Medical Association Journal* 16(1):42–45.

Engelen, M. P. K. J., M. Orozco-Levi, N. E. P. Deutz, E. Barreiro, N. Hernández, E. F. M. Wouters, J. Gea, and A. M. W. J. Schols. 2004. “Glutathione and Glutamate Levels in the Diaphragm of Patients with Chronic Obstructive Pulmonary Disease.” *European Respiratory Journal* 23(4):545–51.

EssÉn-Gustavsson, B. and E. Blomstrand. 2002. “Effect of Exercise on Concentrations of Free

Amino Acids in Pools of Type I and Type II Fibres in Human Muscle with Reduced Glycogen Stores." *Acta Physiologica Scandinavica* 174(3):275–81.

Flodgren, Gerd M., Albert G. Crenshaw, Fredrik Hellström, and Martin Fahlström. 2010. "Combining Microdialysis and Near-Infrared Spectroscopy for Studying Effects of Low-Load Repetitive Work on the Intramuscular Chemistry in Trapezius Myalgia." *Journal of Biomedicine and Biotechnology* 2010.

Fridovich, I. 1995. "Superoxide Radical and Superoxide Dismutases." *Annual Review of Biochemistry* 64(1):97–112.

Fridovich, Irwin. 1989. "Superoxide Dismutases." *The Journal of Biological Chemistry* 264(14):7761–64.

García-Ruiz, Carmen, Albert Morales, Antonio Ballesta, Joan Rodés, Neil Kaplowitz, and José Carlos Fernández-Checa. 1994. "Effect of Chronic Ethanol Feeding on Glutathione and Functional Integrity of Mitochondria in Periportal and Perivenous Rat Hepatocytes." *Journal of Clinical Investigation* 94(1):193–201.

Gerdle, Björn, Britt Larsson, Frida Forsberg, Nazdar Ghafouri, Linn Karlsson, Niclas Stensson, and Bijar Ghafouri. 2014. "Chronic Widespread Pain: Increased Glutamate and Lactate Concentrations in the Trapezius Muscle and Plasma." *Clinical Journal of Pain* 30(5):409–20.

Ghalwash, Mohammad, Ahlam Elmasry, and Nabil El-Adeeb. 2018. "Effect of L-Carnitine on the Skeletal Muscle Contractility in Simvastatin-Induced Myopathy in Rats." *Journal of Basic and Clinical Physiology and Pharmacology* 29(5):483–91.

Griffith, O. W. and A. Meister. 1985. "Origin and Turnover of Mitochondrial Glutathione." *Proceedings of the National Academy of Sciences of the United States of America*

82(14):4668–72.

Grivennikova, Vera G. and Andrei D. Vinogradov. 2006. “Generation of Superoxide by the Mitochondrial Complex I.” *Biochimica et Biophysica Acta - Bioenergetics* 1757(5–6):553–61.

Gu, Yuchao, Claudio P. Albuquerque, Daniel Braas, Wei Zhang, Genaro R. Villa, Junfeng Bi, Shiro Ikegami, Kenta Masui, Beatrice Gini, Huijun Yang, Timothy C. Gahman, Andrew K. Shiau, Timothy F. Cloughesy, Heather R. Christofk, Huilin Zhou, Kun Liang Guan, and Paul S. Mischel. 2017. “MTORC2 Regulates Amino Acid Metabolism in Cancer by Phosphorylation of the Cystine-Glutamate Antiporter XCT.” *Molecular Cell* 67(1):128-138.e7.

La Guardia, P. G., L. C. Alberici, F. G. Ravagnani, R. R. Catharino, and A. E. Vercesi. 2013. “Protection of Rat Skeletal Muscle Fibers by Either L-Carnitine or Coenzyme Q10 against Statins Toxicity Mediated by Mitochondrial Reactive Oxygen Generation.” *Frontiers in Physiology* 4 MAY(May):1–9.

Guo, Weijie, Yingjun Zhao, Zhenfeng Zhang, Ning Tan, Fangyu Zhao, Chao Ge, Linhui Liang, Deshui Jia, Taoyang Chen, Ming Yao, Jinjun Li, and Xianghuo He. 2011. “Disruption of XCT Inhibits Cell Growth via the ROS/Autophagy Pathway in Hepatocellular Carcinoma.” *Cancer Letters* 312(1):55–61.

Hawke, Thomas J. and Daniel J. Garry. 2001. “Myogenic Satellite Cells: Physiology to Molecular Biology.” *Journal of Applied Physiology* 91(2):534–51.

Hoheisel, U. and S. Mense. 1990. “Response Behaviour of Cat Dorsal Horn Neurones Receiving Input from Skeletal Muscle and Other Deep Somatic Tissues.” *J. Physiol.* 426:265–80.

Hoye, Adam T., Jennifer E. Davoren, Peter Wipf, Mitchell P. Fink, and Valerian E. Kagan. 2008.

"Targeting Mitochondria." *Accounts of Chemical Research* 41(1):87–97.

Huff, M. W. and J. R. Burnett. 1997. "3-Hydroxy-3-Methylglutaryl Coenzyme A Reductase Inhibitors and Hepatic Apolipoprotein B Secretion." *Current Opinion in Lipidology* 8(3):138–45.

Hughes, Meghan C., Sofhia V. Ramos, Patrick C. Turnbull, Irena A. Rebalka, Andrew Cao, Cynthia M. F. Monaco, Nina E. Varah, Brittany A. Edgett, Jason S. Huber, Peyman Tadi, Luca J. Delfinis, U. Schlattner, Jeremy A. Simpson, Thomas J. Hawke, and Christopher G. R. Perry. 2019. "Early Myopathy in Duchenne Muscular Dystrophy Is Associated with Elevated Mitochondrial H2O2 Emission during Impaired Oxidative Phosphorylation." *Journal of Cachexia, Sarcopenia and Muscle* 10(3):643–61.

Hunninghake, D. .. 1992. "HMG CoA Reductase Inhibitors." *Current Opinion in Lipidology* 3(1):22–28.

Hutchinson, PJ, MT O'Connell, PG Al-Rawi, LB Maskell, R. Kett-White, AK Gupta, HK Richards, DB Hutchinson, PJ Kirkpatrick, and JD Pickard. 2000. "Clinical Cerebral Microdialysis: A Methodological Study." *Journal of Neurosurgery* 93(1):37–43.

IASP. 2012. "IASP Taxonomy."

IMS Institute for Healthcare Informatics. 2017. "Medicines Use and Spending in the U.S.: A Review of 2015 and Outlook to 2021. New Jersey, USA: IMS Institute." (May 2017).

Irwin, Jordon C., Andrew S. Fenning, and Rebecca K. Vella. 2020. "Statins with Different Lipophilic Indices Exert Distinct Effects on Skeletal, Cardiac and Vascular Smooth Muscle." *Life Sciences* 242(October 2019):117225.

Ishii, Tetsuro, Yoshiki Sugita, and Shiro Bannai. 1987. "Regulation of Glutathione Levels in

Mouse Spleen Lymphocytes by Transport of Cysteine." *Journal of Cellular Physiology* 133(2):330–36.

Istvan, Eva S. and Johann Deisenhofer. 2001. "Structural Mechanism for Statin Inhibition of HMG-CoA Reductase." *Science* 292(5519):1160–64.

Janvier. 2017. *Sprague Dawley Rat*.

Julio-Pieper, Marcela, Peter J. Flor, Timothy G. Dinan, and John F. Cryan. 2011. "Exciting Times beyond the Brain: Metabotropic Glutamate Receptors in Peripheral and Non-Neural Tissues." *Pharmacological Reviews* 63(1):35–58.

Karamouzis, M., H. Langberg, D. Skovgaard, J. Bülow, M. Kjær, and B. Saltin. 2001. "In Situ Microdialysis of Intramuscular Prostaglandin and Thromboxane in Contracting Skeletal Muscle in Humans." *Acta Physiologica Scandinavica* 171(1):71–76.

Kaufmann, P., M. Török, A. Zahno, K. M. Waldhauser, K. Brecht, and S. Krähenbühl. 2006. "Toxicity of Statins on Rat Skeletal Muscle Mitochondria." *Cellular and Molecular Life Sciences* 63(19–20):2415–25.

Kaufmann, Scott H. and Michael O. Hengartner. 2001. "Programmed Cell Death: Alive and Well in the New Millennium." *Trends in Cell Biology* 11(12):526–34.

Kelner, Michael J. and Mark A. Montoya. 2000. "Structural Organization of the Human Glutathione Reductase Gene: Determination of Correct CDNA Sequence and Identification of a Mitochondrial Leader Sequence." *Biochemical and Biophysical Research Communications* 269(2):366–68.

Khayznikov, Maksim, Kallish Hemachrandra, Ramesh Pandit, Ashwin Kumar, Ping Wang, and Charles J. Glueck. 2015. "Statin Intolerance Because of Myalgia, Myositis, Myopathy, or

Myonecrosis Can in Most Cases Be Safely Resolved by Vitamin D Supplementation." *North American Journal of Medical Sciences* 7(3):86–93.

Kniffki, K. D., S. Mense, and R. F. Schmidt. 1978. "Responses of Group IV Afferent Units from Skeletal Muscle to Stretch, Contraction and Chemical Stimulation." *Experimental Brain Research* 31(4):511–22.

Krause, B. R. and R. S. Newton. 1995. "Lipid-Lowering Activity of Atorvastatin and Lovastatin in Rodent Species: Triglyceride-Lowering in Rats Correlates with Efficacy in LDL Animal Models." *Atherosclerosis* 117:237–44.

Kroemer, Guido. 2003. "Mitochondrial Control of Apoptosis: An Introduction." *Biochemical and Biophysical Research Communications* 304(3):433–35.

Kurnik, Daniel, Israel Hochman, Janet Vesterman-Landes, Tali Kenig, Itzhak Katzir, Yosef Lomnicky, Hillel Halkin, and Ronen Loebstein. 2012. "Muscle Pain and Serum Creatine Kinase Are Not Associated with Low Serum 25(OH) Vitamin D Levels in Patients Receiving Statins." *Clinical Endocrinology* 77(1):36–41.

Kwak, Hyo Bum, Anna Thalacker-Mercer, Ethan J. Anderson, Chien Te Lin, Daniel A. Kane, Nam Sihk Lee, Ronald N. Cortright, Marcas M. Bamman, and P. Darrell Neufer. 2012. "Simvastatin Impairs ADP-Stimulated Respiration and Increases Mitochondrial Oxidative Stress in Primary Human Skeletal Myotubes." *Free Radical Biology and Medicine* 52(1):198–207.

Laaksonen, K. S., T. O. Nevalainen, K. Haasio, I. H. E. Kasanen, P. A. Nieminen, and H. M. Voipio. 2013. "Food and Water Intake, Growth, and Adiposity of Sprague-Dawley Rats with Diet Board for 24 Months." *Laboratory Animals* 47(4):245–56.

Langberg, Henning, Dorthe Skovgaard, Michael Karamouzis, Jens Bülow, and Michael Kjær. 1999. “Metabolism and Inflammatory Mediators in the Peritendinous Space Measured by Microdialysis during Intermittent Isometric Exercise in Humans.” *Journal of Physiology* 515(3):919–27.

Leninger, Albert. 1964. *The Mitochondrion; Molecular Basis of Structure and Function*. Wa Benjamin.

Lennernäs, Hans. 2003. “Clin Pharmacokinetics of Atorvastatin.” *Clin Pharmacokinet* 42(13):1141–60.

Li Li Ji, R. Fu, and E. W. Mitchell. 1992. “Glutathione and Antioxidant Enzymes in Skeletal Muscle: Effects of Fiber Type and Exercise Intensity.” *Journal of Applied Physiology* 73(5):1854–59.

Lin, Chun Han, Ke Wei Hsu, Chia Hao Chen, Yow Shieng Uang, and Chun Jung Lin. 2017. “Differential Changes in the Pharmacokinetics of Statins in Collagen-Induced Arthritis Rats.” *Biochemical Pharmacology* 142:216–28.

MacLean, D. A., K. F. LaNoue, K. S. Gray, and L. I. Sinoway. 1998. “Effects of Hindlimb Contraction on Pressor and Muscle Interstitial Metabolite Responses in the Cat.” *Journal of Applied Physiology* (85):1583–92.

Maclean, David A., Lisa M. Vickery, and Lawrence I. Sinoway. 2001. “Elevated Interstitial Adenosine Concentrations Do Not Activate the Muscle Reflex.” *American Journal of Physiology - Heart and Circulatory Physiology* 280(2 49-2):546–53.

Maggs, D. G., R. Jacob, F. Rife, R. Lange, P. Leone, M. J. During, W. V Tamborlane, and R. S. Sherwin. 1995. “Interstitial Fluid Concentrations of Glycerol, Glucose, and Amino Acids in

Human Quadricep Muscle and Adipose Tissue." *Journal of Clinical Investigation* 96(July):370–77.

Mahdy, Mohamed A. A. 2019. "Biotoxins in Muscle Regeneration Research." *Journal of Muscle Research and Cell Motility* 40(3–4):291–97.

Mancini, G. B. Joh., Steven Baker, Jean Bergeron, David Fitchett, Jiri Frohlich, Jacques Genest, Milan Gupta, Robert A. Hegele, Dominic Ng, and Janet Pope. 2011. "Diagnosis, Prevention, and Management of Statin Adverse Effects and Intolerance: Proceedings of a Canadian Working Group Consensus Conference." *Canadian Journal of Cardiology* 27(5):635–62.

Mannery, Y. O., T. R. Ziegler, and D. P. Jones. 2007. "A Chemically Defined Diet with Insufficient Sulfur Amino Acids Induces Oxidation of Plasma Cysteine/Cystine and Glutathione/Glutathione Disulfide Redox State in Humans." *FASEB Journal* 21(5):697.

Mari, M., A. Colell, A. Morales, C. von Montfort, C. Garcia-Ruiz, and J. C. Fernandez-Checa. 2010. "Redox Control of Liver Function in Health and Disease." *Antioxidants and Redox Signaling* 12(11):1295–1331.

Mari, M., A. Morales, A. Colell, C. Garcia-Ruiz, and J. C. Fernandez-Checa. 2009. "Mitochondrial Glutathione, a Key Survival Antioxidant." *Antioxidants and Redox Signaling* 11(11):2685–2700.

Marot, A., J. Morelle, V. A. Chouinard, M. Jadoul, M. Lambert, and N. Demoulin. 2011. "Concomitant Use of Simvastatin and Amiodarone Resulting in Severe Rhabdomyolysis: A Case Report and Review of the Literature." *Acta Clinica Belgica* 66(2):134–36.

Martignoni, Marcella, Geny M. M. Groothuis, and Ruben de Kanter. 2006. "Species Differences between Mouse, Rat, Dog, Monkey and Human CYP-Mediated Drug Metabolism, Inhibition

and Induction." *Expert Opinion on Drug Metabolism and Toxicology* 2(6):875–94.

Martin, L. and L. B. Gardner. 2015. "Stress-Induced Inhibition of Nonsense-Mediated RNA Decay Regulates Intracellular Cystine Transport and Intracellular Glutathione through Regulation of the Cystine/Glutamate Exchanger SLC7A11." *Oncogene* 34(32).

Matsubara, T., H. J. Kim, M. Miyata, M. Shimada, Kiyoshi Nagata, and Y. Yamazoe. 2004. "Isolation and Characterization of a New Major Intestinal CYP3A Form, CYP3A62, in the Rat." *Journal of Pharmacology and Experimental Therapeutics* 309(3):1282–90.

McKenney, James M. 2003. "Pharmacologic Characteristics of Statins." *Clinical Cardiology* 26(S3):32–38.

Meister, Alton. 1995. "Glutathione Metabolism." *Methods in Enzymology* 251(C):3–7.

Mense, S. 1993. "Nociception from Skeletal Muscle in Relation to Clinical Muscle Pain." *Pain* 54(3):241–89.

Miao, Lu and Daret K. St. Clair. 2009. "Regulation of Superoxide Dismutase Genes: Implications in Disease." *Free Radical Biology and Medicine* 47(4):344–56.

Michalska-Kasiczak, Marta, Amirhossein Sahebkar, Dimitri P. Mikhailidis, Jacek Rysz, Paul Muntner, Peter P. Toth, Steven R. Jones, Manfredi Rizzo, G. Kees Hovingh, Michel Farnier, Patrick M. Moriarty, Vera A. Bittner, Gregory Y. H. Lip, and Maciej Banach. 2015. "Analysis of Vitamin D Levels in Patients with and without Statin-Associated Myalgia - A Systematic Review and Meta-Analysis of 7 Studies with 2420 Patients." *International Journal of Cardiology* 178:111–16.

Miller, Sharon, David Chinkes, David A. MacLean, Dennis Gore, and Robert R. Wolfe. 2004. "In Vivo Muscle Amino Acid Transport Involves Two Distinct Processes." *American Journal of*

Physiology - Endocrinology and Metabolism 287(1 50-1):136–41.

Morrison, Justin T., Chris T. Longenecker, Alison Mittelsteadt, Ying Jiang, Sara M. Debanne, and Grace A. McComsey. 2016. "Effect of Rosuvastatin on Plasma Coenzyme Q10 in HIV-Infected Individuals on Antiretroviral Therapy." *HIV Clinical Trials* 17(4):140–46.

Morville, Thomas, Tine LovsØ Dohlmann, Anja Birk Kuhlman, Ronni E. G. Sahl, Margit Kriegbaum, Steen Larsen, Flemming Dela, and JØrn Wulff Helge. 2019. "Aerobic Exercise Performance and Muscle Strength in Statin Users - The LIFESTAT Study." *Medicine and Science in Sports and Exercise* 51(7):1429–37.

Mudd, S. H., J. D. Finkelstein, F. Irreverre, and L. Laster. 1965. "Transsulfuration in Mammals. Microassays and Tissue Distributions of Three Enzymes of the Pathway." *Journal of Biological Chemistry* 240(11):4382–92.

Muir, A., L. V. Danai, D. Gui, C. Y. Waingarten, C. A. Lewis, and M. G. Vander Heiden. 2017. "Environmental Cystine Drives Glutamine Anaplerosis and Sensitizes Cancer Cells to Glutaminase Inhibition." *Elife* 6:27713.

Newsholme, Philip, Joaquim Procopio, Manuela Maria Ramos Lima, Tania Cristina Pithon-Curi, and Rui Curi. 2003. "Glutamine and Glutamate - Their Central Role in Cell Metabolism and Function." *Cell Biochemistry and Function* 21(1):1–9.

Nicholls, David and Stuart Ferguson. 2002. *Bioenergetics*. Elsevier.

Nkabyo, Yvonne S., Young Mi Go, Thomas R. Ziegler, and Dean P. Jones. 2005. "Extracellular Cysteine/Cystine Redox Regulates the P44/P42 MAPK Pathway by Metalloproteinase-Dependent Epidermal Growth Factor Receptor Signaling." *American Journal of Physiology - Gastrointestinal and Liver Physiology* 289(1 52-1):70–78.

Nunes-Silva, Albená, Priscila T. T. Bernardes, Bárbara M. Rezende, Fernando Lopes, Elisa C. Gomes, Pedro E. Marques, Paulo M. A. Lima, Cândido C. Coimbra, Gustavo B. Menezes, Mauro M. Teixeira, and Vanessa Pinho. 2014. "Treadmill Exercise Induces Neutrophil Recruitment into Muscle Tissue in a Reactive Oxygen Species-Dependent Manner. An Intravital Microscopy Study." *PLoS ONE* 9(5).

Okado-Matsumoto, Ayako and Irwin Fridovich. 2001. "Subcellular Distribution of Superoxide Dismutases (SOD) in Rat Liver. Cu,Zn-SOD in Mitochondria." *Journal of Biological Chemistry* 276(42):38388–93.

Olson. 2011. "Review Article." *Journal of Medieval Religious Cultures* 37(1):60.

Omote, Keiichi, Tomoyuki Kawamata, Mikito Kawamata, and Akiyoshi Namiki. 1998. "Formalin-Induced Release of Excitatory Amino Acids in the Skin of the Rat Hindpaw." *Brain Research* 787(1):161–64.

Ong, H. T. 2005. "The Statin Studies: From Targeting Hypercholesterolaemia to Targeting the High-Risk Patient." *Qjm* 98(8):599–614.

Ozdemir, O., M. Boran, V. Gokce, and Y. Uzun. 2000. "A Case with Severe Rhabdomyolysis and Renal Failure Associated with Cerivstatin-Gemfibrozil Combination Therapy: A Case Report." *Angiology* 51(8):695.

Parker, Beth A., Amanda L. Augeri, Jeffrey A. Capizzi, Kevin D. Ballard, Christopher Troyanos, Aaron L. Baggish, Pierre A. D'Hemecourt, and Paul D. Thompson. 2012. "Effect of Statins on Creatine Kinase Levels before and after a Marathon Run." *American Journal of Cardiology* 109(2):282–87.

Pierno, S., M. P. Didonna, V. Cippone, A. De Luca, M. Pisoni, A. Frigeri, G. P. Nicchia, M. Svelto,

G. Chiesa, C. Sirtori, E. Scanziani, C. Rizzo, D. De Vito, and D. Conte Camerino. 2006. "Effects of Chronic Treatment with Statins and Fenofibrate on Rat Skeletal Muscle: A Biochemical, Histological and Electrophysiological Study." *British Journal of Pharmacology* 149(7):909–19.

Pinal-fernandez, Iago, Maria Casal-dominguez, Andrew L. Mammen, Skin Diseases, United States, and United States. 2018. "HHS Public Access." 150(10):398–402.

Powers, Scott K., Jose Duarte, Andreas N. Kavazis, and Erin E. Talbert. 2010. "Reactive Oxygen Species Are Signalling Molecules for Skeletal Muscle Adaptation." *Experimental Physiology* 95(1):1–9.

Quinlan, Casey L., Adam L. Orr, Irina V. Perevoshchikova, Jason R. Treberg, Brian A. Ackrell, and Martin D. Brand. 2012. "Mitochondrial Complex II Can Generate Reactive Oxygen Species at High Rates in Both the Forward and Reverse Reactions." *Journal of Biological Chemistry* 287(32):27255–64.

Ramkumar, Satish, Ajay Raghunath, and Sudhakshini Raghunath. 2016. "Statin Therapy: Review of Safety and Potential Side Effects." *Acta Cardiologica Sinica* 32(6):631–39.

Rebalka, Irena A., Andrew W. Cao, Linda L. May, Mark A. Tarnopolsky, and Thomas J. Hawke. 2019. "Statin Administration Activates System XC- in Skeletal Muscle: A Potential Mechanism Explaining Statin-Induced Muscle Pain." *American Journal of Physiology. Cell Physiology* 317(5):C894–99.

Ribas, Vicent, Carmen García-Ruiz, and José C. Fernández-Checa. 2014. "Glutathione and Mitochondria." *Frontiers in Pharmacology* 5 JUL(July):1–19.

Rimaniol, Anne Cécile, Patricia Mialocq, Pascal Clayette, Dominique Dormont, and Gabriel Gras.

2001. “Role of Glutamate Transporters in the Regulation of Glutathione Levels in Human Macrophages.” *American Journal of Physiology - Cell Physiology* 281(6 50-6):1964–70.

Robinson, Michael and Joseph Coyle. 1987. “Glutamate and Related Acidic Excitatory Neurotransmitters: From Basic Science to Clinical Application.” *FASEB Journal* 1(6):446–55.

Rosenson, Robert S., Steven K. Baker, Terry A. Jacobson, Stephen L. Kopecky, and Beth A. Parker. 2014. “An Assessment by the Statin Muscle Safety Task Force: 2014 Update.” *Journal of Clinical Lipidology* 8(3 SUPPL):S58–71.

Ross, David. 1988. “Glutathione, Free Radicals and Chemotherapeutic Agents. Mechanisms of Free-Radical Induced Toxicity and Glutathione-Dependent Protection.” *Pharmacology and Therapeutics* 37(2):231–49.

Rott, David, David Leibowitz, Ilan Goldenberg, and Robert Klempfner. 2016. “Effect Of Coenzyme Q 10 Supplementation On Statin-Induced Myalgia, A Randomized Double-Blind, Placebo-Controlled Study.” *Journal of Preventive Medicine And Care* 1(1):16–22.

Rutten, Erica P. A., Mariëlle P. K. J. Engelen, Annemie M. W. J. Schols, and Nicolaas E. P. Deutz. 2005. “Skeletal Muscle Glutamate Metabolism in Health and Disease: State of the Art.” *Current Opinion in Clinical Nutrition and Metabolic Care* 8(1):41–51.

Saoi, Michelle, Alice Li, Chris McGlory, Tanner Stokes, Mark T. von Allmen, Stuart M. Phillips, and Philip Britz-Mckibbin. 2019. “Metabolic Perturbations from Step Reduction in Older Persons at Risk for Sarcopenia: Plasma Biomarkers of Abrupt Changes in Physical Activity.” *Metabolites* 9(7):1–19.

Sarchielli, Paola, Massimiliano di Filippo, Katiuscia Nardi, and Paolo Calabresi. 2007. “Sensitization, Glutamate, and the Link between Migraine and Fibromyalgia.” *Current Pain*

and Headache Reports 11(5):343–51.

Sato, Hideyo, Ayako Shiiya, Mayumi Kimata, Kanako Maebara, Michiko Tamba, Yuki Sakakura, Nobuo Makino, Fumihiro Sugiyama, Ken Ichi Yagami, Takashi Moriguchi, Satoru Takahashi, and Shiro Bannai. 2005. "Redox Imbalance in Cystine/Glutamate Transporter-Deficient Mice." *Journal of Biological Chemistry* 280(45):37423–29.

Sayin, Volkan I., Sarah E. LeBoeuf, Simranjit X. Singh, Shawn M. Davidson, Douglas Biancur, Betul S. Guzelhan, Samantha W. Alvarez, Warren L. Wu, Triantafyllia R. Karakousi, Anastasia Maria Zavitsanou, Julian Ubriaco, Alexander Muir, Dimitris Karagiannis, Patrick J. Morris, Craig J. Thomas, Richard Possemato, Matthew G. Vander Heiden, and Thales Papagiannakopoulos. 2017. "Activation of the NRF2 Antioxidant Program Generates an Imbalance in Central Carbon Metabolism in Cancer." *ELife* 6:1–23.

Schaefer, William H., Jeffery W. Lawrence, Amy F. Loughlin, Dana A. Stoffregen, Lori A. Mixson, Dennis C. Dean, Conrad E. Raab, Nathan X. Yu, George R. Lankas, and Clay B. Frederick. 2004. "Evaluation of Ubiquinone Concentration and Mitochondrial Function Relative to Cerivastatin-Induced Skeletal Myopathy in Rats." *Toxicology and Applied Pharmacology* 194(1):10–23.

Shakunthala, Narasimhulu. 2010. "New Cytochrome P450 Mechanisms: Implications for Understanding Molecular Basis for Drug Toxicity at the Level of the Cytochrome." *Expert Opinion on Drug Metabolism and Toxicology* 6(1):1–15.

Shan, Xiaoqin, Tak Yee Aw, and Dean P. Jones. 1990. "Glutathione-Dependent Projection against Oxidative Injury." *Pharmacology and Therapeutics* 47(1):61–71.

Shimada, A., E. E. Castrillon, L. Baad-Hansen, B. Ghafouri, B. Gerdle, K. Wåhlén, M. Ernberg, B. E.

Cairns, and P. Svensson. 2016. “Increased Pain and Muscle Glutamate Concentration after Single Ingestion of Monosodium Glutamate by Myofascial Temporomandibular Disorders Patients.” *European Journal of Pain (United Kingdom)* 20(9):1502–12.

Sidaway, J., Y. Wang, A. M. Marsden, T. C. Orton, F. R. Westwood, C. T. Azuma, and R. C. Scott. 2009. “Statin-Induced Myopathy in the Rat: Relationship between Systemic Exposure, Muscle Exposure and Myopathy.” *Xenobiotica* 39(1):90–98.

Singh, François, Joffrey Zoll, Urs Duthaler, Anne Laure Charles, Miljenko V. Panajatovic, Gilles Laverny, Thomas G. McWilliams, Daniel Metzger, Bernard Geny, Stephan Krähenbühl, and Jamal Bouitbir. 2019. “PGC-1β Modulates Statin-Associated Myotoxicity in Mice.” *Archives of Toxicology* 93(2):487–504.

Sirvent, Pascal, Sylvain Bordenave, Marianne Vermaelen, Belle Roels, Guy Vassort, Jacques Mercier, Eric Raynaud, and Alain Lacampagne. 2005. “Simvastatin Induces Impairment in Skeletal Muscle While Heart Is Protected.” *Biochemical and Biophysical Research Communications* 338(3):1426–34.

Siska, P. J., B. Kim, X. Ji, M. D. Hoeksema, P. P. Massion, K. E. Beckermann, J. Wu, J. Chi, J. Hong, and J. C. Rathmell. 2016. “Fluorescence-Based Measurement of Cystine Uptake through XCT Shows Requirement for ROS Detoxification in Activated Lymphocytes.” *Journal of Immunilogical Methods* 438:51–58.

Sleire, L., B. S. Skeie, I. A. Netland, H. E. Førde, E. Dodoo, F. Selheim, L. Leiss, J. I. Heggdal, P. H. Pedersen, J. Wang, and P. Enger. 2015. “Drug Repurposing: Sulfasalazine Sensitizes Gliomas to Gamma Knife Radiosurgery by Blocking Cystine Uptake through System Xc-, Leading to Glutathione Depletion.” *Oncogene* 34(49):5951–59.

Stacey, MJ. 1969. “Free Nerve Endings in Skeletal Muscle of the Cat.” *J. Anut.* 105:231–54.

Stern, R. H., D. M. Gibson, and L. R. Whitfield. 1998. “Cimetidine Does Not Alter Atorvastatin Pharmacokinetics or LDL- Cholesterol Reduction.” *European Journal of Clinical Pharmacology* 53(6):475–78.

Stone, Neil J., Jennifer G. Robinson, Alice H. Lichtenstein, C. Noel Bairey Merz, Conrad B. Blum, Robert H. Eckel, Anne C. Goldberg, David Gordon, Daniel Levy, Donald M. Lloyd-Jones, Patrick McBride, J. Sanford Schwartz, Susan T. Shero, Sidney C. Smith, Karol Watson, and Peter W. F. Wilson. 2014. “2013 ACC/AHA Guideline on the Treatment of Blood Cholesterol to Reduce Atherosclerotic Cardiovascular Risk in Adults: A Report of the American College of Cardiology/American Heart Association Task Force on Practice Guidelines.” *Journal of the American College of Cardiology* 63(25 PART B):2889–2934.

Sugano, Kenji, Kiyoshi Maeda, Hiroshi Ohtani, Hisashi Nagahara, Masatsune Shibutani, and Kosei Hirakawa. 2015. “Expression of XCT as a Predictor of Disease Recurrence in Patients with Colorectal Cancer.” *Anticancer Research* 35(2):677–82.

Svensson, P., B. E. Cairns, K. Wang, J. W. Hu, T. Graven-Nielsen, L. Arendt-Nielsen, and B. J. Sessle. 2003. “Glutamate-Evoked Pain and Mechanical Allodynia in the Human Masseter Muscle.” *Pain* 101(3):221–27.

Svensson, P., K. Wang, L. Arendt-Nielsen, BE Cairns, and BJ Sessle. 2005. “Pain Effects of Glutamate Injection into Human Jaw or Neck Muscles.” *J Orofac Pain* 19(2):109–18.

Taha, Dhiaa A., Cornelia H. De Moor, David A. Barrett, and Pavel Gershkovich. 2014. “Translational Insight into Statin-Induced Muscle Toxicity: From Cell Culture to Clinical Studies.” *Translational Research* 164(2):85–109.

Takeshige, K. and S. Minakami. 1979. “NADH- and NADPH-Dependent Formation of Superoxide Anions by Bovine Heart Submitochondrial Particles and NADH-Ubiquinone Reductase Preparation.” *Biochemical Journal* 180(1):129–35.

Tapiero, Haim, G. Mathé, P. Couvreur, and K. D. Tew. 2002. “II. Glutamine and Glutamate.” *Biomedicine and Pharmacotherapy* 56(9):446–57.

Toussirot, Éric, Fabrice Michel, and Nicolas Meneveau. 2015. “Rhabdomyolysis Occurring under Statins after Intense Physical Activity in a Marathon Runner.” *Case Reports in Rheumatology* 2015(Table 1):1–2.

Trumpower, B. 1990. “The Protonmotive Q Cycle.” *Journal of Biological Chemistry* 265(20):11409–12.

Turinsky, J. and C. L. Long. 1990. “Free Amino Acids in Muscle: Effect of Muscle Fiber Population and Denervation.” *American Journal of Physiology - Endocrinology and Metabolism* 258(3 21-3).

Turrens, Julio F. 2003. “Mitochondrial Formation of Reactive Oxygen Species.” *Journal of Physiology* 552(2):335–44.

Tzagoloff, Alexander. 1982. *Mitochondria*. Plenum Press.

Ungard, Robert G., Katja Linher-Melville, Mina Nashed, Manu Sharma, Jianping Wen, and Gurmit Singh. 2019. “XCT Knockdown in Human Breast Cancer Cells Delays Onset of Cancer-Induced Bone Pain.” *Molecular Pain* 15.

Ungard, Robert G., Eric P. Seidlitz, and Gurmit Singh. 2014. “Inhibition of Breast Cancer-Cell Glutamate Release with Sulfasalazine Limits Cancer-Induced Bone Pain.” *Pain* 155(1):28–36.

Vaccaro, M., C. Riva, L. Tremolizzo, M. Longoni, A. Aliprandi, E. Agostoni, A. Rigamonti, M. Leone, G. Bussone, and C. Ferrarese. 2007. "Platelet Glutamate Uptake and Release in Migraine with and without Aura." *Cephalalgia* 27(1):35–40.

Venditti, Paola, Lisa Di Stefano, and Sergio Di Meo. 2013. "Mitochondrial Metabolism of Reactive Oxygen Species." *Mitochondrion* 13(2):71–82.

Vento, Peter J., Meghan E. Swartz, Lisa B. E. Martin, and Derek Daniels. 2008. "Food Intake in Laboratory Rats Provided Standard and Fenbendazole- Supplemented Diets." *Journal of the American Association for Laboratory Animal Science* 47(6):46–50.

Vitvitsky, Victor, Sanjana Dayal, Sally Stabler, You Zhou, Hong Wang, Steven R. Lentz, and Ruma Banerjee. 2004. "Perturbations in Homocysteine-Linked Redox Homeostasis in a Murine Model for Hyperhomocysteinemia." *American Journal of Physiology - Regulatory Integrative and Comparative Physiology* 287(1 56-1):39–46.

Ward, Natalie C., Gerald F. Watts, and Robert H. Eckel. 2019. "Statin Toxicity: Mechanistic Insights and Clinical Implications." *Circulation Research* 124(2):328–50.

Waters. 2007. "UPLC Amino Acid Analysis Solution - System Guide."

Weisiger, Richard and Irwin Fridovich. 1973. "Mitochondrial Superoxide Dismutase." *The Journal of Biological Chemistry* 248(13):4793–96.

Westwood, F. Russell, Alison Bigley, Kevin Randall, Alan M. Marsden, and Robert C. Scott. 2005. "Statin-Induced Muscle Necrosis in the Rat: DistributioN, Development, and Fibre Selectivity." *Toxicologic Pathology* 33(2):246–57.

Westwood, F. Russell, Robert C. Scott, Alan M. Marsden, Alison Bigley, and Kevin Randall. 2008. "Rosuvastatin: Characterization of Induced Myopathy in the Rat." *Toxicologic Pathology*

36(2):345–52.

Yang, Wan Seok, Rohitha Sriramaratnam, Matthew E. Welsch, Kenichi Shimada, Rachid Skouta, Vasanthi S. Viswanathan, Jaime H. Cheah, Paul A. Clemons, Alykhan F. Shamji, Clary B. Clish, Lewis M. Brown, Albert W. Girotti, Virginia W. Cornish, Stuart L. Schreiber, and Brent R. Stockwell. 2014. "Regulation of Ferroptotic Cancer Cell Death by GPX4." *Cell* 156(1–2):317–31.

Yeter, Ekrem, Telat Keles, Tahir Durmaz, and Engin Bozkurt. 2007. "Rhabdomyolysis Due to the Additive Effect of Statin Therapy and Hypothyroidism: A Case Report." *Journal of Medical Case Reports* 1:2–3.

Yokoyama, Masayoshi, Toru Seo, Taesik Park, Hiroaki Yagyu, Yunying Hu, Huiping Son Ni, Ayanna S. Augustus, Reeba K. Vikramadithyan, Rajasekhar Ramakrishnan, Leslie K. Pulawa, Robert H. Eckel, and Ira J. Goldberg. 2007. "Effects of Lipoprotein Lipase and Statins on Cholesterol Uptake into Heart and Skeletal Muscle." *Journal of Lipid Research* 48(3):646–55.

Young, Jette F., Salka E. Nielsen, Jóhanna Haraldsdóttir, Bahram Daneshvar, Søren T. Lauridsen, Pia Knuthsen, Alan Crozier, Brittmarie Sandström, and Lars O. Dragsted. 1999. "Effect of Fruit Juice Intake on Urinary Quercetin Excretion and Biomarkers of Antioxidative Status." *American Journal of Clinical Nutrition* 69(1):87–94.

Young, Joanna M., Christopher M. Florkowski, Sarah L. Molyneux, Roberta G. McEwan, Christopher M. Frampton, Peter M. George, and Russell S. Scott. 2007. "Effect of Coenzyme Q10 Supplementation on Simvastatin-Induced Myalgia." *American Journal of Cardiology* 100(9):1400–1403.

Zala, KS, PA Bhatt, and HR Rajput. 2019. “Evaluation of Efficacy of Formoterol Fumarate on Simvastatin Induced Myopathy in Rats.” *Indian J Physiol Pharmacol* 63(4):324–31.

Zhao, Heng, Jiani Liu, Shinong Pan, Yingwei Sun, Qi Li, Fei Li, Li Ma, and Qiyong Guo. 2013. “SOD MRNA and MDA Expression in Rectus Femoris Muscle of Rats with Different Eccentric Exercise Programs and Time Points.” *PLoS ONE* 8(9):1–9.

Zhou, Qian and James K. Liao. 2010. “Pleiotropic Effects of Statins - Basic Research and Clinical Perspectives.” *Circulation Journal* 74(5):818–26.

Zhu, Yong Fang, Katja Linher-Melville, Jianhan Wu, Jennifer Fazzari, Tanya Miladinovic, Robert Ungard, Kan Lun Zhu, and Gurmit Singh. 2020. “Bone Cancer-Induced Pain Is Associated with Glutamate Signalling in Peripheral Sensory Neurons.” *Molecular Pain* 16.